

Exploring the Acute Effects of Glucocorticoids on Rabbit Vocal Fold Tissue

by

Gary Joseph Gartling

B.S. Communication Sciences and Disorders, James Madison University, 2015

M.S. Communication Sciences and Disorders, Bloomsburg University of Pennsylvania, 2017

Submitted to the Graduate Faculty of the
School of Health and Rehabilitation Sciences in partial fulfillment
of the requirements for the degree of
Doctor of Philosophy

University of Pittsburgh

2021

UNIVERSITY OF PITTSBURGH
SCHOOL OF HEALTH AND REHABILITATION SCIENCES

This dissertation was presented

by

Gary Joseph Gartling

It was defended on

October 13, 2021

and approved by

Dr. Leah B. Helou, Ph.D., CCC-SLP; Assistant Professor, Department of Communication Science and Disorders, School of Health and Rehabilitation Sciences, University of Pittsburgh

Dr. James L. Coyle, Ph.D., CCC-SLP, BCS-S, F-ASHA; Professor, Department of Communication Science and Disorders and Otolaryngology, School of Health and Rehabilitation Sciences and School of Medicine, University of Pittsburgh

Dr. Bradley C. Nindl, Ph.D., FACSM; Professor and Vice Chair for Research, Department of Sports Medicine and Nutrition; Director of Neuromuscular Research Laboratory/Warrior Human Performance Research Center, School of Health and Rehabilitation Sciences, University of Pittsburgh

Dr. Ryan C. Branski, Ph.D., CCC-SLP, F-ASHA; Vice Chair for Research, Department of Rehabilitation Medicine; Howard A. Rusk Associate Professor of Rehabilitation Research; Associate Professor, Department of Otolaryngology-Head and Neck Surgery, New York University

Dissertation Director: Dr. Bernard Rousseau, Ph.D., MMHC, CCC-SLP, F-ASHA; Associate Dean for Equity, Inclusion, and Community Engagement; Professor and Chair, Department of Communication Science and Disorders, School of Health and Rehabilitation Sciences, University of Pittsburgh

Copyright © by Gary Joseph Gartling

2021

Exploring the Acute Effects of Glucocorticoids on Rabbit Vocal Fold Tissue

Gary Joseph Gartling, Ph.D., CCC-SLP

University of Pittsburgh, 2021

Glucocorticoids (GCs) are frequently used to treat vocal fold (VF) inflammation due to their potent anti-inflammatory effects. Glucocorticoids have varying pharmacodynamic properties with effects ranging from reduced angiogenesis, changes in epithelial/endothelial barrier integrity, reduced therapeutic effect after long-term use, and skeletal muscle atrophy. Despite the known diversity of drug activity and associated negative effects, otolaryngologists typically rely on subjective clinical judgments when prescribing GCs, rather than objective evidence of differential efficacy. Elucidating GC-induced VF tissue changes and delineating effects between GCs is necessary for physicians to accurately modify drug selection for patient-specific needs. To inform these knowledge gaps, *in-vivo* animal models are frequently used due to the ability to study experimentally induced tissue changes that would be impossible to conduct in humans. However, knowledge of the existence and localization of key VF constituents involved in the regulation of VF homeostasis in rabbits - a commonly used model in this field - has not yet been investigated.

The purpose of this study was to: 1) Compare the localization of integral membrane proteins involved in the regulation of VF tissue homeostasis between human and rabbit VF tissue. 2) Investigate the acute effects of intramuscular injections of dexamethasone and methylprednisolone on VF tight junctions, vascularity, therapeutic efficacy, and thyroarytenoid (TA) muscle morphology in rabbit VFs. 3) Investigate the effects of an intracordal injection of dexamethasone on atrophy-associated gene expression and TA muscle morphology in rabbit VFs.

The results of these experiments revealed: 1) Similar localization of key ion transport channels and cell adhesion proteins between rabbit and human VFs. 2) Increases in VF epithelial and endothelial tight junction expression in rabbits treated with 6-daily intramuscular injections of dexamethasone and decreases in global body mass in rabbits treated with methylprednisolone. 3) No evidence of GC-induced atrophy in the VFs of rabbits receiving an intracordal injection of dexamethasone. These findings provide support for the use of rabbits as an experimental model when studying key VF constituents, and evidence of differential effects of GCs at a systemic and VF level. These findings identify an important role for tailored GC selection dependent on patient-specific needs when treating voice disorders.

Table of Contents

1.0 Introduction.....	1
1.1 Etiology of Voice Disorders	1
1.2 Structure of the Vocal Folds.....	3
1.2.1 Stratified Squamous Epithelium.....	4
1.2.2 Lamina Propria	6
1.2.3 Thyroarytenoid Muscle	7
1.3 Physiology of Voice Production.....	8
1.4 Vocal Fold Injury	9
1.4.1 Causes of VF Injury	10
1.4.2 Wound Healing Cascade.....	11
1.4.2.1 Inflammatory Phase	11
1.4.2.2 Proliferation Phase	13
1.4.2.3 Remodeling Phase.....	15
1.4.3 Vocal Fold Wound Healing	16
1.5 Glucocorticoids	19
1.5.1 Glucocorticoid Mechanism of Action	19
1.5.1.1 Direct Genomic Mechanism of Action.....	20
1.5.1.2 Indirect Genomic Mechanism of Action.....	21
1.5.1.3 Non-Genomic Mechanism of Action	22
1.5.2 Effects of Glucocorticoids on the Vocal Folds and Other Tissue	24
1.5.2.1 Mechanisms of Glucocorticoid-Induced Atrophy.....	26

1.5.2.1.1	Systems Involved in Synthesis and Degradation of Muscle	28
1.5.2.1.2	Inhibitory Effects	31
1.5.2.1.3	Stimulatory Effects	33
1.6	Specific Aims	34
1.6.1	Power Analyses.....	36
2.0	Methodology	38
2.1	Human Tissue Procurement.....	38
2.2	Animal Surgical Procedures	38
2.2.1	Intramuscular Injections	38
2.2.2	Intracordal Injection.....	39
2.2.3	Rabbit Vocal Fold Tissue Acquisition	40
2.2.4	Frozen Vocal Fold Tissue Sectioning	42
2.2.5	Paraffin Embedded Vocal Fold Tissue Sectioning.....	42
2.2.6	Immunofluorescence Labeling.....	43
2.2.7	Hematoxylin and Eosin Staining	44
2.2.8	Image Acquisition	45
2.2.9	Protein Localization Ratings.....	45
2.2.10	Fluorescence Quantification.....	45
2.2.11	Muscle Fiber Cross-sectional Area Quantification.....	46
2.2.12	Quantitative Polymerase Chain Reaction Primer and Probe Design	46
2.2.13	Electrophoresis	47
2.2.14	Standard Curve	47
2.2.15	RNA Extraction.....	48

2.2.16 Reverse Transcription	48
2.2.17 Quantitative Polymerase Chain Reaction.....	48
3.0 Results	51
3.1 Localization of Integral Membrane Proteins in Human and Rabbit Vocal Folds .	52
3.1.1 Aquaporin 1	52
3.1.2 Aquaporin 4.....	52
3.1.3 Aquaporin 7	53
3.1.4 Sodium-potassium Adenosine Triphosphatase	54
3.1.5 E-cadherin.....	55
3.1.6 Occludin	56
3.1.7 Zonula Occludin-1.....	56
3.2 Acute Effects of Daily Intramuscular Glucocorticoid Treatment on Rabbit Vocal Folds.....	58
3.2.1 Body Mass	58
3.2.2 Thyroarytenoid Muscle Cross-sectional Area	59
3.2.3 Immunofluorescence Expression	60
3.3 Occurrence of Vocal Fold Atrophy after Intracordal Dexamethasone Injection... 	61
3.3.1 Thyroarytenoid Muscle Cross-sectional Area.....	61
3.3.2 MuRF-1 Gene Expression	63
3.3.3 Atrogin-1 Gene Expression	63
4.0 Discussion.....	65
4.1 Localization of Integral Membrane Proteins in Human and Rabbit Vocal Folds .	65
4.2 Acute Effects of Daily Intramuscular GC Treatment on Rabbit Vocal Folds.....	69

4.3 Occurrence of Vocal Fold Atrophy After Intracordal Dexamethasone Injection..	71
4.4 Limitations	72
5.0 Conclusion and Clinical Implications	74
6.0 Future Directions	75
Appendix A Subjective localization rating form.....	77
Appendix B Depiction of muscle fiber CSA quantification	78
Bibliography	83

List of Tables

Table 1. Summary of temporal tissue changes in VFs after injury	18
Table 2. Anti-inflammatory and biological half-life properties of GCs.....	26
Table 3: Probe and primer sequences.....	49
Table 4: Results of positive labeling of tissue structures in rabbit and human VFs	58

List of Figures

Figure 1. Coronal-section of the larynx and VF.....	4
Figure 2. Coronal-section of the VF SSE.....	6
Figure 3. Cycle of phonation.....	9
Figure 4. Illustration of the inflammatory phase of wound healing.....	13
Figure 5. Illustration of proliferation phase of wound healing.....	15
Figure 6. Remodeling phase of wound healing.....	16
Figure 7. Illustration of the direct genomic mechanism of GCs.....	21
Figure 8. Illustration of the indirect genomic mechanism of GCs.....	22
Figure 9. Illustration of the non-genomic mechanism of GCs in the cell cytoplasm.....	23
Figure 10. Illustration of the non-genomic mechanism of GCs in the cell membrane.....	24
Figure 11. Inhibitory effect of GCs on protein synthesis and muscle growth.....	32
Figure 12. Stimulatory effects of GCs on protein proteolysis and muscle degradation.....	33
Figure 13. Percutaneous VF injection using the trans-cricothyroid membrane approach .	40
Figure 14. Schematic of experimental paradigm for rabbits receiving intramuscular injections.....	41
Figure 15. Schematic of experimental paradigm for rabbits receiving intracordal injections	42
Figure 16: qPCR with dual labeled 5'FAM, 3'TAMRA probes.....	49
Figure 17: Representative immunofluorescence images labeled for AQP1, 4, and 7.....	53
Figure 18: Representative immunofluorescence images labeled for Na⁺/K⁺-ATPase.....	55

Figure 19: Representative immunofluorescence images labeled for E-cadherin, Occludin, and ZO-1.....	57
Figure 20: Scatter plots showing pre and post-treatment body mass (kg)	59
Figure 21: H&E stained TA muscle fibers and scatter plot.....	60
Figure 22: Immunofluorescence images of rabbit VF epithelium and LP layers.	61
Figure 23: H&E stained TA muscle fibers and scatter plot.....	62
Figure 24: MuRF-1 gene expression in VFs injected with dexamethasone, saline, and untreated controls	63
Figure 25: Atrogin-1 gene expression in VFs injected with dexamethasone, saline, and untreated controls	64

List of Abbreviations

GC	Glucocorticoid
VF	Vocal fold
TA	Thyroarytenoid
ECM	Extracellular matrix
SSE	Stratified squamous epithelial
BMZ	Basement membrane zone
LP	Lamina propria
Na ⁺ /K ⁺ -ATPase	Sodium-potassium adenosine triphosphatase
AQP	Aquaporin
TJ	Tight junction
AJ	Anchoring junction
ZO-1	Zonula occludin-1
HA	Hyaluronic acid
IL	Interleukins
TNF	Tumor necrosis factor
PDGF	Platelet-derived growth factor
TGF	Transforming growth factor
COX	Cyclooxygenase
VEGF	Vascular endothelial growth factor
FGF	Fibroblast growth factor
KGF	Keratinocyte growth factor
MMP	Matrix metalloproteinases
NF- κ B	Nuclear factor kappa B
CRH	Corticotropin-releasing hormone
GCR	Glucocorticoid receptor
GRE	Glucocorticoid-responsive elements
ATP	Adenosine triphosphate
AA	Arachidonic acid
TCR	T-cell receptors
LCK	Lymphocyte-specific protein tyrosine kinase
UPS	Ubiquitin-proteasome system
IGF	Insulin-like growth factor
IRS	Insulin receptor substrate
PI3K	Phosphatidylinositol-3-kinase
PIP2	Phosphatidylinositol-(4,5)-bisphosphate
PIP3	Phosphatidylinositol-(3,4,5)-trisphosphate
mTOR	Mammalian target of rapamycin
Akt	Protein kinase B

S6K1	S6 kinase beta-1
Ub	Ubiquitin
MuRF	Muscle really interesting new gene finger
CSA	Cross-sectional area
CD	Cluster of differentiation
OCT	Optimal cutting temperature
IV	Intravenous
SpO2	Spot oxygen saturation
H&E	Hematoxylin and eosin
PBS	Phosphate-buffered saline
RT	Room temperature
DAPI	4',6-diamidino-2-phenylindole
dH2O	Distilled water
qPCR	Quantitative polymerase chain reaction
SDHA	Succinate dehydrogenase subunit a
Ct	Cycle threshold
ANOVA	Analysis of variance
CI	Confidence intervals
TEER	Trans-electrical epithelial resistance

1.0 Introduction

Portions of this dissertation have been previously published. It is reprinted with permission from *The Laryngoscope* (Gartling, Sayce, Kimball, Sueyoshi, & Rousseau, 2021) © 2021. Gartling GJ, Sayce L, Kimball EE, Sueyoshi S, Rousseau B. A Comparison of the Localization of Integral Membrane Proteins in Human and Rabbit Vocal Folds. *The Laryngoscope*. 2021 Apr;131(4):E1265-71.

1.1 Etiology of Voice Disorders

Voice disorders are the most common communication ailment across the lifespan; approximately 20 million Americans are diagnosed with a voice disorder each year¹ with total annual health care costs approaching \$13 billion dollars.² A voice disorder can be defined as an abnormality in a person's voice production characterized by irregularities in pitch, loudness, resonance, and/or quality that negatively impact their ability to meet daily communication needs.^{1,3-5} Voice disorders can be generally classified as being organic or functional. Organic voice disorders can have structural origins, where there are physical changes to any of the mechanisms involved in voice production, or neurogenic origins, where the voice mechanism is altered from iatrogenic damage, idiopathic damage, or degeneration of the central or peripheral nervous system. Functional voice disorders are characterized by abnormal voice production in the absence of any organic origin. These classifications are not mutually exclusive and vary across etiological factors including occupation, age, and sex.⁶

Regarding the prevalence of voice disorders across occupations, studies often use cross-sectional methods without the use of controls, and combine occupations including telemarketers, tour guides, salespeople, and professional singers into a single category of “professional voice users”, making differentiating the prevalence of voice disorders across the wide variety of specific occupations difficult. However, it is reported that teachers are considered the most at-risk population for voice disorders, comprising approximately 5.2% to 20% of caseloads in voice clinics,^{7,8} likely due to the increased vocal burden required for projecting voice in the classroom.

The age group that is at the highest risk of having a voice-related disability are people 40 to 59-years-old.^{7,9} However, children and adults are similarly affected by voice disorders with causes varying by age. In younger children between 1 and 18-years-old, the most common organic voice disorders are acute laryngotracheobronchitis, VF nodules, and VF cysts.⁹⁻¹¹ Vocal fold nodules are observed more frequently among males ages 4 to 10-years-old.⁹⁻¹¹ However, between 12 to 60-years-old, VF nodules are seen more frequently in females.^{9,12} This age and gender discrepancy is likely due to males experiencing substantial laryngeal growth and subsequent lesion regression into the VF tissue during adolescence,^{13,14} while the female VFs remain much smaller compared to males after puberty. Female VFs also contain different extracellular matrix (ECM) components which increase the likelihood of traumatic collisions during phonation (i.e. phonotrama).¹⁵⁻¹⁸

In general, voice disorders affect more females than males, as evidenced by organic voice disorders such as VF polyps, VF nodules, Reinke’s edema, reflux laryngitis, VF paralysis, and presbyphonia disproportionately affecting females.⁹ Additionally, functional voice disorders are reported to be the leading cause of voice-related disability in females 19 to 60-years-old,⁹ believed to be partly associated with higher reported occurrences of depression and anxiety in the general

female population,¹⁹ which can contribute to functional voice disorders such as muscle tension dysphonia.^{20,21} The higher incidence of voice disorders among the female population may also be due to the well-documented findings that females are more likely to report a voice disorder,⁸ while males are less likely.²² It is important to note the sparsity of evidence and underrepresentation of diverse participants in studies exploring the etiology of voice disorders, making findings regarding the prevalence of voice disorder in underrepresented groups of individuals challenging.

1.2 Structure of the Vocal Folds

The VFs are bilateral membranous bands of tissue located within the larynx (Figure 1A). Each VF is composed of five layers; the outermost luminal layer is comprised of stratified squamous epithelial (SSE) cells anchored to a basement membrane zone (BMZ). Deeper into the tissue is the lamina propria (LP), which is segmented into three distinct sections: the superficial, intermediate, and deep layers, which gradually increase in elastin and collagen density and elastin flexibility toward the muscle. The final layer of the VF is the TA muscle (Figure 1B).

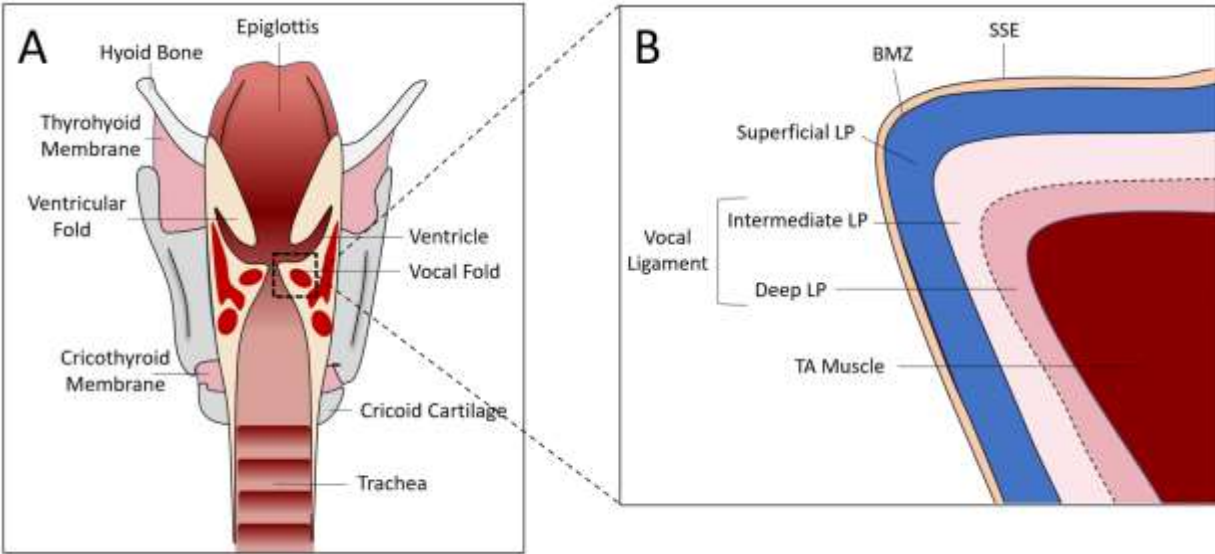


Figure 1. Coronal-section of the larynx and VF

1.2.1 Stratified Squamous Epithelium

Efficient voice production primarily depends on the unique layered structure of the VFs allowing for this specialized tissue to withstand amazingly rapid vibration (i.e. phonation), and extreme stress and strain during phonation and other biological processes. Each VF consists of 5-10 tightly packed layers of SSE^{23,24} (Figure 2A-C) which consist of integral protein complexes in the cell's membrane which function to maintain cellular homeostasis and barrier integrity. Integral membrane proteins contributing to the specialized function of the SSE are transepithelial ion channels and cell junctions.

Ion channels regulate the influx and efflux of positively and negatively charged molecules, serving multiple functions: regulating osmotic potential, providing energy for active transport, and driving cellular polarization and depolarization for cellular signaling. Sodium-potassium adenosine triphosphatase (Na⁺/K⁺-ATPase) is a transepithelial ion channel in the SSE believed to be involved in maintaining a thin layer of fluid on the VF epithelium, which contributes

to efficient VF oscillation and voice production.²⁵ This protein functions by using active transport to simultaneously pump three positively charged sodium ions out of the cell and two positively charged potassium ions into the cell, creating an osmotic gradient²⁶ This osmotic gradient is believed to contribute to passive water transport between cells via aquaporin (AQP) water channels (Figure 2 D).²⁷

Cellular junctions connect adjacent SSE cells and anchor the epithelial layer to the BMZ and underlying connective tissue, providing the first line of defense to the VFs. Two main types of cell junctions found in the VF SSE are tight junctions (TJ)s, and anchoring junctions (AJ)s. Tight junctions function by connecting and sealing the apical borders of adjacent SSE together, preventing any outside pathogens from entering the paracellular space.^{28,29} Examples of TJs in the VF include zonula occludin (ZO)-1 and occludin.³⁰⁻³³ Anchoring junctions in the VF, including e-cadherin, connect adjacent epithelial cells and also contribute to sealing paracellular spaces.³⁴ E-cadherin is also believed to facilitate the formation of TJs.³⁴ Other AJs, such as hemidesmosomes, connect the basal epithelium to the LP via fastening structures in the BMZ, attaching the SSE to the LP (Figure 2 D).³⁵

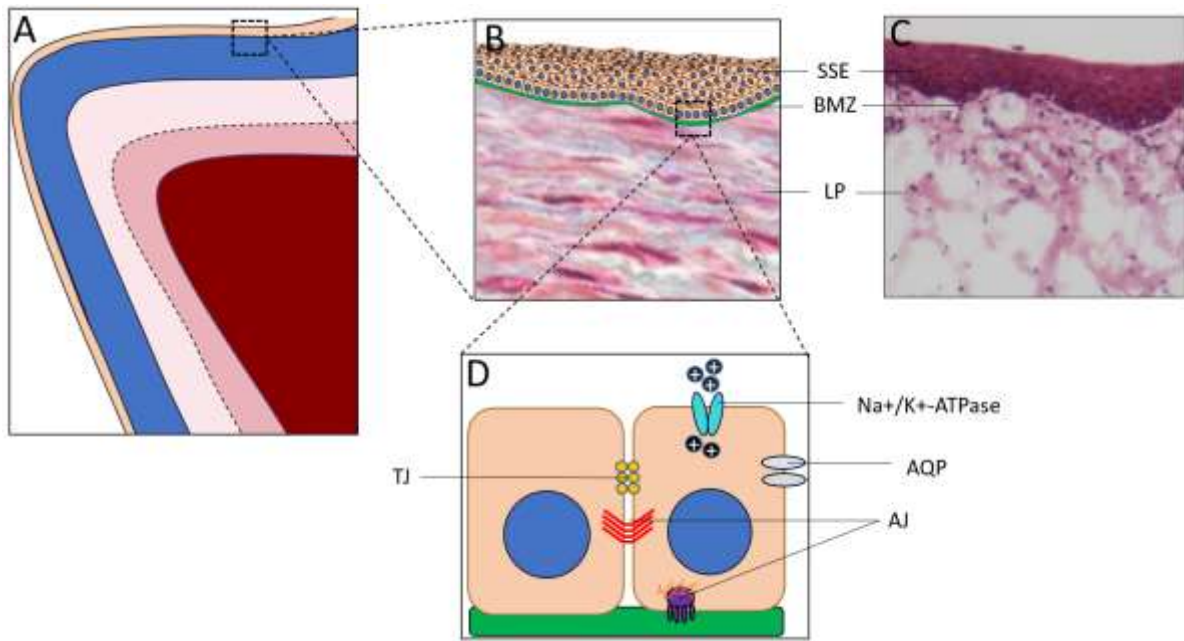


Figure 2. Coronal-section of the VF SSE

1.2.2 Lamina Propria

The LP is separated into three sections made up of the superficial, intermediate, and deep layers. These layers are distinctly characterized by their histological elements consisting of different concentrations of ECM components including collagen, elastin, and interstitial proteins. Collagen is an abundant fibrous protein that provides the tissue with tensile strength and functions as scaffolding for many cellular processes.³⁶ Elastin is essential for the elasticity and ability to stretch and recoil under the forces of phonation.³⁷ Interstitial proteins, including hyaluronic acid (HA), occupy the spaces within the ECM and acts as a shock absorber during the impacts of the VFs during phonation^{17,38,39} and are involved in cell proliferation, cell migration, and ECM organization.⁴⁰⁻⁴² Collagen and elastin are mostly organized parallel to the anterior/posterior plane of the VFs, with the density of distribution varying throughout the layers. The superficial layer of the VF has the least collagen and elastin, with loosely organized fibers interspersed throughout the

ECM.^{38,43} The superficial LP contains elastin in the form of eulanin and oxytalan, which are relatively brittle and fracture/reform with relative ease.^{38,44} The intermediate layer has the highest concentration of HA of the three layers⁴⁵ and is more densely concentrated with collagen and elastin than the superficial layer, with the elastin predominating over the collagen. Finally, the deep layer of the LP has the densest concentration of collagen and elastin, with collagen predominating.⁴⁶ The intermediate and deep layers of the LP comprise the vocal ligament, which attaches to the underlying TA muscle.⁴³

1.2.3 Thyroarytenoid Muscle

The TA is a paired skeletal muscle that is innervated by the recurrent laryngeal nerve, which contributes to the anterior-posterior shortening of the VFs, thereby decreasing tension in the covering layers and subsequently reducing speaking pitch.⁴⁷ Although an area of debate, it is speculated that different parts of the TA are responsible for different functions. For example, some researchers believe that the TA is separated into two parts; the lateral portion, called the muscularis, and the medial portion, called the vocalis. The muscularis consists of primarily type II fast-twitch muscle fibers and is reported to have roles in VF adduction and airway protection. The vocalis consists primarily of type I slow twitch muscle fibers^{48,49} and is believed to be the primary portion involved in modulating speaking pitch.^{49,50}

1.3 Physiology of Voice Production

The seemingly effortless production of voice is a complex physiological activity involving the coordinated activation of the respiration, phonation, and resonance systems. In order to produce adequate voice, it is necessary for these systems to work seamlessly in unison. The biomechanics of self-sustained VF vibration is the product of the composition of the VF layers and various aerodynamic principles.

Although the VF contains five unique layers as discussed in the previous section, it is often biomechanically simplified into two layers: the body - consisting of the stiffer TA and vocal ligament which remains, for the most part, stationary during phonation, - and the cover - consisting of the more pliable superficial LP and SSE, which moves separately over “the body” during phonation. The difference in the biomechanical properties and vibratory characteristics between the cover and body give rise to the characteristic vertical phase difference (known as the mucosal wave) during VF opening and closing, which is necessary for self-sustained VF vibration.⁵¹ As previously eluded to, the composition of collagen and elastin fibers in each layer differs to lend the biomechanical properties described.

Activation of the lateral cricoarytenoid, interarytenoid, and the TA muscles adduct the VFs to meet at the laryngeal midline. While approximated, the VFs obstruct airflow from the lungs, allowing for the buildup of subglottal pressure (Figure 3A). This accumulation of subglottal air pressure eventually overcomes the resistance of the folds (i.e. phonation threshold pressure), separating the VFs in an inferior to superior fashion to create a convergent glottal shape (Figure 3B). The lateral opening of the VFs continues until the natural elasticity of the tissue draws the VFs inward in a divergent shape. Additionally, the divergent glottal geometry results in airflow separation at the opening duct, producing intraglottal vortices (Figure 3C).⁵² These vortices are

believed to result in negative pressure that pulls the VFs to midline again, decreasing the airflow velocity and allowing for subglottal pressure to accumulate to repeat the vibratory cycle and sustain vibration for voice (Figure 3D).⁵³

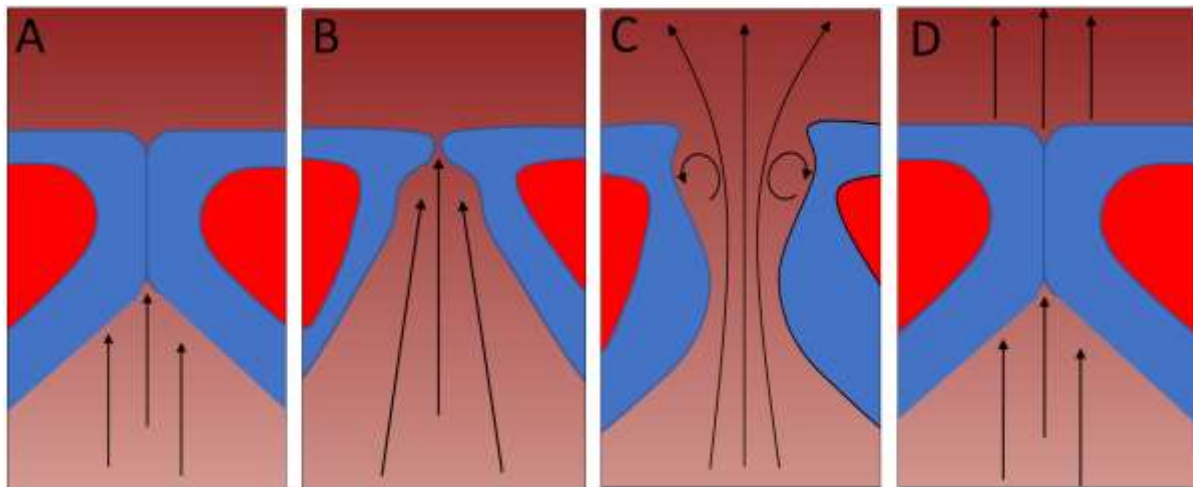


Figure 3. Cycle of phonation

1.4 Vocal Fold Injury

The VFs have the potential to be exposed to a variety of injurious stimuli including vibratory, surgical, and chemical trauma that often results in inflammation, lesions, and scarring of the mucosa and underlying tissue. These injuries often change the structure of the SSE and LP, resulting in changes in the biomechanical function of the VFs which can adversely affect healthy voice production.⁵⁴⁻⁵⁷ Vocal fold inflammation can result from a variety of different conditions including infections, laryngopharyngeal reflux, systemic inflammatory diseases, and mechanical VF injuries. A heightened laryngeal inflammatory response may exacerbate scarring,⁵⁸ which is the leading post-surgical contributor to poor voice quality.⁵⁶

1.4.1 Causes of VF Injury

Viral and bacterial infections are common sources of laryngitis and often result in acute laryngotracheobronchitis, which is characterized by inflammation of the subglottis and VFs resulting in a dry barking cough, hoarse voice, and inspiratory stridor.⁵⁹ Laryngopharyngeal reflux results from the retrograde flow of gastric contents into the laryngopharynx. This is often caused by insufficient closure of the upper and lower esophageal sphincters and ineffective esophageal peristalsis,⁶⁰ permitting digestive liquids such as hydrochloric acid and activated pepsin to enter the larynx and irritate the delicate VF tissue.

Systemic diseases that present with laryngeal inflammation include relapsing polychondritis, Wegener's granulomatosis, and rheumatoid arthritis. Polychondritis is rare a disease characterized by recurring episodes of inflammation of cartilaginous tissues. This disease affects the larynx in approximately 50% of cases and can cause dysphonia and airway stenosis.⁶¹ Wegener's granulomatosis is an autoimmune disease characterized by the systemic inflammation of the blood vessels including the small vessels and arteries in the airway, resulting in strider and subglottic stenosis.⁶² The laryngeal manifestation of rheumatoid arthritis may present as swelling of the arytenoid cartilage and/or rheumatoid nodules near the cartilage or other parts of the larynx.^{63,64}

Mechanical VF injuries can occur from loud or extended speaking situations where striking forces between the VFs are prolonged and/or increased. Although the VFs can withstand this stress to a high degree, a threshold exists where the mechanical stress of vibration overcomes the tissue integrity, resulting in phonotraumatic damage to the VFs and initiation of a full-scale wound healing response. Acutely, phonotrauma may present as VF inflammation. However, repeated phonotraumatic events may lead to scarring of the VF tissue or the development of benign lesions

such as VF nodules, polyps, and cysts.^{13,65-67} Mechanical VF injuries can also occur from surgical procedures performed to remove such lesions, resulting in damage to the SSE and LP, ultimately leading to VF scarring.⁶⁸

1.4.2 Wound Healing Cascade

To provide better treatment outcomes for patients with these injuries, it is necessary to understand the foundations of the dynamic wound healing process. Although literature regarding VF wound healing is still emerging, knowledge of the dermal wound healing process is relatively well established. The wound healing cascade can be divided into at least three overlapping phases; inflammation, proliferation, and tissue remodeling.⁶⁹ The inflammatory phase includes hemostasis, vasodilation, and infiltration of immune cells responsible for various healing functions. The infiltrating immune cells release proteins that initiate the proliferation phase, characterized by the growth of granulation tissue in the wound bed. During the remodeling phase, the collagen fibers reorganize, remodel, and mature to provide the tissue with tensile strength and functional competence.

1.4.2.1 Inflammatory Phase

The purpose of the inflammatory phase is to clean bacteria and debris from the injured area to prevent infection. Immediately after an injury, blood vessels are disrupted resulting in fluid leakage into the wound area. In response to the injury, the adrenal medulla releases epinephrine to constrict blood vessels, followed by platelets in the bloodstream binding to exposed collagen fibers in the sub-endothelium of the vessels to form a plug.^{70,71} The exposed molecules of the sub-endothelium, such as tissue factor, form a protein complex that initiates the coagulation cascade

resulting in thrombin formation. Thrombin, a principal enzyme of hemostasis, aggregates additional platelets to the site of vessel injury and converts fibrinogen into fibrin strands.⁷² Fibrin composes the provisional cross-links stabilizing the newly formed platelet plug to prevent blood from flowing out, achieving hemostasis.

During the first 24 to 36-hours following an injury, mast cells residing in nearby connective tissue release histamine. Histamine dilates blood vessels which causes the traditional redness, swelling, and heat associated with inflammation. The resulting increased vascular permeability allows immune cells, such as neutrophils, to slip through the vessel walls. Concurrently, various small proteins involved in cell signaling, called cytokines, are released from mast cells and platelets, including interleukins (IL), tumor necrosis factor (TNF), transforming growth factor (TGF)- β , and platelet-derived growth factor (PDGF), which induce cyclooxygenase (COX)-2 production - an enzyme that synthesizes prostaglandins that further promote platelet aggregation and initiate inflammatory cytokine release by immune cells.⁷³ These cytokines also chemoattract neutrophils which utilize the fibrin clot as scaffolding to infiltrate and clean bacteria and other foreign substances from the wound area.^{74,75} Once the bacteria have been removed, the neutrophils begin to die off.

Around 48 to 72-hours after an injury, many of the same cytokines that attracted neutrophils chemoattract other immune cells called monocytes.⁷⁶ Monocytes migrate to the wound area through dilated vessels and mature into macrophages, devouring damaged tissue debris and dead neutrophils in a process called phagocytosis.⁷⁴ Macrophages play a pivotal role in the following stage of wound healing by attracting and stimulating other cell types to initiate several tissue reconstructive tasks (Figure 4).

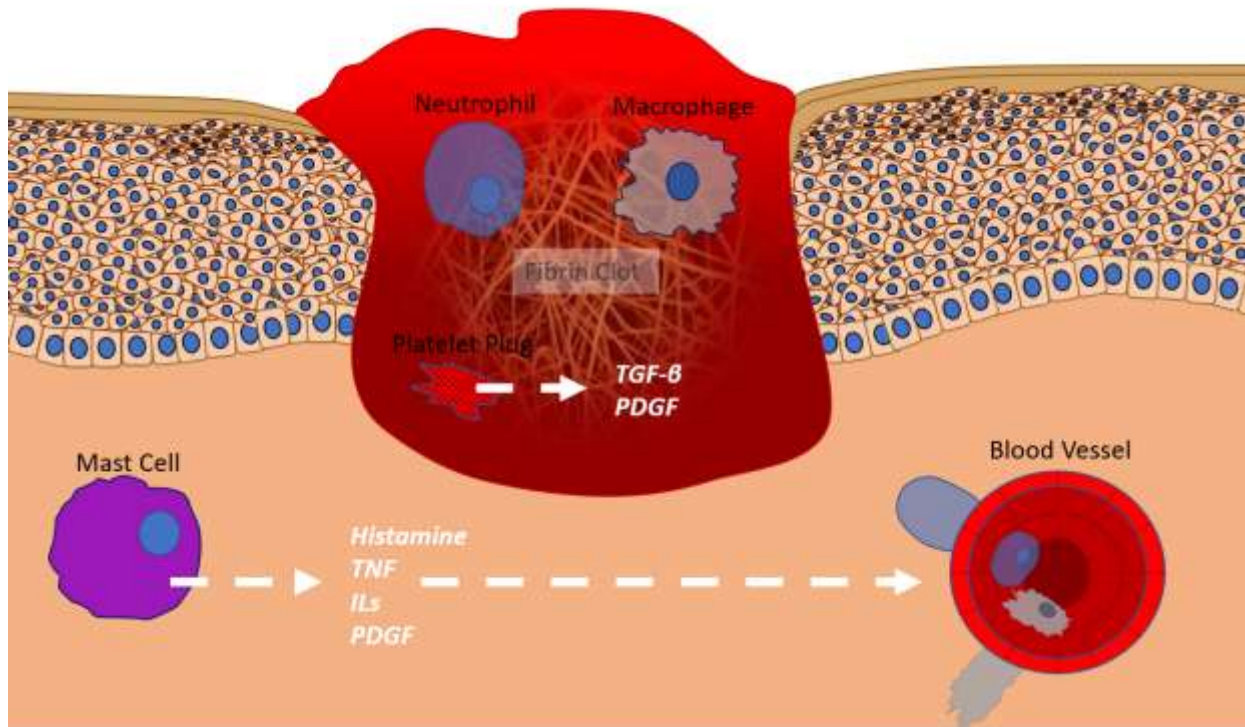


Figure 4. Illustration of the inflammatory phase of wound healing

1.4.2.2 Proliferation Phase

The inflammatory response sets the stage for the next phase in healing - the proliferation phase. The purpose of the proliferation phase is to supply blood and oxygen to the wound area and reestablish a protective barrier. This phase is characterized by the formation of pinkish granulation tissue, and begins 3 to 4-days post-injury, and lasts for about 2 to 3-weeks.^{69,76,77} Granulation tissue is comprised of macrophages, fibroblasts, and blood vessels and serves as the foundation for scar tissue development.⁶⁹ Macrophages supply a continuous source of growth factors such as vascular endothelial growth factor (VEGF) to induce the growth of new blood vessels in a process called angiogenesis. The newly formed vessels provide oxygen and nutrition to the growing tissue. Macrophages also release TGF-β and fibroblast growth factor (FGF) to recruit and proliferate fibroblasts to the wound site in a process known as fibroplasia.⁶⁹ Fibroblasts are responsible for

the production of the ECM components including collagen types I and III, fibronectin, elastin, and HA.^{66,78} Although the ECM components are immature and disorganized at this time, the ECM provides structural support for surrounding cells and provides a reservoir for cell migration, proliferation, and differentiation.^{66,74}

In healthy tissue, collagen type I constitutes approximately 80% of the collagens in the ECM, while collagen type III constitutes 10%.⁷⁴ However, during the proliferation phase, collagen type III is the main collagen type synthesized. The collagens bind to fibronectin in the ECM and predominantly replace the provisional fibrin scaffolding.⁷⁹

Fibroblasts also produce several growth factors that aid in tissue re-epithelialization. Re-epithelialization is the process of the re-establishment of a functional epithelial barrier through proliferation, migration, and differentiation of epithelial cells at the wound's edge and can only be accomplished in the presence of the living, vascular granulation tissue.⁸⁰ Fibroblasts and macrophages release keratinocyte growth factor (KGF) and TGF- α , respectively, to induce epithelialization by attracting and proliferating keratinocytes - the most prevalent cells of the epidermis.⁷⁷ The proliferating and migrating keratinocytes seal the wound site and create a BMZ that anchors down the epidermis to the dermal connective tissue. Epithelialization is usually complete in 3 to 4-days.^{81,82}

At about 2-weeks post-injury, the wound site continues to fill with granulation tissue, and the margins of the wound contract. Wound contraction is characterized by fibroblast differentiation to their myofibroblast phenotype, which has characteristics of both smooth muscle cells and fibroblasts. Myofibroblast cells bind to fibronectin in the ECM and connect to collagen fibers in the fibrin clot/granulation tissue, resulting in wound contraction (Figure 5).⁷⁴

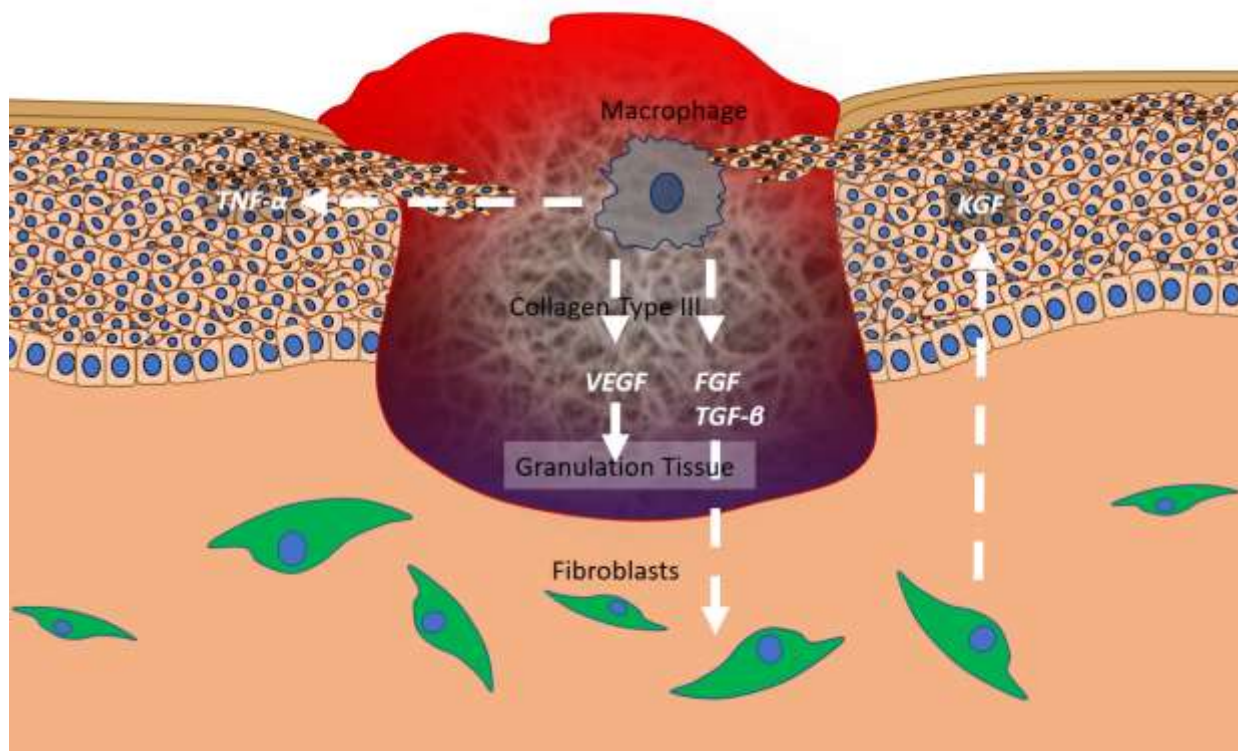


Figure 5. Illustration of proliferation phase of wound healing

1.4.2.3 Remodeling Phase

The remodeling phase begins with the replacement of the fibrin clot with granulation tissue and starts as early as 2 to 3-days after injury and can last as long as 2-years.⁸⁰ When wound closure commences, cells and capillaries from the granulation tissue that are no longer needed begin to thin out. Starting at about 3-weeks after injury, collagen type III undergoes degradation while the synthesis of the stronger collagen type I surges. The degradation and turnover of collagen are controlled by matrix metalloproteinases (MMP)s secreted by fibroblasts, epidermal cells, endothelial cells, and macrophages.⁸³ Collagen type I begins to arrange in a more favorable pattern, and the wound continues to contract.^{84,85} At the end of this phase, the wound is sealed with collagen-rich scar tissue that has only about 70% of the original strength as normal, non-damaged skin.⁶⁹

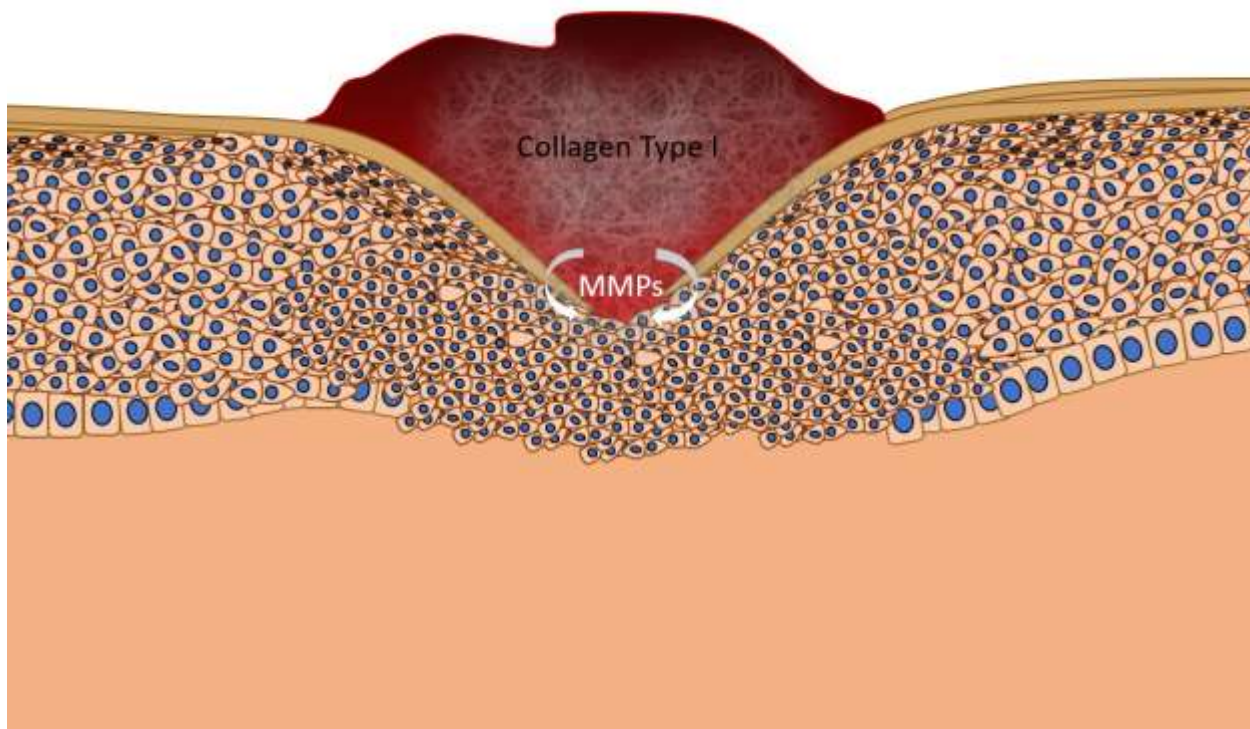


Figure 6. Remodeling phase of wound healing

1.4.3 Vocal Fold Wound Healing

The VFs differ from other tissue types in the human body due to their ability to withstand continuous sheering forces and stress during phonation without being compromised. There is a growing body of literature characterizing the wound healing cascade in VFs using a variety of experimental models to more precisely investigate the wound healing progression in this specialized tissue. Although limited studies have been conducted in human subjects, laryngeal secretions taken from a single subject after a 1-hour vocal loading task revealed increases in inflammatory and profibrotic mediators including IL-1 β , TNF- α , and MMP-8.⁸⁶ Other studies inducing VF injuries in animal models revealed similar findings regarding IL-1 β , TGF- β 1, COX-2,^{87,88} TNF- α ,⁸⁷ HA,⁸⁷⁻⁸⁹ MMP-1,^{90,91} MMP-9,⁹⁰ fibronectin, and collagen^{89,90} during the first 3-

days after injury. Increases in procollagen - a collagen precursor, and nuclear factor kappa B (NF- κ B) - a prototypical proinflammatory signaling pathway, were also observed.⁸⁷ Similar studies using animals also observed decreases in gene transcript levels of the epithelial cell junctions adhesion including occludin,⁹²⁻⁹⁴ tjp-1 (ZO-1 precursor), e-cadherin,^{93,94} and β -catenin⁹² in the days following injury. Branski et al.⁹⁵ observed complete epithelial coverage to occur by day five after iatrogenic injury in a rabbit model.

Regarding the proliferation and remodeling phases of VF injury, studies in various animal models revealed increases in collagen^{89,95-97} and fibronectin,⁹⁶ and decreases in HA^{97,98} approximately 2 to 3-weeks following VF injury. In the months following injury, increases in procollagen⁹⁹ and collagen^{96,100,101} and decreases in HA⁹⁶ and elastin¹⁰⁰ were observed. However, a study in rabbits revealed a decrease in collagen fiber density 2-months after injury.⁹⁹ A summary of these findings is displayed in Table 1. Although there is a paucity in the literature distinguishing the morphological differences between VF scar, nodules, polyps, and cysts, human VF nodule biopsies have demonstrated increased collagen deposition and increased fibronectin deposition,¹⁰² while polyps had less fibronectin deposition compared to nodules.¹⁰³

Table 1. Summary of temporal tissue changes in VFs after injury

	30m	1h	2h	4h	8h	16h	24h	72h	5d	7d	10d	2w	3w	4w	2m	3m	6m
ECM Components																	
Procollagen I & III								↑							↑		
Collagen							↑	↑				↑	↑	↑	↑	↕	↑
Elastin															↓		↓
Fibronectin							↑	↑				↑		↑			
HAS		↑		↑		↑		↕	↑		↓	↓		↓	↓		
Cell Junctions																	
ZO-1	↓						↓	↓									
E-cadherin	↓		↓		↓		↓			↓							
Occludin	↓		↓	↓	↓		↓	↓									
Inflammatory Mediators																	
NF-κβ				↑													
COX-2	↑	↑		↑	↑		↑						↔				
TGF-β1					↑	↑	↑	↑		↔							
TNF-α		↑			↑												
IL-1β		↑		↑	↑		↑	↑					↔				
MMP-1		↑		↑				↑									
MMP-8		↑															
MMP-9					↑			↑									

1.5 Glucocorticoids

Glucocorticoids are frequently prescribed off-label for the direct treatment of VF inflammation and scar due to their known anti-inflammatory properties in other indications. Glucocorticoids have been administered via various clinical approaches including inhalation, intramuscular injections, and intracordal injections to treat a variety of pathologies affecting the larynx. Intramuscular injections have been used effectively to treat laryngotracheobronchitis.^{104,105} Intracordal injections, which are injections delivered directly to the VF percutaneously, transnasally, or orally, are the most commonly used route¹⁰⁶ for the treatment of VF granuloma, scar,^{107–109} Reinke's edema,¹¹⁰ nodules,^{109,111–113} and polyps.^{109,112}

The principal effect of GCs is to reduce expression of multiple inflammatory cytokines that are stimulated during the inflammation process, including TNF- α ,^{76,114–116} TGF- β ,¹¹⁷ IL-1 β ,^{114–116,118} and IL-6.^{114–116,118} Suppression of these proteins attenuates VF edema, decreasing the effective mass of the tissue relative to an inflamed phenotype, allowing for easier phonation. If given at a high enough dose, GCs may also promote anti-inflammatory protein production, including IL-10,¹¹⁹ Annexin-1,¹²⁰ and inhibitor of NF- κ B (I- κ B).¹²¹ Although information regarding the precise mechanisms of GCs in VF tissue is still emerging, these mechanisms have been well established in other tissue types.

1.5.1 Glucocorticoid Mechanism of Action

During an injury or traumatic event, the body produces free endogenous GCs called cortisol. The basic actions of endogenous GCs are regulated by the hypothalamic-pituitary-adrenal axis. After an injury, neural, endocrine, and cytokine signals promote the hypothalamic secretion

of corticotropin-releasing hormone (CRH) into the anterior pituitary via a group of capillaries called the hypophyseal portal system.¹²² Corticotropin-releasing hormone induces the anterior pituitary to release corticotropin, inducing the adrenal glands to secrete cortisol systemically and eventually to the cells and tissue at the site of inflammation. Elevation of GCs in the bloodstream will attenuate the production of CRH in the hypothalamus through a negative feedback loop.¹²⁰

Cortisol passes through the plasma membrane of the cell and enters the cytoplasm, binding to the GC receptor (GCR). The GCR is present in almost all cells and plays a key role in the anti-inflammatory signaling pathway. Once bound, the GC-GCR complex dissociates from chaperone proteins, revealing specific binding domains enabling the protein complex to influence inflammatory gene expression via direct genomic, indirect genomic, and non-genomic mechanisms.

1.5.1.1 Direct Genomic Mechanism of Action

Direct genomic effects of GCs involve the GC-GCR complex entering the nucleus and dimerizing to become a chain of two identical proteins (i.e. homodimer). The homodimer binds to promoter regions of DNA called glucocorticoid-responsive elements (GRE), increasing the transcription of anti-inflammatory mRNA.^{119,123} The mRNA then exits the nucleus and codes for the translation and synthesis of specific anti-inflammatory proteins that inhibit inflammation induced by the original injury (Figure 7).

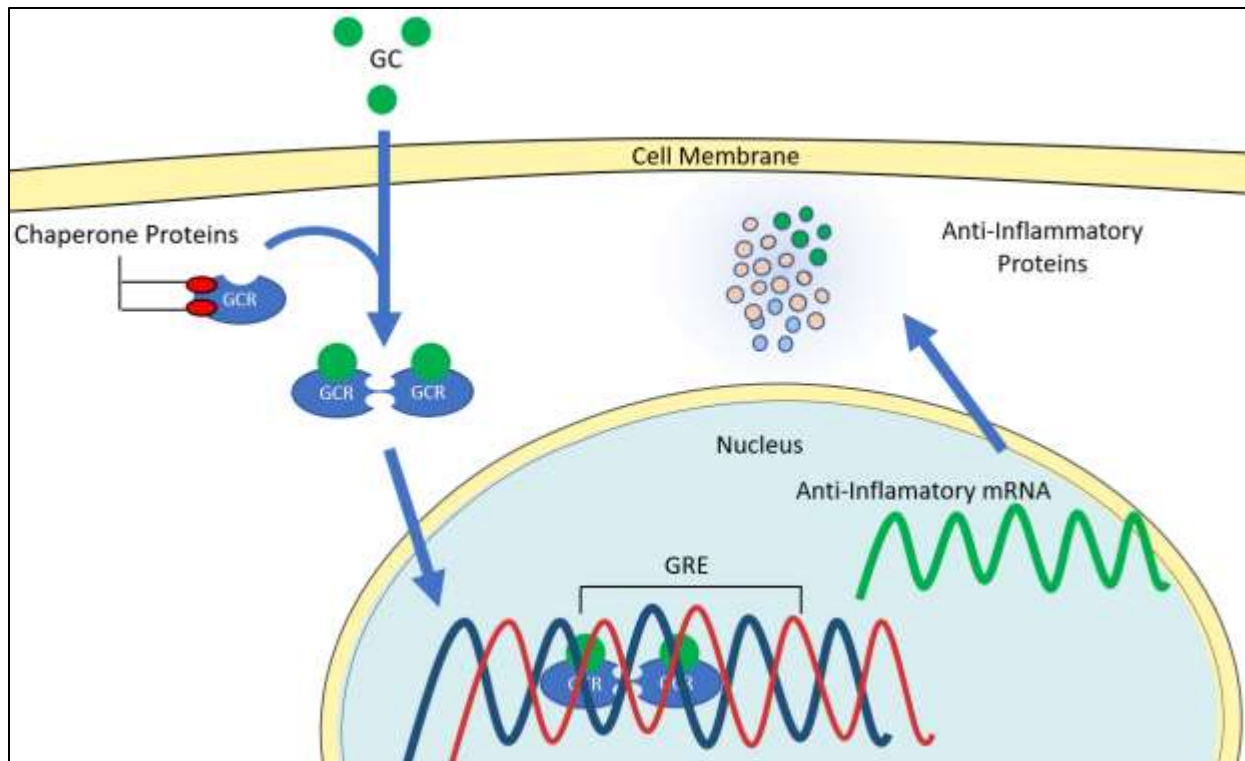


Figure 7. Illustration of the direct genomic mechanism of GCs

1.5.1.2 Indirect Genomic Mechanism of Action

Indirect genomic mechanisms of GCs also involve the GC-GCR complex entering the nucleus, homodimerizing, and interfering with NF- κ B genomic binding affinity. During the uninterrupted inflammatory process, the transcription factor NF- κ B typically binds to specific DNA sequences and transcribes inflammatory mRNA for downstream translation of inflammatory cytokines.¹²⁴ However, the GC-GCR complex interacts with NF- κ B and competes for DNA binding sites, inhibiting the binding affinity of NF- κ B and downstream production of inflammatory cytokines (Figure 8).^{125,126}

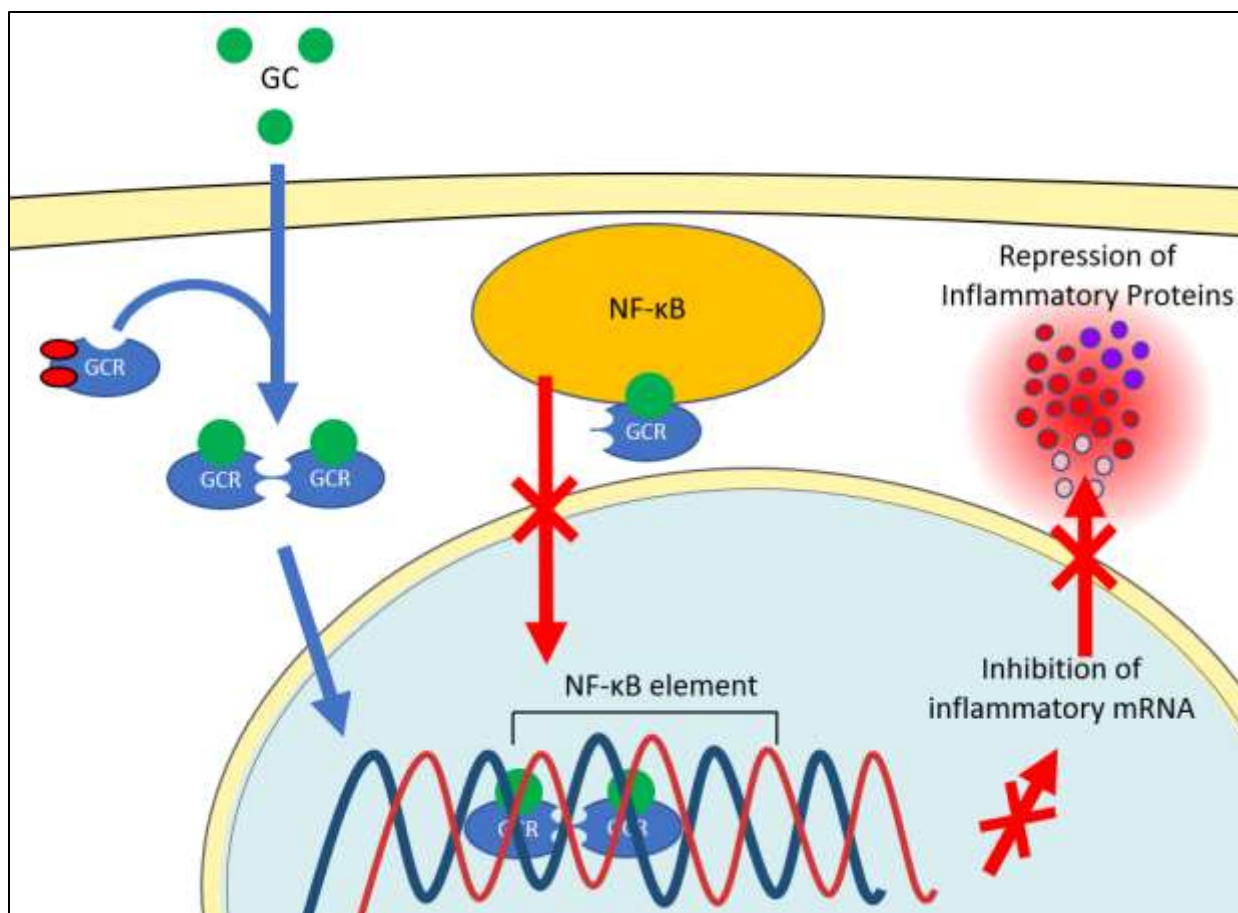


Figure 8. Illustration of the indirect genomic mechanism of GCs

1.5.1.3 Non-Genomic Mechanism of Action

Non-genomic mechanisms of GCs are less understood but are believed to occur in the cytoplasm of cells and at cell and organelle membranes. The mitochondria is a cell organelle that produces adenosine triphosphate (ATP), a chemical that provides energy for critical cell processes like cytokine synthesis, migration, and phagocytosis.¹²⁷ Glucocorticoids interact with the mitochondrial membrane to inhibit the metabolic process of ATP synthesis, thus suppressing immune cell processes essential for inflammation.¹²⁸ Cytosolic mechanisms of GCs involve the GC-GCR complex interfering with the synthesis of arachidonic acid (AA), a substance essential for several inflammatory chemotactic reactions.¹²⁹ This occurs by the GC-GCR complex inhibiting

phospholipase A2 release of AA from the cell membrane into the cytoplasm and inhibiting COX-2 from converting AA into inflammatory mediators, such as prostaglandins and leukotrienes (Figure 9).¹³⁰

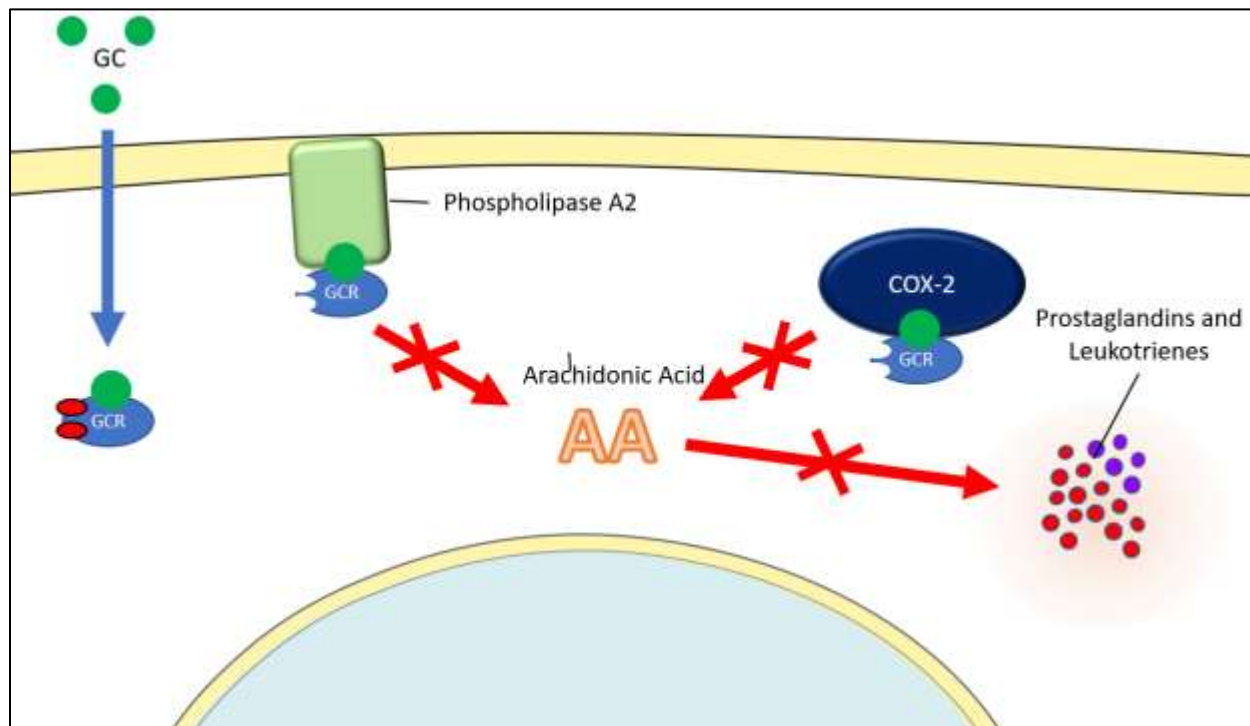


Figure 9. Illustration of the non-genomic mechanism of GCs in the cell cytoplasm

Glucocorticoids also disrupt membrane-bound T-cell receptors (TCR) in T lymphocytes, which are immune cells responsible for pro-inflammatory cytokine production. T-cell receptors recruit a multiprotein complex consisting of GCR, chaperone proteins, and lymphocyte-specific protein tyrosine kinase (LCK), which is critical for TCR signaling. Upon GC binding to the GCR, the multiprotein complex dissociates, reducing LCK enzymatic activities in the cytoplasm and impairing TCR signaling (Figure 10A-E).¹³¹

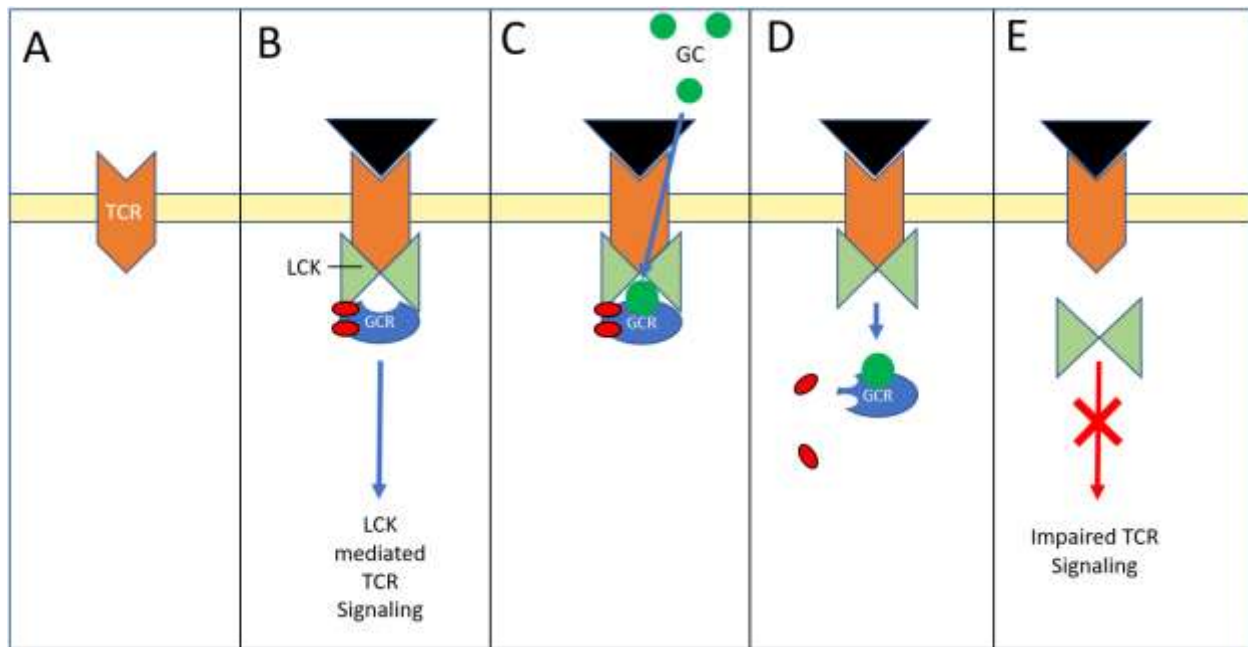


Figure 10. Illustration of the non-genomic mechanism of GCs in the cell membrane

1.5.2 Effects of Glucocorticoids on the Vocal Folds and Other Tissue

Glucocorticoids have varying pharmacodynamic properties including differences in drug potency, duration, and mineralocorticoid activity (Table 2) with effects ranging from reduced angiogenesis (decrease blood vessel production), changes in epithelial/endothelial barrier integrity, reduced therapeutic effect after long-term use, and skeletal muscle atrophy. For example, studies of prednisolone treatment in a juvenile porcine model observed fewer and disorganized capillaries in tibia growth plates.¹³² Similarly, capillary shrinkage occurred in cultured bone endothelial cells after hydrocortisone treatment¹³³ as well as reduced endothelial proliferation and capillary density in rabbit and human brain tissue after betamethasone treatment.¹³⁴ In airway tissue, the number of vessels in bronchial biopsies decreased after 6-weeks of high dose fluticasone propionate.¹³⁵

Long-term cortisol treatment has also been observed to reduce epidermal barrier function in human^{136,137} and mouse¹³⁶ epidermal cells. Conversely, GC's have also been observed to improve epithelial and endothelial barrier integrity, as demonstrated by improved barrier function in intestinal epithelium^{138,139} and brain endothelium.^{133,140–146} In the context of VF and airway tissue, rabbits treated with a high dose of triamcinolone showed reduced TJ expression, which may lead to a compromised VF epithelial barrier.¹⁴⁷ However, the authors also observed increases in VF TJ expression in rabbits treated with a low dose of triamcinolone, which has also been observed in dexamethasone-treated cultured human tracheal epithelium.¹⁴⁸

Many inflammatory conditions require long-term GC treatment, which has the potential to result in GC resistance and reduced therapeutic effect. A reduced therapeutic effect is believed to be in part due to down regulation of the GCR due to chronic exposure,¹⁴⁹ as demonstrated in patients given repeated doses of prednisone to treat inflammatory bowel disease,¹⁵⁰ and Nephrotic syndrome.¹⁵¹ Additionally, researchers have also observed a positive correlation between GCR level and response to GC therapy when treating leukemia.¹⁵² A small number of patients who suffer from severe asthma are resistant to GC treatment.^{153,154} This insensitivity is believed to be partially due to inherently lower GCR expression levels in the airway smooth muscle in this population, rather than GC-induced resistance.¹⁵⁵

Although the exact mechanisms of GC effects on TJ, angiogenesis, and GCR are still being elucidated, the underlying molecular mechanisms of GC-induced atrophy are better understood.^{156,156,157} Many catabolic conditions resulting in muscle atrophy (e.g. sepsis, cachexia, starvation, and metabolic acidosis) are characterized by increased GC levels.¹⁵⁸ Additionally, catabolic responses in skeletal muscle have been observed after GC treatment *in vitro* and *in vivo*. The use of intracordal injections of GCs for various laryngeal indications has been associated with

atrophy of the TA muscle of the VFs. For example, a series of prospective case studies observed VF atrophy in two subjects receiving a weekly injection of dexamethasone for 5 and 6-weeks respectively, resulting in perceived breathy dysphonia and incomplete glottal closure.¹⁵⁹ Additionally, intracordal injection of triamcinolone in rabbits showed increased degrees of TA muscle atrophy in the weeks following treatment.¹⁶⁰ These findings are also supported by anecdotal evidence of VF atrophy following intracordal injections.¹¹³

Table 2. Anti-inflammatory and biological half-life properties of GCs

Drug	Anti-Inflammatory Strength	Biologic Half-life (Hours)
Hydrocortisone	1	8-12
Cortisone	0.8	8-12
Prednisone	4	12-36
Prednisolone	5	12-36
Methylprednisolone	5	12-36
Triamcinolone	5	12-36
Betamethasone	25	24-72
Dexamethasone	25	24-72

1.5.2.1 Mechanisms of Glucocorticoid-Induced Atrophy

As discussed in section 1.5.1, the initial mechanism of action of GCs involves the GC entering the cell membrane and binding the GCR. The GC-GCR complex then enters the nucleus and homodimerizes and binds to GRE, increasing the transcription of mRNA that has inhibitory effects on muscle growth. Glucocorticoids also directly induce stimulatory effects on the Ubiquitin-Proteasome System (UPS) to increase muscle protein breakdown. To fully elucidate the

mechanistic action of this process, it is first necessary to understand the process of healthy muscle growth and renewal.

1.5.2.1.1 Systems Involved in Synthesis and Degradation of Muscle

Myofibrillar proteins are fundamental for the normal growth and renewal of muscle cells (i.e. myocytes). Muscle size is controlled by balanced rates of myofibrillar protein synthesis and degradation,¹⁶¹ and the maintenance of a healthy balance of myocytes is regulated by the IGF-I/PI3K/Akt/mTOR signaling pathway and the UPS.¹⁶² IGF-I/PI3K/Akt/mTOR signaling is a widely studied molecular pathway of muscle growth and renewal and begins with insulin-like growth factor-I (IGF-I) binding to its receptor (IGF-R) and activating insulin receptor substrate (IRS)-1. The IRS-1 activates phosphatidylinositol-3-kinase (PI3K), which is an enzyme responsible for the conversion of phosphatidylinositol-(4,5)-bisphosphate (PIP₂) to phosphatidylinositol-(3,4,5)-trisphosphate (PIP₃) - a substrate involved in many downstream signaling pathways required for cell growth.¹⁶³ Once PIP₃ is activated, it stimulates protein kinase B (Akt) and the mammalian target of rapamycin (mTOR), which initiates ribosomal protein S6 kinase beta-1 (S6K1) to activate factors that induce mRNA translation for muscle protein synthesis.¹⁶⁴

In contrast to the IGF-I/PI3K/Akt/mTOR pathway, the UPS is responsible for identifying and destroying damaged or excess proteins to support homeostasis.¹⁶⁵ The process of the UPS begins with E1 ubiquitin (Ub)-activating enzyme binding to Ub - an abundant protein found in almost all eukaryotic cells. Ub is then transferred to a second enzyme, E2 Ub-conjugating enzyme, which escorts Ub to the E3 ligase enzyme.¹⁶⁵ E3 ligase enzymes recognize and bind to a target protein and act as a platform for the E2-Ub complex to transfer Ub to the target protein.¹⁶⁶ This process is repeated to produce a polyubiquitin chain attached to the target protein. A protein complex responsible for breaking down proteins, called a proteasome, recognizes and binds to the polyubiquitin chain. The target protein is released from the polyubiquitin chain, unfolded, and

catalyzed for entry into the proteasome where protein degradation occurs.¹⁶⁷ This highly regulated system assures that ubiquitin is specifically attached to target proteins to avoid unintended protein destruction.

Although most eukaryotic cells only contain a single type of E1 enzyme, they have several types of protein-specific E3 ligases.¹⁶⁸ Different E3 ligases recognize and bind to different target proteins. Muscle-specific E3 ligases include muscle atrophy F-box (also known as atrogin-1) and muscle RING (really interesting new gene) Finger-1 (MuRF-1),¹⁶⁹ and their corresponding genes have been upregulated in several atrophy models. For example, De Boer et al.¹⁷⁰ investigated muscle cross-sectional area (CSA) and MuRF-1 gene expression of leg muscle biopsies from men subjected to unilateral lower leg suspension for 23-days. On day 10, rates of myofibrillar protein synthesis and muscle fiber size significantly decreased, and MuRF-1 mRNA significantly increased compared to baseline measures. Similarly, increases in MuRF-1 and atrogin-1 mRNA in hind leg biopsies have been observed in the days and weeks following experimentally applied limb immobilization.^{171,172} Other studies in humans showing increases in atrophy associated genes resulting from muscle unloading or immobilization¹⁷³ are supported by increases in these genes in animal models subjected to atrophic conditions such as hind limb suspension,¹⁷⁴ denervation,^{174,175} cachexia,¹⁷⁶ and spinal cord transection.¹⁷⁷ To further support evidence of the role of these genes in muscle atrophy, mice genetically modified to lack atrogin-1 and MuRF-1 were resistant to muscle atrophy after being subjected to hind leg denervation.¹⁷⁴

A major protein involved in stimulating the UPS and inducing atrogin-1 and MuRF-1 production is myostatin.¹⁷⁸ Myostatin is a protein that is prevalent in the muscle ECM, but typically remains inactive in healthy tissue.¹⁶⁴ When activated in atrophic conditions, myostatin binds to its receptor and directly stimulates Smad3¹⁷⁹ and indirectly stimulates FoxO through Akt

suppression.¹⁷⁸ These transcription factors then translocate to the nucleus to induce the expression of atrogin-1^{180,181} and MuRF-1,^{181,182} increasing proteolysis of myofibrillar proteins resulting in muscle degradation and atrophy.¹⁸³ Myostatin has been observed to be increased in conditions of atrophy. For example, patients receiving anterior cruciate ligament reconstruction had increased levels of circulating myostatin in their blood up to two weeks after surgery compared to presurgical measures.¹⁸⁴ In more controlled experiments using animal models, rats subjected to 17-days of zero gravity space flight displayed a 24% decrease in skeletal muscle mass associated with up to 5-fold increases in myostatin mRNA and protein,¹⁸⁵ with similar findings observed in a separate study subjecting rats to 10-days of hind leg unloading.¹⁸⁶

1.5.2.1.2 Inhibitory Effects

The inhibitory effects of GCs involve disrupting the transport of essential amino acids across the plasma membrane of myocytes, likely preventing the synthesis of proteins necessary to support muscle growth.¹⁸⁷ Glucocorticoids also inhibit the activating action of IGF-I on muscle growth and renewal, which reduces the downstream synthesis of proteins and muscle growth through suppression of IGF-I/PI3K/Akt/mTOR signaling (Figure 11). This has been shown in studies involving mice receiving 5-daily injections of triamcinolone or methylprednisolone, revealing decreased IGF-I mRNA and muscle mass compared to pair-fed controls.¹⁸⁸ Studies in humans receiving daily oral dexamethasone for 4-days reveal decreased levels of skeletal muscle IGF-I mRNA expression from leg muscle biopsies compared to biopsies taken pre-GC administration.¹⁸⁹ Additional evidence of inhibitory effects of GCs include GC mediated decreases in IRS-1, an upstream component of the PI3K/AKT/mTOR pathway responsible for protein synthesis.¹⁹⁰

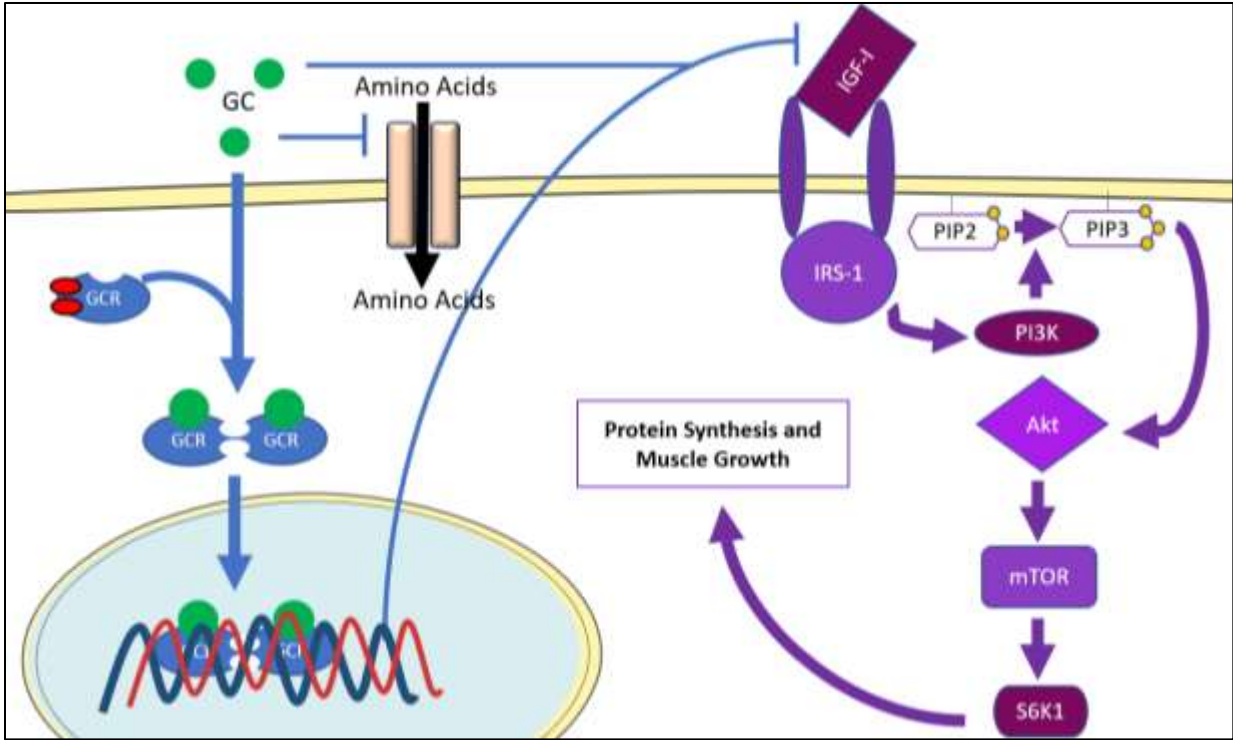


Figure 11. Inhibitory effect of GCs on protein synthesis and muscle growth

1.5.2.1.3 Stimulatory Effects

The stimulatory effects of GCs are believed to involve activation of the UPS primarily through the stimulation of myostatin (Figure 12).¹⁹¹ Myostatin has been found to be upregulated *in-vitro* in human cell lines¹⁹² and *in-vivo* in mice¹⁹³ after dexamethasone treatment. For example, mice treated with dexamethasone showed myofibrillar disorganization and degradation accompanied by increased myostatin gene expression.¹⁹⁴ To further support the role of myostatin in regulating muscle growth, a study in mice lacking the myostatin gene were resistant to muscle atrophy after dexamethasone treatment compared to wild-type mice.¹⁹⁵ These marked GC-induced shifts in myostatin are thought to stimulate the previously described downstream targets that induce muscle protein degradation,¹⁹¹ as demonstrated by increases in MuRF-1^{195,196} and atrogin-1¹⁹⁵⁻¹⁹⁷ gene expression and decreases in muscle fiber area measures in rats receiving dexamethasone treatment.^{188,196,197}

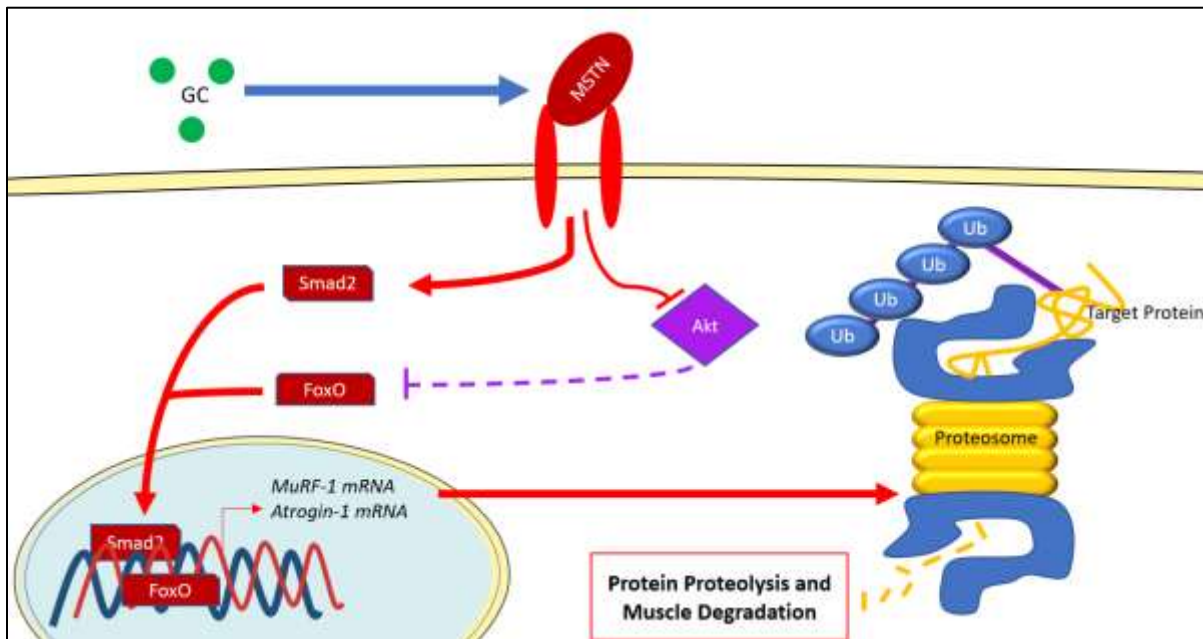


Figure 12. Stimulatory effects of GCs on protein proteolysis and muscle degradation

1.6 Specific Aims

To better understand human VF physiology and explore treatments for voice disorders, various animal models have been used. Although no other animal shares the identical tissue layered structure of the VFs compared to humans, in the absence of fresh procurement of human donor larynges, animal models provide a reasonable approximation and opportunity for the study of conserved proteins between species on the regulation of VF homeostasis. Animal larynges are also generally more accessible than fresh human larynges and offer reasonable advantages in the control of extraneous environmental variables, as well as better access to tissue primers and antibodies for routine molecular biological assays.

Preference for animal models broadly depends on the specific research questions being addressed. For example, canine larynges are commonly used in excised larynx experiments due to similarities in laryngeal size and gross tissue structure compared to human larynges.¹⁹⁸ However, the use of canines in histological studies has relative disadvantages due to differences in layered structure and tissue biomechanical properties.¹⁹⁹ Other comparably sized animal models, such as porcine, offer relative advantages to canine models due to similarities in collagen and elastin distribution with human VFs.^{198,200,201} However, porcine VF tissue is not as well characterized as rabbit, mouse, and rat VFs, and pigs can be inherently more challenging to work with within the experimental setting. Smaller animal models such as rabbits, mice, and rats have been widely used due to their ease of procurement and handling.

Due to the relative advantages of smaller species, there has been a growing body of work using the rabbit as a small animal solution for studies of VF tissue biology. Our lab has developed an *in-vivo* rabbit model^{33,202-205} to investigate the biological characteristics of VF tissue. Rabbits demonstrate similarities to humans relative to VF tissue microarchitectural properties and ECM

components.^{99,206,207} The rabbit is an innately quiet animal, allowing for increased control over unsolicited vocalizations outside of the research setting.²⁰² Rabbits also provide the relative advantage of being easier to handle and more affordable than larger species.^{101,208} Information about proteins involved in the regulation of VF tissue homeostasis is still evolving in rabbits. However, their advantageous characteristics make them a useful model when investigating research questions related to the safety and efficacy of current pharmacological treatments used to treat voice disorders, such as GCs.

Glucocorticoids are commonly used as off-label treatments for a wide variety of voice disorders due to their potent anti-inflammatory and anti-fibrotic properties.^{209–211} While these immunomodulatory properties have made GCs an attractive therapeutic within otolaryngology, it remains unclear how GCs induce physiologic changes within the VF tissue. Glucocorticoids have been administered using a variety of different routes including intramuscular and intracordal injections to treat various laryngeal diseases, which have been associated with off-target effects including VF atrophy to the injected area.^{113,159,160} Despite the known diversity of drug activity and associated negative effects, otolaryngologists reported that they typically rely on subjective clinical judgments when prescribing GCs, such as familiarity with the drug, rather than objective evidence of differential efficacy.²⁰⁹

The purpose of this study was to identify the localization of key VF constituents in rabbit and human VFs, as well as understand and characterize the temporal effects of acute GC treatment on the VF tissue. Characterization of GC-induced tissue changes in the VFs, especially any differential effects between GCs, is necessary for physicians to better understand the utility of GCs and to accurately modify drug selection for patient-specific needs.

The specific aims and hypotheses for this study were as follows:

Aim 1: Compare the localization of integral membrane proteins including Na⁺/K⁺-ATPase, AQPs, e-cadherin, ZO-1, and occludin in human and rabbit VF tissue. The following hypothesis was investigated: Integral membrane proteins will be similarly localized between species.

Aim 2: Investigate the acute effects of intramuscular dexamethasone and methylprednisolone injections on TA muscle morphology and the fluorescence expression of ZO-1, vascularity marker cluster of differentiation (CD)31, and GCR in rabbit VFs. The following hypotheses were investigated: Due to differential mechanisms of action, dexamethasone will increase ZO-1 expression compared to controls, while methylprednisolone will decrease ZO-1 expression compared to controls. Both GCs will decrease CD31, GCR, and TA muscle fiber CSA compared to controls.

Aim 3: Investigate the effects of an intracordal injection of dexamethasone on atrophy-associated gene expression, including MuRF-1 and atrogin-1, and TA muscle morphology in rabbit VFs. The following hypotheses were investigated: Dexamethasone-treated VFs will show increases in transcription levels of atrophy associated genes and decreases in TA muscle fiber CSA in comparison to saline-treated VFs and untreated controls.

1.6.1 Power Analyses

Statistical power analyses were conducted *a priori* to determine an adequate sample size to address the proposed hypotheses in aims 2 and 3. The expected effect sizes of $f = 0.9$ and 1.5 were used and based on preliminary fluorescence expression changes in relevant proteins following GC treatment, and previously published reports of changes in atrophy-associated gene

expression and muscle CSA, respectively.^{197,212} Based on these relative effect sizes, a sample size of five VF specimens per condition will allow the study to achieve 80% power ($\beta = 0.20$) for detecting differences between conditions, at an adjusted alpha level of $p = 0.001$ for aim 2, and $p = 0.016$ for aim 3. This sample size has also been used to achieve adequate power in our previous studies and similar reports in the literature.^{88,90,213–217}

2.0 Methodology

2.1 Human Tissue Procurement

Five human donor larynges (1 Male; 4 Female) ranging from 27 to 83 years of age (\bar{x} = 52; SD = 23.8) were procured by pathologists from the Cooperative Human Tissue Network. The samples were harvested within 24-hours of each donor's death and transported to Vanderbilt University Medical Center (Nashville, TN). Each VF was determined to be healthy and absent of any gross tissue abnormalities by an otolaryngologist. The left VF from each specimen was mounted and flash-frozen in Optimal Cutting Temperature (OCT) compound.

2.2 Animal Surgical Procedures

A total of 65 male New Zealand white rabbits weighing 2.6 to 3.6 kg (\bar{x} = 2.97; SD = 0.22) were used for these experiments. All procedures in these experiments were approved by the Vanderbilt Institutional Review Board, #170371, and by the University of Pittsburgh Institutional Animal Care and Use Committee Institutional Review Board, #417962 and in compliance with the Animal Welfare Act and Guide for the Care and Use of Laboratory Animals²¹⁸

2.2.1 Intramuscular Injections

Forty-five rabbits were randomized to receive intramuscular injections to the iliocostalis/longissimus muscle of 4.5mg of methylprednisolone (n = 15), 450 μ g of dexamethasone

(n = 15), or volume matched saline (n = 15) for six consecutive days. Doses were based on the typical dosing range for GC intramuscular injections, which are between 1-9 mg for dexamethasone²¹⁹ and 10-90 mg for methylprednisolone.²²⁰ Based on these standard human doses for each drug, the dose for rabbits was calculated based on weight (human: 60 kg, rabbit: 3 kg).

2.2.2 Intracordal Injection

An additional 10 rabbits were sedated with intravenous (IV) ketamine (0.06 mg/kg) and dexmedetomidine (7.5 mg/kg) via the marginal ear vein. Once sedated, the animals were placed on the surgical platform in the supine position and shaved from the submentum down to the chest. Artificial tears were applied to the eyes to prevent drying and the eyes were taped closed. Heart rate, blood pressure, respiratory rate, body temperature, and spot oxygen saturation (SpO₂) were monitored every 15-minutes throughout the procedure. The neck was sterilized with a minimum of three applications of iodine and isopropyl alcohol. At this point, the lead surgeon observed an aseptic technique to ensure a sterile field. A pediatric laryngoscope and 0° 4-mm rigid endoscope was inserted into the mouth by the non-sterile assisting surgeon to visualize the VFs. Five rabbits were randomized to receive bilateral percutaneous VF injection with either 40µl of dexamethasone (10 mg/ml) or volume matched saline using a 30-gauge Exel Comfort Point Micro Syringe utilizing the trans-cricothyroid membrane approach (Figure 13). Once the injections were complete, rabbits received an IV injection of Atipamezole (0.5 mg/kg) and were recovered and returned to their cage.

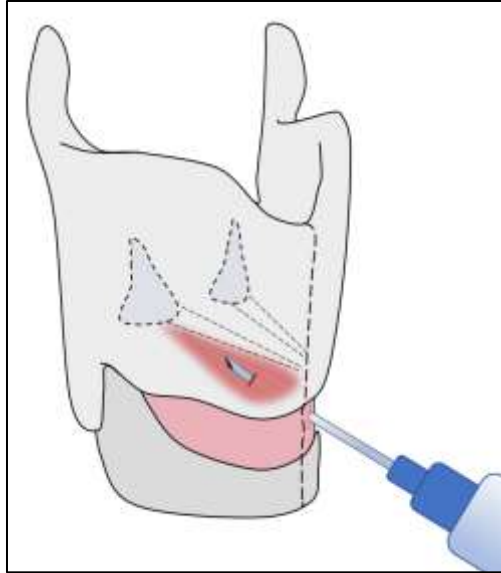


Figure 13. Percutaneous VF injection using the trans-cricothyroid membrane approach

2.2.3 Rabbit Vocal Fold Tissue Acquisition

All rabbits were sedated with ketamine (20 mg/kg) and dexmedetomidine (0.125 mg/kg) via intramuscular injection into the iliocostalis/longissimus muscle. Heart rate, blood pressure, respiratory rate, body temperature, SpO₂ were monitored throughout the procedure to assess the animals' state of sedation and general well-being. Once sedated, the animals were placed on the surgical platform in the supine position and shaved from the submentum down to the chest. Lidocaine was subcutaneously injected along the midline of the shaved region to locally anesthetize the incision area. The larynx and trachea were exposed by an incision along the midline from the sternal notch to the hyoid bone. Once the larynx and trachea were exposed, the animal was euthanized via IV injection of sodium pentobarbital (390 mg/kg). Once euthanized, the entire larynx was excised and hemisected. For the five larynges being used for human comparison, the left half of each larynx was mounted in OCT medium.

The 45 rabbits receiving intramuscular GC injections were sedated and euthanized as previously described either 1-day following termination of GC injections (n = 15), 3-days following termination of injections (n = 15), or 7-days following termination of injections (n = 15) Larynges were excised and hemisected, and the right half was fixed in formalin for Hematoxylin and Eosin (H&E) staining, and the left half was fresh frozen in OCT medium for immunolabeling (Figure 14).

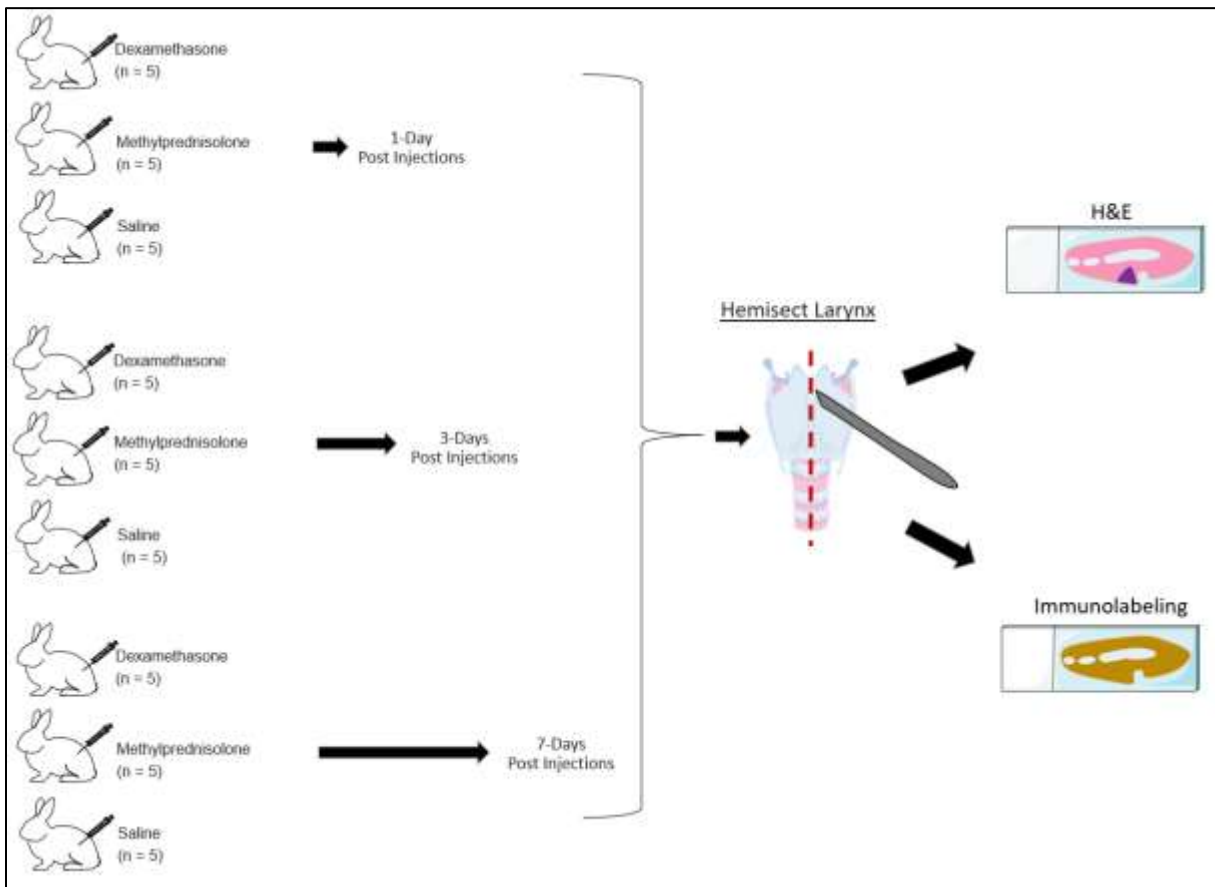


Figure 14. Schematic of experimental paradigm for rabbits receiving intramuscular injections

For the 10 rabbits receiving intracordal injections, animals were survived 7-days post injections, and then humanely sacrificed as described previously. Larynges were excised and

hemisected (Figure 15), and the right half was stored in 10% neutral buffered formalin and the TA muscle was placed in RNAlater Stabilization Solution™ and stored at -20°C until further processing.

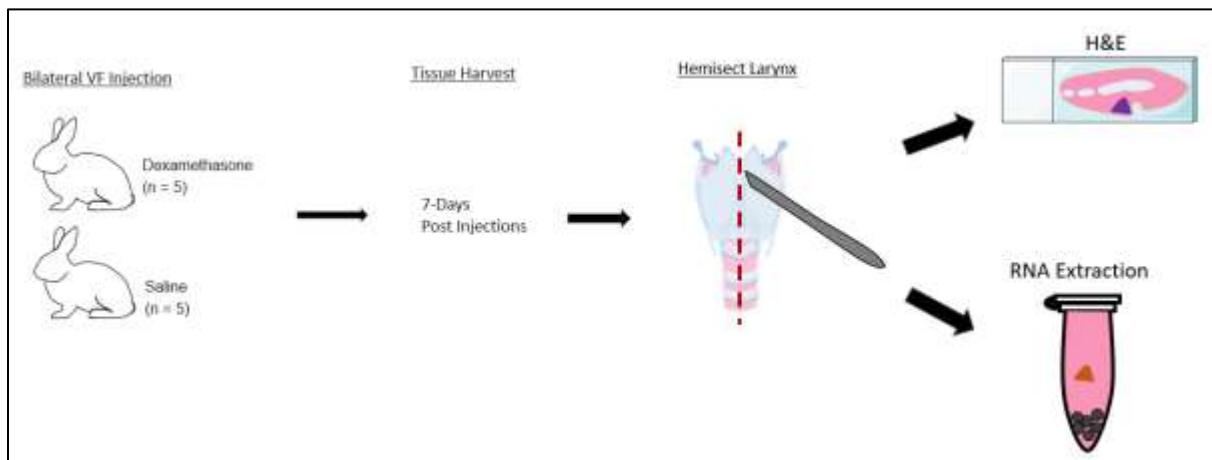


Figure 15. Schematic of experimental paradigm for rabbits receiving intracordal injections

2.2.4 Frozen Vocal Fold Tissue Sectioning

Frozen OCT blocks of all VF samples were sectioned in the coronal orientation at 12 μ m thickness using a Leica CM1900 cryostat and mounted onto positively charged slides. Samples were stored at -80°C until further processing.

2.2.5 Paraffin Embedded Vocal Fold Tissue Sectioning

A Leica™ TP1020 Automatic Tissue Processor was used for paraffin embedding. Formalin-fixed VF samples were inserted into the tissue basket and dehydrated in increasing concentrations of ethanol (70%; 80%; 96%; 100%; 100%, 100%) for equal durations of 1.5-hours

in each concentration. Samples were then cleared in two 1.5-hour baths of xylene and then in two 2-hour baths of paraffin wax. The VFs were placed in a tissue mounting cassette and embedded in paraffin wax. Once hardened, the paraffin blocks were sectioned in the coronal orientation at 10 μ m using a Leica™ HistoCore BIOCUT microtome. Once sectioned, the tissue was floated in a Leica™ HI1210 heated water bath and adhered to positively charged slides. Slides were stored at room temperature until further processing.

2.2.6 Immunofluorescence Labeling

Immunofluorescence labeling was performed in triplicate per sample using primary antibodies against AQP1 (Santa Cruz Biotechnology Cat# sc-70371), AQP4 (Santa Cruz Biotechnology Cat# sc-390636), AQP7 (Santa Cruz Biotechnology Cat# sc-376407,) alpha subunit Na⁺/K⁺-ATPase (Abcam Cat# ab7671), e-cadherin (BD Biosciences Cat# 610182), ZO-1 (Innovative Research Cat# 33-9100), occludin (Santa Cruz Biotechnology Cat# sc-271842), CD31 (Novus Cat# NB600-562), and GCR (Abcam Cat# ab2768). Samples labeled for AQP4, AQP7, e-cadherin, ZO-1, occludin, CD31, and GCR were fixed in methanol for 10-minutes at -20°C. These were washed in three changes of phosphate-buffered saline (PBS) for 5-minutes per wash and permeabilized in 200 μ l of Triton X-100 (diluted 1:1000 in PBS), and then washed in one change of PBS for 5-minutes. Samples labeled for AQP1 and Na⁺/K⁺-ATPase were fixed and permeabilized in acetone for 10-minutes at -20°C and then washed in three changes of PBS for 5-minutes per wash. For antigen blocking, samples in all conditions were blocked in 200 μ l of 10% goat serum for 1-hour at room temperature. After blocking, samples were treated with 200 μ l of the appropriate primary antibody diluted 1:100 in 1% goat serum for 1-hour at room temperature (RT) and then washed in three changes of PBS. For secondary antibody treatment, Alexa Fluor®

594 Goat anti-Mouse Immunoglobulin G conjugate (Molecular Probes Cat# A-11032) in 1% goat serum was used (dilution 1:500) and incubated for 1-hour in the dark at RT. Samples were washed in three changes of PBS. Samples labeled for AQP1 and Na⁺/K⁺-ATPase were incubated in 200 µl 4',6-diamidino-2-phenylindole (DAPI) (Thermo Fisher Scientific Cat# D1306) (dilution 1:50) for 5-minutes in the dark at RT. Samples were washed in three changes of PBS and mounted under glass coverslips using Vectashield[®] Mounting Medium (Vector Laboratories Cat# H-1000). Samples labeled for AQP4, AQP7, e-cadherin, ZO-1, occludin, CD31, and GCR were mounted under glass coverslips using Vectashield[®] Mounting Medium with DAPI (Vector Laboratories Cat# H-1200). Samples that were not treated with the primary antibody served as controls to ensure specific protein labeling.

2.2.7 Hematoxylin and Eosin Staining

Hematoxylin and eosin staining was performed in triplicate for each sample. Slides were deparaffinized using three changes of xylene for 3-minutes each and then dehydrated in three decreasing concentrations of ethanol (100%, 95%, 85%, respectively) for 3-minutes each. Slides were then immersed in hematoxylin for 15-minutes and then washed in distilled water (dH₂O) for 15-minutes. Slides were immersed in eosin for 30-seconds followed by a 30-second wash in dH₂O. Samples were then submerged in three increasing concentrations of ethanol (85%, 95%, 100%, respectively) for 3-minutes each, and then in three changes of xylene for 3-minutes each. Coverslips were mounted onto slides using SecureMount[™] low viscosity mounting medium.

2.2.8 Image Acquisition

Images were captured digitally using a Nikon Eclipse 90i microscope and Hamamatsu C10600 Camera. All samples were captured at 10x and 20x magnification at a fixed exposure time per experiment.

2.2.9 Protein Localization Ratings

To identify and compare the localization of proteins between species, two raters familiar with rabbit and human VF histology identified the location of positive protein labeling in tissue samples. Raters were aware of species and image magnification when rating but blinded to specific protein labeling. Raters identified positive labeling in tissue structures including the apical epithelium, basal epithelium, basement membrane, and LP layers (Appendix A).

2.2.10 Fluorescence Quantification

Positive immunolabeling of ZO-1, GCR, CD31 was quantified using ImageJ's "threshold" tool. Images were separated into color channels. The "Triangle" threshold presets were used to select CD31, GCR, ZO-1, and DAPI nuclear counterstain. The "analyze particles" function was then applied to calculate the percent area positively labeled within each sample. The positive area for each immunolabel of interest was normalized to the DAPI area and reported as a % value.

2.2.11 Muscle Fiber Cross-sectional Area Quantification

To calculate TA muscle fiber CSA, ImageJ software was used to manually select a region of interest containing the muscle fibers in H&E stained samples. Default thresholding was performed, and the particle analysis tool was used to calculate the total muscle fiber CSA in each sample. Individual muscle fibers were then manually counted using the multipoint tool, and the average individual muscle fiber CSA for each image was calculated (Appendix B) using the formula:

$$\frac{\text{Total muscle fiber area}}{\text{Muscle fiber count}} = \bar{x} \text{ individual muscle fiber}$$

2.2.12 Quantitative Polymerase Chain Reaction Primer and Probe Design

To assess transcript levels, quantitative polymerase chain reaction (qPCR) assays were developed and validated. Rabbit sequences for the genes of interest were obtained from Ensembl v.104²²¹ and GenScript Real-time PCR (TaqMan) Primer and Probes Design Tool was utilized to design assays that met the following specifications:

- 1) Primers or probes designed to span exon (protein-coding region) junctions to ensure sequence specificity
- 2) Primer melting temperature ~ 60°C and Probe melting temperature ~ 70°C
- 3) Absence of possible self-annealing sites (e.g. hairpins, primer dimers)

Once designed, primers were run through the nBLAST tool (NCBI) to ensure unique sequence identity within the rabbit genome, such that cDNA from other genes will not be recognized and amplified.

2.2.13 Electrophoresis

Polymerase chain reaction and gel electrophoresis were performed to evaluate primer specificity. cDNA was amplified for 35 cycles at 95°C, 60°C, and 72°C using standard protocol for the 2X complete PCR Master Mix (Thermofisher). Products were separated on a 2% agarose gel, at 120V, for approximately 45-minutes and visualized using a GelDoc (BioRad). The size was determined by comparison to a 100bp protein ladder. Primers that yielded products that were of the incorrect size, or multiple products, were not determined to be specific to the cDNA sequence and were excluded from further use.

2.2.14 Standard Curve

Once primer specificity was confirmed, the primer and probe combination (TaqMan assay) were evaluated for efficiency by generating a standard curve. In order to compare between assays (e.g. to perform relative expression analysis with a control gene), each assay must have similar efficiency. For these experiments, an efficiency of 90 – 110% was considered optimal. A 5-point standard curve of cDNA was generated at 1:5 dilution steps and added to identical wells containing Universal Fast qPCR master mix (BioRad) and the TaqMan assay of interest. Samples were plated in triplicate, and qPCR was performed for 40 cycles at 95°C, and 60°C. Sample efficiency was determined by plotting the fluorescence expression at each dilution and calculating their linear relationship.

2.2.15 RNA Extraction

RNA was extracted from VF samples using the manufacturer's directions for the Direct-Zol RNA kit (Zymo Research). Samples were homogenized in 500ul TRIzol reagent using a Precellys homogenizer coupled to the Cryolys chamber with dry ice to prevent RNA degradation. Homogenized samples were mixed with 100% ethanol and passed through a column to bind the RNA. Samples were then treated with DNase I, to prevent enzymatic contamination for 15-minutes at RT. Following this step, the RNA was washed with several proprietary solutions, before being eluted in DNase/RNase free water and nanodropped to determine concentration.

2.2.16 Reverse Transcription

Reverse transcription was undertaken with the High Capacity cDNA kit (BioRad) following the manufacturer's instructions. Briefly, RNA was added in equal volume to a PCR mix containing random primers and free-floating nucleotides that could be recruited to replicate the complementary strand to the RNA (cDNA). The reaction was amplified at 60°C for 2-hours and then stored at 4°C until used.

2.2.17 Quantitative Polymerase Chain Reaction

Quantitative PCR was performed using the TaqMan Universal Fast Mix (ThermoFisher) at 95°C for 40 Cycles. Reactions were run in triplicate, with five samples per condition. Each sample was evaluated for the following transcripts: MuRF-1, atrogin-1, and succinate

dehydrogenase subunit A (SDHA; the internal control). The sequences for primers and probes are found in Table 3 as well as an illustration of transcript level quantification in qPCR (Figure 16).

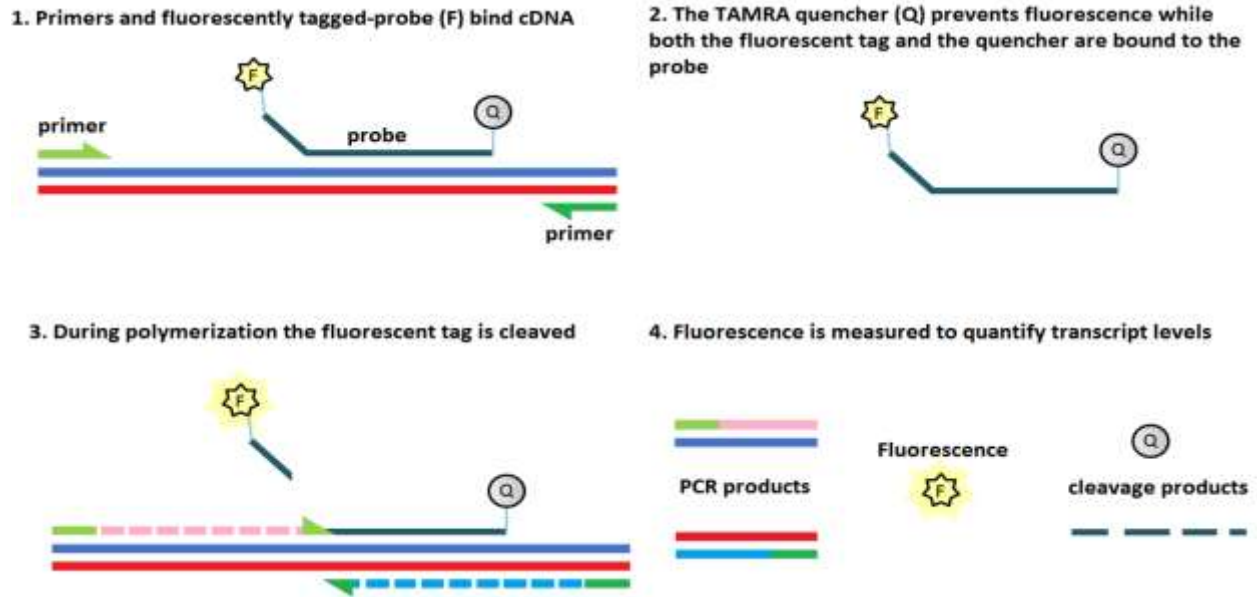


Figure 16: qPCR with dual labeled 5'FAM, 3'TAMRA probes TaqMan assays are designed with primers that flank a region of the gene of interest, and a probe that anneals between these two primers. The probe has a 5' fluorescent dye attached (6-FAM) and 3' quencher (TAMRA - which prevents 6-FAM from fluorescing when they are both attached to the probe). When the DNA is amplified by PCR it is transcribed from the 5' end, releasing the 6-FAM dye which can then fluoresce. The fluorescence is quantified by the StepOne qPCR machine and can be used to determine relative expression to a control gene SDHA.

Table 3: Probe and primer sequences

	Forward Primer	Reverse Primer	Probe
Atrogin-1	CGATGCTACCCGAGGAGGGA	GGTCAGTGCCCTTCCAGGAC	AGACACCCTCCAGCTCTGCAAGCA
MuRF-1	CATCCTGCCGTGTCAGCACA	TGCAGCCTGGAAGATGTCGT	ACCTCTGCCGCAAGTGTGCCA
SDHA	GCTGCATTTGGCCTCTCGGA	CAGAGCCCTTCACGGTGTCTG	TGCCTCCCTGTGCCGCCACA

Results were analyzed using StepOne software (ThermoFisher) and the $2^{-\Delta\Delta Ct}$ method. Samples were first evaluated for internal consistency between replicates, and anomalous data points were excluded. Next, the means of each gene of interest were compared within the sample to generate a cycle threshold (Ct) for the onset of detection of fluorescence. This is then averaged across samples within the condition to provide an average delta Ct. Next, the Ct of the internal control group (SDHA) is subtracted from the Ct of the gene of interest to derive a normalized $\Delta\Delta Ct$. Finally, 2 is raised to the power of $-\Delta\Delta Ct$ to calculate fold change of expression.

3.0 Results

All statistical analyses were calculated using IBM SPSS Statistics V.26 (SPSS, INC, Chicago, IL) and GraphPad Prism V.7.0 (GraphPad Software, San Diego, California, USA) with a significant alpha level determined at $p < 0.05$.

To establish inter-rater reliability for localization ratings, a weighted Cohen's kappa (κ_w) was used. The weighted extension of the kappa coefficient was necessary because this statistic considers the degree of disagreement between observers, unlike the traditional kappa which treats any slight disagreement between raters as total disagreement.²²² Samples were considered positive for the presence of protein if both raters identified positive labeling in the tissue of interest. The κ_w was 0.62 ($p < 0.01$), indicating moderate-substantial agreement between raters as determined by Viera and Garret.²²³

For variables attained from rabbits receiving intramuscular injections, two-way repeated-measures analyses of variance (ANOVA)s with Sidak's multiple comparisons tests and two-way ANOVAs with Tukey's multiple comparisons tests were conducted. For variables attained from rabbits receiving intracordal injections, one-way ANOVAs with Tukey's multiple comparisons tests were conducted. If assumptions for parametric analysis were not met, an analogous non-parametric Kruskal-Wallis with Dunn's multiple comparison tests were used. Confidence intervals (CI) of 95% were reported with statistically significant findings. The practical significance of statistically significant findings was evaluated using Cohen's d and f effect size measurements.

3.1 Localization of Integral Membrane Proteins in Human and Rabbit Vocal Folds

3.1.1 Aquaporin 1

The integral transport protein AQP1 was present in the basal epithelium/basement membrane, superficial LP, and deep/intermediate LP of both species (Figure 16A and B). Out of the 13 rabbit samples positive for AQP1 labeling, eight (62%) had positive labeling in the basal epithelium/basement membrane, 12 (92%) in the superficial LP, and 13 (100%) in the deep LP. Out of the seven human samples positive for labeling, four (57%) had positive labeling in the basal epithelium/basement membrane, seven (100%) in the superficial LP, and six (85%) in the intermediate LP.

3.1.2 Aquaporin 4

Aquaporin 4 was present in the apical epithelium, basal epithelium/basement membrane, superficial LP of both species (Figure 16C and D). Out of the eight positive rabbit samples, five (62%) had positive labeling in the apical epithelium, six (75%) in the basal epithelium/basement membrane, seven (88%) in the superficial LP, and two (25%) in the deep LP. Out of the seven human samples positive for labeling, three (43%) had positive labeling in the apical epithelium, two (28%) in the basal epithelium/basement membrane, and one (14%) in the superficial LP.

3.1.3 Aquaporin 7

Aquaporin 7 was present in the apical epithelium, basal epithelium/basement membrane, superficial LP of both species (Figure 17 E and F). Out of the seven positive rabbit samples, six (86%) had positive labeling in the apical epithelium, seven (100%) in the basal epithelium/basement membrane, six (86%) in the superficial LP, and three (43%) in the deep LP. Out of the six human samples positive for labeling, two (33%) had positive labeling in the apical epithelium, three (50%) in the basal epithelium/basement membrane, and one (16%) in the superficial LP.

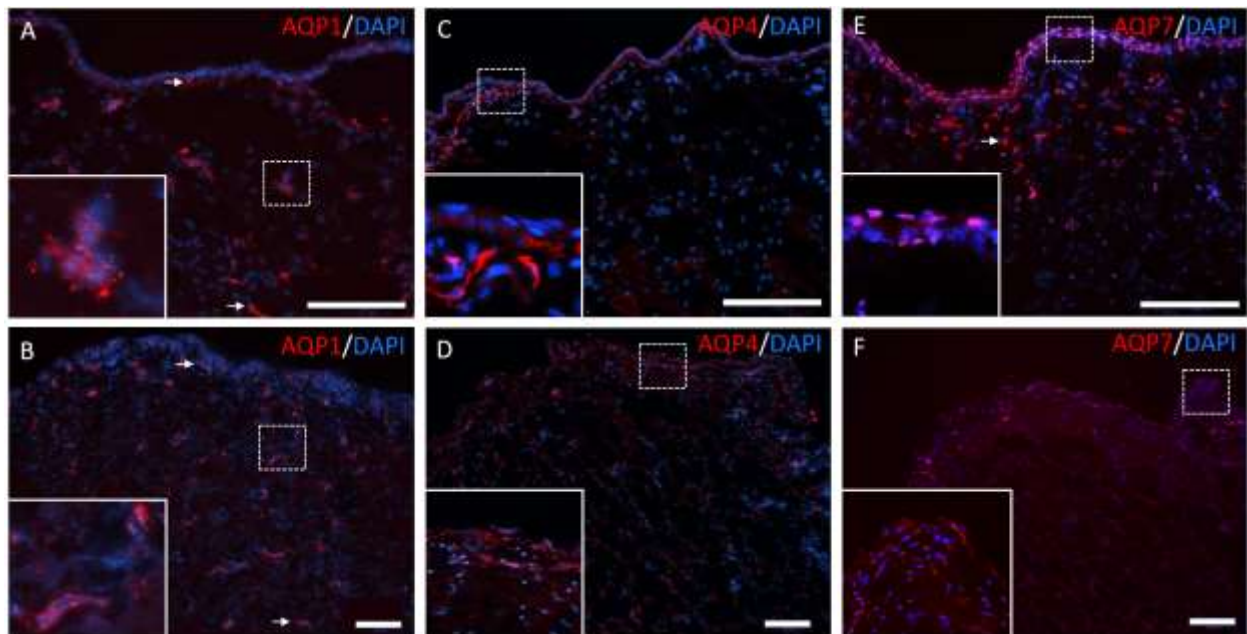


Figure 17: Representative immunofluorescence images labeled for AQP1, 4, and 7. Rabbit (A, C, and E) and human (B, D, and F) VF epithelium, superficial LP, and intermediate/deep LP labeled for DAPI are shown in blue and AQP1 (A-B), AQP4 (C-D), and AQP7 (E-F) in red. Dotted white boxes represent the magnified portion of the image and are displayed in the bottom left corner of each image. White arrows indicate other areas of positive labeling. Scale bars: 100 μ m.

3.1.4 Sodium-potassium Adenosine Triphosphatase

The integral transport protein Na^+/K^+ -ATPase was present in the apical epithelium and basal epithelium/basement membrane region in both species (Figure 18A and B). Out of the 15 rabbit samples positive for Na^+/K^+ -ATPase labeling, six (40%) were positive in the apical epithelium while 15 (100%) were positive in the basal epithelium/basement membrane region. Out of the 10 human samples positive for labeling, eight (80%) were positive in both apical epithelium and basal epithelium/basement membrane regions.

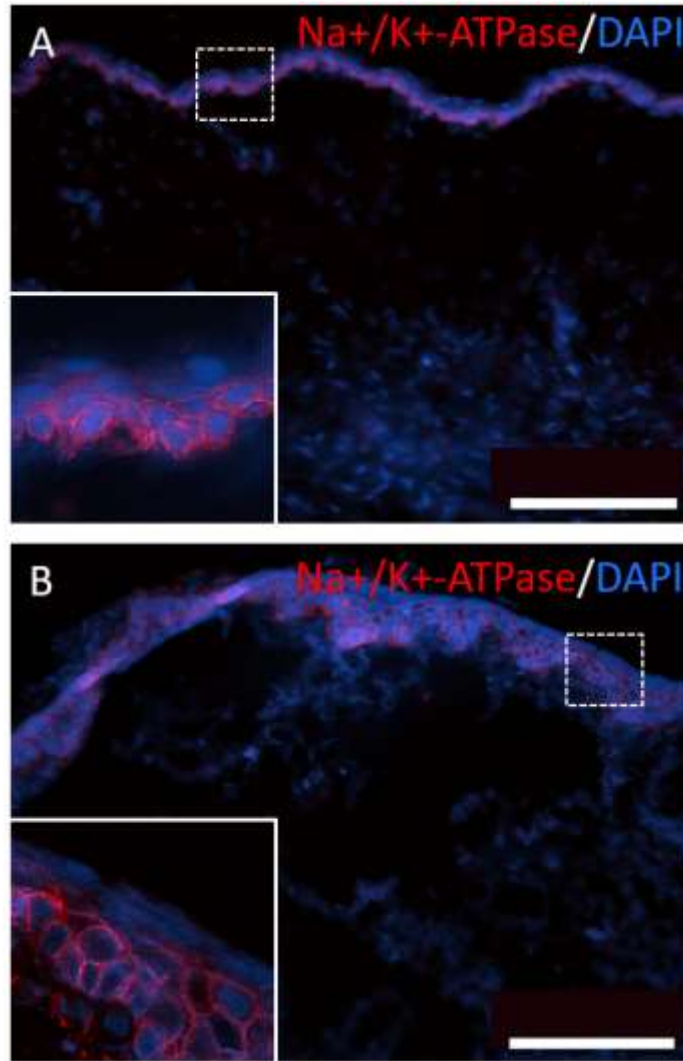


Figure 18: Representative immunofluorescence images labeled for Na⁺/K⁺-ATPase. Rabbit (A) and human (B) VF epithelium, superficial LP, and intermediate/deep LP labeled for DAPI in blue and Na⁺/K⁺-ATPase in red. Dotted white boxes represent the magnified portion of the image and are displayed in the bottom left corner of each image. Scale bars: 100 μ m.

3.1.5 E-cadherin

The cell-cell adhesion protein e-cadherin was present in the apical epithelium and basal epithelium/basement membrane region (Figure 19A and B) in all 14 rabbit samples. Out of the 11

human samples, 10 (91%) had protein labeled in both the apical epithelium and basal epithelium/basement membrane regions.

3.1.6 Occludin

The TJ protein occludin was present in the epithelium of both species (Figure 19C and D). Out of the 10 positive rabbit samples, nine (90%) were positive in the apical epithelium and three (30%) were positive in the basal epithelium. All rabbit samples also had positive labeling throughout the LP layers. In the seven human samples positive for labeling, only two (29%) showed presence in the apical epithelium and basal epithelium/basement membrane regions.

3.1.7 Zonula Occludin-1

The TJ protein ZO-1 was present in the apical epithelium, basal epithelium/basement membrane, and LP of both species (Figure 19E and F). Out of the eight positive rabbit samples, seven (88%) were positive in the apical and basal epithelium/basement membrane region, eight (100%) were positive in the superficial LP, and five (63%) were positive in the deep LP. Out of five positive human samples, three (60%) were positive in the apical epithelium, two (40%) were positive in the basal epithelium/basement membrane region, four (80%) were positive in the superficial LP, and two (40%) were positive in the intermediate LP. A summary of these findings is presented in Table 3.

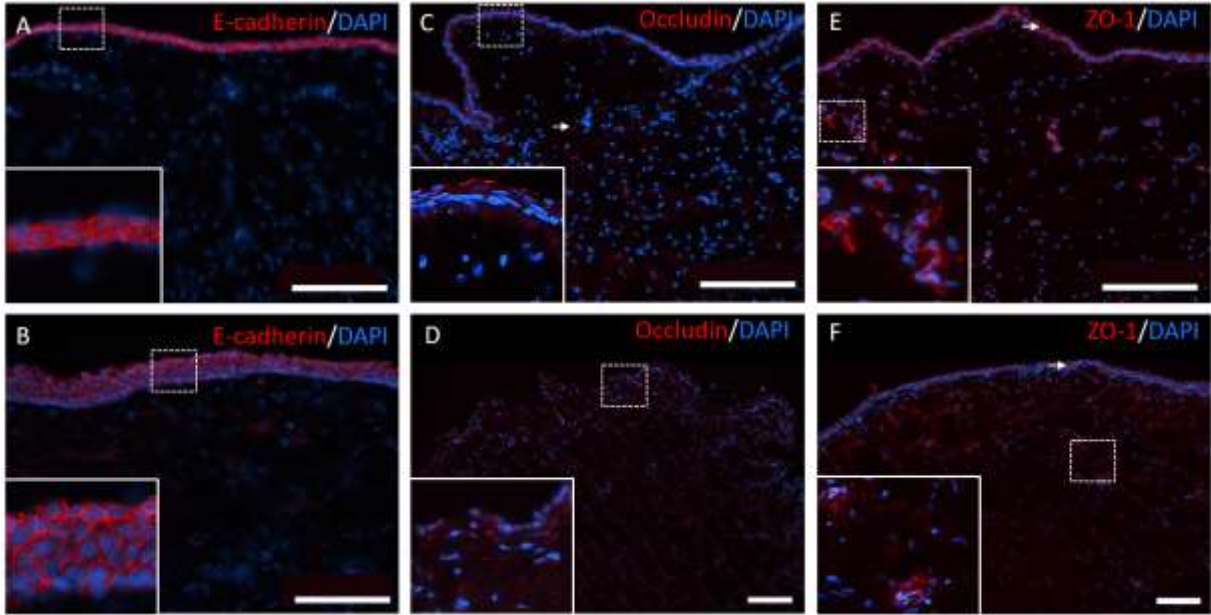


Figure 19: Representative immunofluorescence images labeled for E-cadherin, Occludin, and ZO-1. Representative immunofluorescence labeled images of rabbit (A, C, and E) and human (B, D, and F) VF epithelium, superficial LP, and intermediate/deep LP labeled for DAPI in blue and e-cadherin (A-B), occludin (C-D), and ZO-1 (E-F) in red. Dotted white boxes represent the magnified portion of the image and are displayed in the bottom left corner of each image. White arrows indicate other areas of positive labeling.

Scale bars: 100 μ m.

Table 4: Results of positive labeling of tissue structures in rabbit and human VFs

Protein	Apical Epithelium		Basal Epithelium/Basement Membrane		Superficial LP		Deep/ Intermediate LP	
	Rabbit	Human	Rabbit	Human	Rabbit	Human	Rabbit	Human
AQP1	-	-	62%	57%	92%	100%	100%	85%
AQP4	63%	43%	75%	28%	88%	14%	25%	-
AQP7	86%	33%	100%	50%	85%	16%	43%	-
Na ⁺ /K ⁺ -ATPase	40%	80%	100%	80%	-	-	-	-
E-cadherin	100%	100%	91%	91%	-	-	-	-
Occludin	90%	29%	30%	29%	100%	-	100%	-
ZO-1	88%	60%	88%	40%	100%	80%	63%	40%

3.2 Acute Effects of Daily Intramuscular Glucocorticoid Treatment on Rabbit Vocal Folds

3.2.1 Body Mass

A two-way repeated measures ANOVA with Sidak's multiple comparisons test revealed a significant increase in pre and post-treatment body mass in saline treated rabbits euthanized at the 1-day timepoint ($F(13, 13) = 10.06$; $p = 0.04$; $d = 0.86$; $CI = -0.16$ to -0.002) (Figure 20A). No significant differences between pre-post treatment weight were observed in rabbits euthanized at the 3-day timepoint (Figure 20B). There was a significant body mass decrease in rabbits treated with methylprednisolone ($F(12, 12) = 15.55$; $p = 0.001$; $d = 1.11$; $CI = 0.097$ to 0.35), and a significant body mass increase in rabbits treated with saline ($F(12, 12) = 15.55$; $p = 0.044$; $d = 0.81$; $CI = -0.25$ to -0.003) at the 7-day timepoint (Figure 20C).

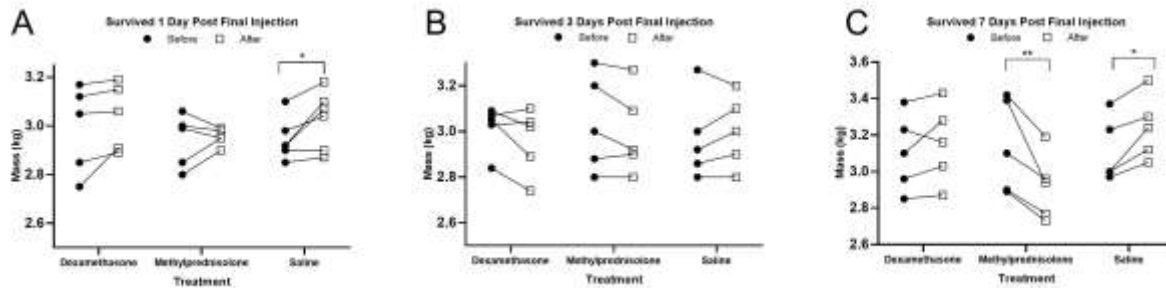


Figure 20: Scatter plots showing pre and post-treatment body mass (kg) for rabbits treated with dexamethasone, methylprednisolone, or saline (vehicle control), and euthanized at 1-day following termination of injections (A), 3-days following termination of injections (B), and 7-days following termination of injections (C). * = $p < 0.05$; ** = $p < 0.01$

3.2.2 Thyroarytenoid Muscle Cross-sectional Area

A two-way ANOVA revealed no significant interactions or main effects of treatment conditions or euthanasia time points on TA CSA (Figure 21A-D). To establish intra-rater reliability, 10% of the samples were randomly selected and redundantly analyzed. The calculated correlation coefficient revealed excellent reliability ($r = 0.96$) between ratings.

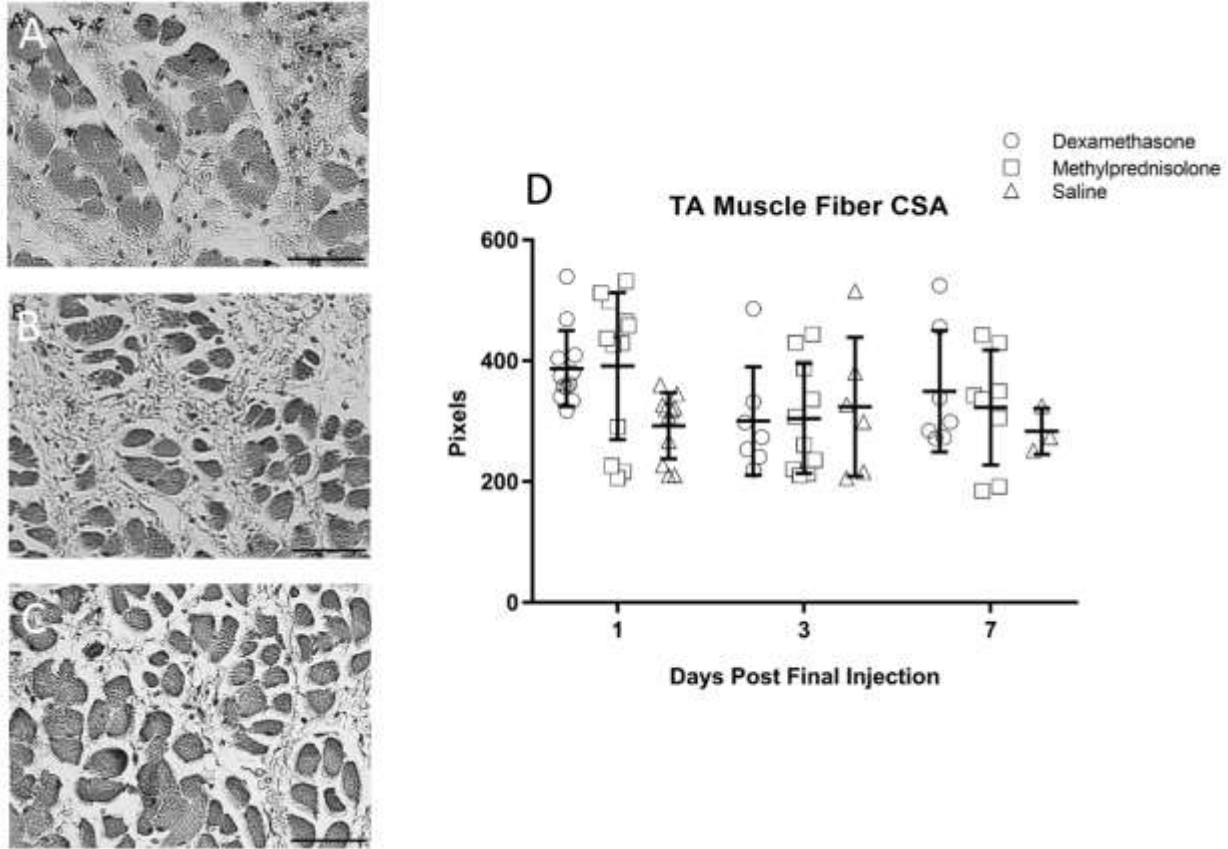


Figure 21: H&E stained TA muscle fibers and scatter plot from rabbits treated with dexamethasone (A), methylprednisolone (B), and saline (C). Scatter plot displays means and SDs for TA muscle CSA measures across drug and euthanasia timepoints. Scale bars: 150 μm.

3.2.3 Immunofluorescence Expression

A two-way ANOVA and Tukey’s multiple comparisons test revealed a significant increase in ZO-1 fluorescence expression with dexamethasone treatment compared to saline treatment at all time points ($F(2, 107) = 3.66$; $p = 0.04$; $f = 0.07$; $CI = 0.003$ to 0.10) (Figure 22A-D). There were no significant interactions or main effects of treatment conditions or euthanasia time points on CD31 or GCR fluorescence expression (Figure 22E-L).

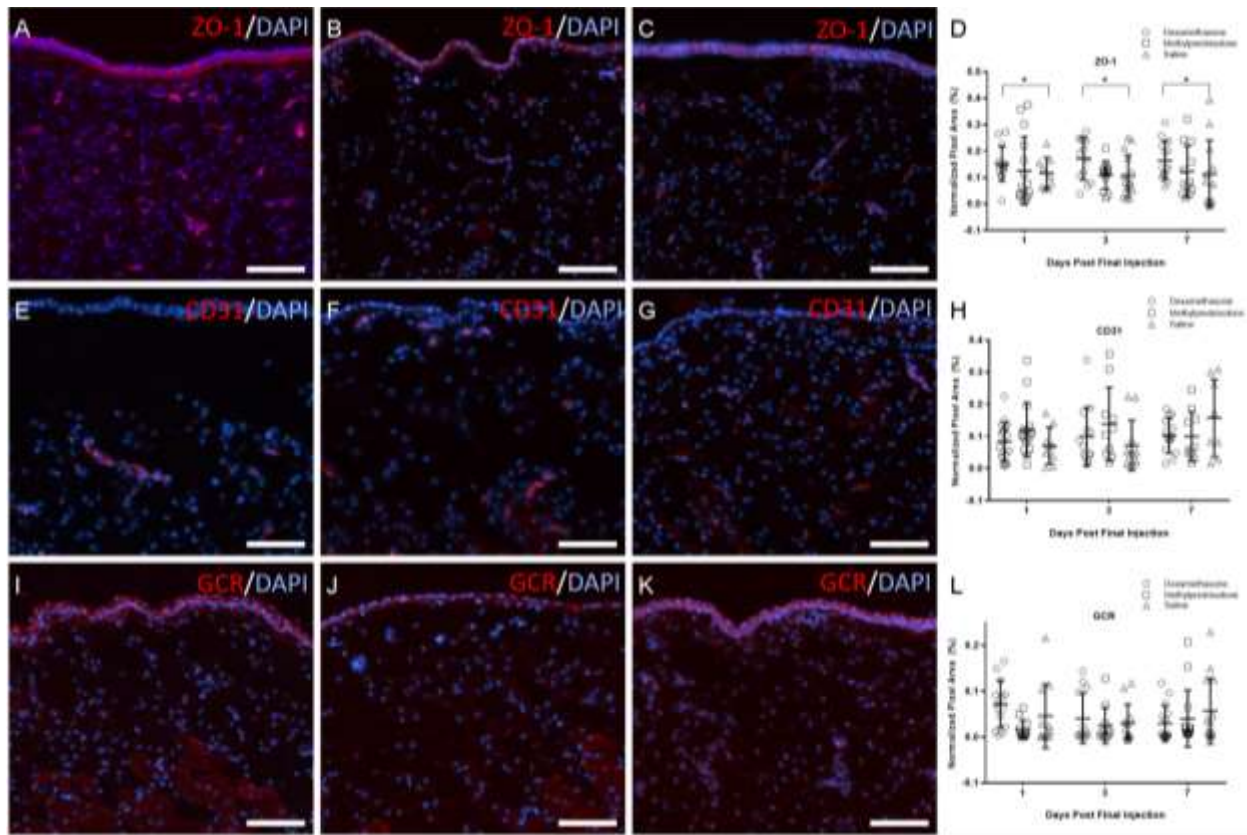


Figure 22: Immunofluorescence images of rabbit VF epithelium and LP layers. Labeling for ZO-1 (A-C), CD31 (E-G), and GCR (I-K) from rabbits treated with dexamethasone (A,E,I), methylprednisolone (B,F,J), and saline (C,G,K) is colored red. DAPI counterstain is colored blue. Scatter plot displays means and SDs for normalized pixel area measures across drug and euthanasia timepoints (D,H,L). Scale bars: 150 μm . * = $p < 0.05$

3.3 Occurrence of Vocal Fold Atrophy after Intracordal Dexamethasone Injection

3.3.1 Thyroarytenoid Muscle Cross-sectional Area.

A non-parametric Kruskal-Wallis test was used due to apparent differences in variance between experimental groups. No significant differences in TA muscle CSA were observed. To

establish intra-rater reliability, 10% of the samples were randomly selected and redundantly analyzed. The calculated correlation coefficient revealed good reliability ($r = 0.85$) between ratings (Figure 23A-D).

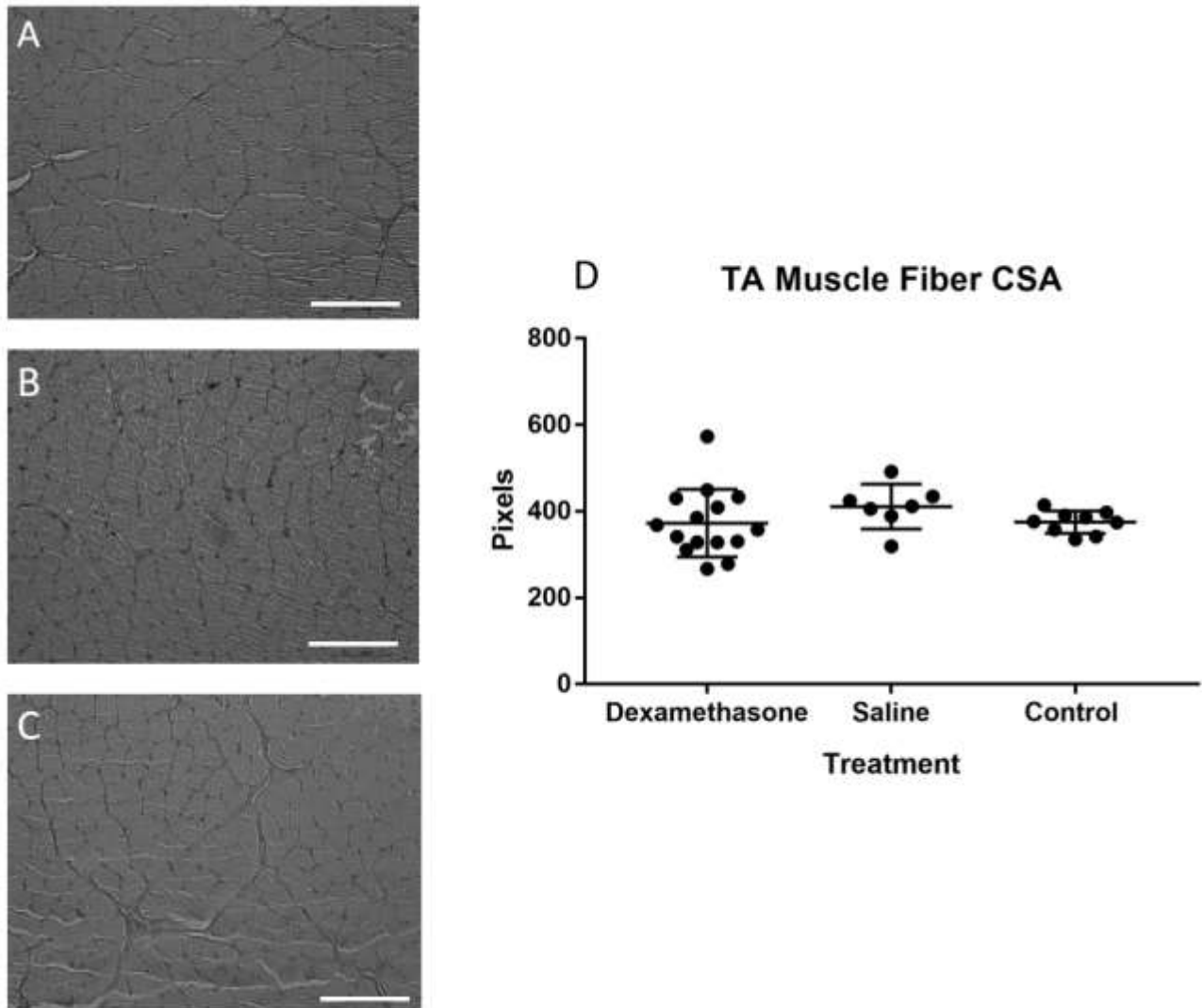


Figure 23: H&E stained TA muscle fibers and scatter plot from rabbit VFs injected with dexamethasone (A), saline (B), and untreated controls (C). Scatter plot (D) displays means and SDs for TA muscle CSA measures across treatment. Scale bars: 150 μm .

3.3.2 MuRF-1 Gene Expression

Two outliers from the dexamethasone ($2^{-\Delta\Delta Ct} = 123.48; 172.38$) and saline ($2^{-\Delta\Delta Ct} = 40.27; 22.71$) treated VFs and three outliers from the untreated control VFs ($2^{-\Delta\Delta Ct} = 133.69; 132.25; 145.2$) were excluded from analysis. A Kruskal-Wallis test revealed no significant differences between experimental groups (Figure 24).

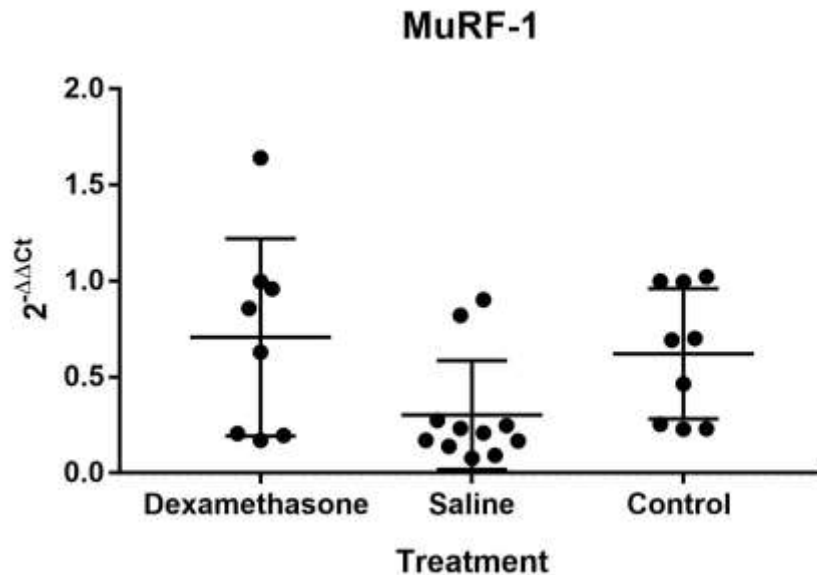


Figure 24: MuRF-1 gene expression in VFs injected with dexamethasone, saline, and untreated controls

3.3.3 Atrogin-1 Gene Expression

A Kruskal-Wallis test revealed no significant differences in atrogin-1 gene expression between experimental groups (Figure 25).

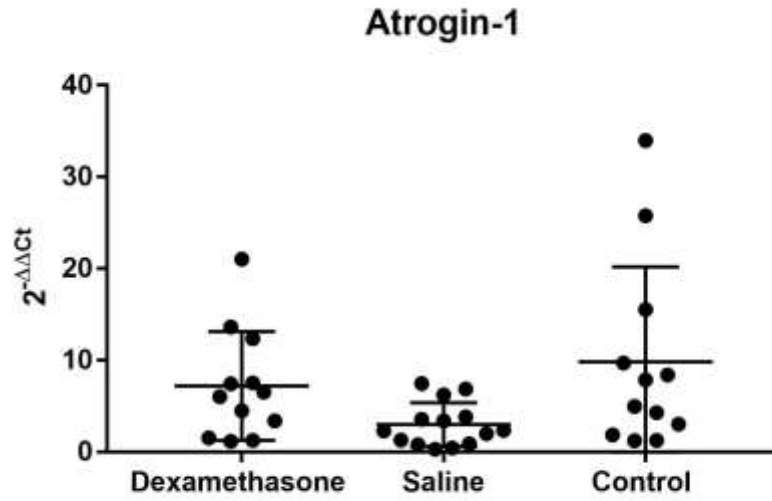


Figure 25: Atrogin-1 gene expression in VFs injected with dexamethasone, saline, and untreated controls

4.0 Discussion

4.1 Localization of Integral Membrane Proteins in Human and Rabbit Vocal Folds

The use of rabbits as a small animal model has gained increased attention in the voice literature due to its relative advantages to larger animals and as a reasonable alternative to smaller species, such as mice and rats. The localization of these proteins in the rabbit VFs provides an opportunity for further characterization in this species and similarities in localization of these critical membrane proteins relative to humans. The purpose of the present study was to identify and compare the localization of these integral membrane proteins between species to validate the suitability of the rabbit for future studies of VF tissue homeostasis and epithelial barrier integrity.

The integral membrane transport protein AQP1 was primarily localized in the superficial LP in both human and rabbit VFs, which is supported by findings of AQP1 in mouse VFs.²²⁴ Aquaporin 1 may serve an important role in the vascular permeability of the VF LP. In corneal and respiratory tissue in mice, the deletion of this gene reduces fluid production in the eyes²²⁵ and fluid movement across the endothelium that lines blood vessels in the lungs.²²⁶ Furthermore, studies in pulmonary tissue revealed that humans expressing the AQP1 gene demonstrate an increase in airway wall thickness, following IV injection of saline, compared to humans deficient in AQP1.²²⁷ This increase was not a result of vascular distention, suggesting that AQP1 may be involved in promoting vascular permeability. Blood vessel permeability enables the flow of small molecules such as drugs, nutrients, and water, and is critically important during the inflammatory and wound healing process.

Between species, the localization of AQP4 was most comparable in the VF epithelium, which is also supported by findings in mouse VFs²²⁴ and studies in the airway epithelium of rats.²²⁸ Although few studies claim a minimal role of AQP4 in transepithelial water transport in airway tissue,^{226,229} AQP4 is believed to contribute to neural signaling²³⁰ and cell migration²³¹ in glial cells.

Aquaporin 7 is involved in water/glycerol transport in adipocytes (i.e. fat cells),²³² and was primarily observed in the epithelium of both species. Although AQP7 has been previously localized to submucosal laryngeal glands in mice,²²⁴ our study seems to be the first to identify AQP7 in the epithelium of rabbit and human VFs. Most rabbit samples also had positive labeling in the superficial LP, which may be due to the presence of adipocytes in the connective tissue. Although the presence of adipocytes in the VF LP has not been confirmed to our knowledge, studies in bladder mucosa revealed that adipocytes constitute the ECM composing the LP.²³³

Sodium-potassium adenosine triphosphatase functions by using active transport to pump three positively charged sodium ions out of the cell, while simultaneously pumping two positively charged potassium ions into the cell.²⁶ This results in a difference in charge between the interior and exterior of the cell, forming an osmotic gradient. Fisher and colleagues²³⁴ were the first to determine that this osmotic gradient is the driving force of water diffusion and transport across the cell membrane of VF epithelium. Water transfer and hydration of the VFs have been reported to increase the efficiency of VF oscillation and voice production through its contributions to phonation threshold pressure.²⁵ In the current study, Na⁺/K⁺-ATPase was localized to intracellular membranes of the epithelium in both species. The rabbit samples demonstrated more intense labeling in the basal-most region of the epithelium. This finding is comparable to those identified by Fisher et al.²³⁴ who identified Na⁺/K⁺-ATPase in the cell membranes of the basal-most

epithelium in canine larynges. The human samples demonstrated an equal distribution in both apical and basal regions of the epithelium. The slight distribution variations of Na⁺/K⁺-ATPase may be due to the differences in epithelial layers between species, as humans have 5-10 layers of SSE while rabbits have only 2-4.^{24,235}

E-cadherin is a cell adhesion molecule present in epithelial cells and is believed to maintain the epithelial barrier created by TJs.³⁴ This protein was similarly localized to intercellular junctions throughout the SSE in both species. E-cadherin plays a crucial role in the maintenance of mucosal integrity and barrier function. Reduced expression of e-cadherin has been observed in biopsy samples of patients with laryngopharyngeal reflux.^{236,237} Disruptions in barrier integrity may result in the undesirable entry of environmental pathogens into the VFs, and the development of disease. Although e-cadherin has been localized throughout the VF epithelium of multiple species including humans, it had not been localized until now in rabbit VFs.

The role of the TJ proteins like ZO-1 and occludin is to facilitate intercellular signaling and adhere to adjacent cells to create an effective barrier.^{28,29} The presence of these proteins in VF tissue has been described in rabbits^{31,238} pigs,³⁰ and sheep,³² but the distribution of these proteins has only been localized to the epithelium of rat VFs.²³⁹ Similar to these findings in rats, our study found that ZO-1 and occludin were localized to the rabbit and human epithelium. There was also substantial ZO-1 labeling in the superficial LP of both species, likely due to their presence in endothelial cells.^{28,240(p1)} There was only substantial occludin labeling in the superficial LP in rabbit samples, possibly due to inherent differences in the layered LP structure between species and subsequent distribution of blood vessels.

The disparity of specific protein labeling in matching structures within species may be due to the heterogeneity between VF tissue in both human and rabbit samples used in this study. For

example, humans are inherently genetically diverse, and information regarding previous voice use and preexisting pathologies in our acquired human samples was nonexistent. Additionally, our rabbit samples were not from homogeneous inbred colonies, but rather from genetically diverse outbred stocks.

On the whole, similarities in these integral membrane proteins provide an opportunity to further investigate the role and function of these proteins following experimentally induced challenges that might otherwise be difficult to perform in humans. These experiments may include exploring the effects of therapeutic drugs such as GCs, phonotrauma, and iatrogenic injury on VF barrier integrity and ion transport. Unpublished data in our laboratory revealed dose-dependent increases in e-cadherin labeling in human and rabbit cultured VF epithelial cells after dexamethasone treatment and dose-dependent decreases in ZO-1 and trans-electrical epithelial resistance (TEER) after methylprednisolone treatment, indicating improved barrier function. Regarding *in-vivo* studies in our laboratory, rabbits treated with 6-daily intramuscular injections of dexamethasone revealed no changes in AQP-1, Na⁺/K⁺-ATPase, ZO-1, and occludin fluorescence expression 14-days after injections were terminated. Similarly, rabbits receiving the same treatment regimen of methylprednisolone revealed no changes in AQP-1, Na⁺/K⁺-ATPase, and occludin fluorescence expression, but did show decreases in ZO-1 fluorescence and tjp-1 gene expression, indicating the possibility of compromised barrier integrity following methylprednisolone treatment.

4.2 Acute Effects of Daily Intramuscular GC Treatment on Rabbit Vocal Folds

Due to the frequent off-label use of GCs to treat a variety of voice disorders, it is critical to characterize and delineate GC effects in healthy VF tissue to provide insight regarding the utility of dexamethasone and methylprednisolone to improve clinical outcomes and to mitigate potential adverse drug effects. Although the current study did not observe VF TA muscle atrophy for the variables of GC treatment or euthanasia timepoint, rabbits revealed global body mass loss 7-days post methylprednisolone treatment. This global body mass loss may be due to the inhibitory effects methylprednisolone has on the endocrine system, specifically IGF-1.^{188,241} Dose-dependent body mass decreases have been observed in rats after repeated methylprednisolone treatment,²⁴² which was postulated to result from decreased circulating IGF-I. There have also been mixed reports regarding GCs' effect on appetite. Studies in rats revealed dose-dependent decreases in food intake and body mass,^{243,244} while other studies in rats and humans found increases in food intake and body mass.²⁴⁵⁻²⁴⁷ However, the rabbits in the current study had open access to food, and conclusions about any association between food intake, body mass, and GC treatment are unavailable.

The role of ZO-1, an epithelial and endothelial TJ protein, is to adhere adjacent cells together to decrease paracellular permeability and maintain barrier integrity.²⁸ Decreased ZO-1 expression is associated with increased endothelial and epithelial paracellular permeability.^{240,248} In the current study, rabbits treated with daily intramuscular dexamethasone injections revealed an up-regulation of ZO-1 across all euthanasia time points compared to controls. This finding is supported by several studies that observed increased ZO-1 expression associated with increased TEER and decreased paracellular permeability in epithelial and endothelial cells after dexamethasone treatment.¹⁴⁰⁻¹⁴² Previous research in our group revealed decreases in ZO-1

transcript levels in rabbits subjected to acute phonotraumatic injury.^{31,238} Similarly, a study by Shen et al.²⁴⁹ revealed significant decreases in ZO-1 expression in rat intestinal epithelium after ischemia-reperfusion injury. These decreases in ZO-1 expression are believed to result from the structural damage to the tissue, which may increase the size of paracellular spaces to allow entry of harmful toxins and pathogens that impede the homeostasis of the mucosa.²⁵⁰ Our findings reveal that dexamethasone may be a useful therapeutic in up-regulating ZO-1 for re-establishing and preserving a functional endothelial and epithelial barrier in VF tissue. As stated previously in section 4.1, unpublished data in our laboratory revealed decreases in ZO-1 in the 14-days following intramuscular methylprednisolone injections, which may be detrimental to epithelial and epithelial barrier function. However, the current study did not demonstrate any effects of methylprednisolone on ZO-1 in the 7-days following treatment.

The potential anti-angiogenic properties of GCs led to the investigation of this phenomenon in VF tissue, which may be detrimental to the VF wound healing process. However, the current study did not find any effects of GCs on VF tissue vascularity using the endothelial marker CD31. Interestingly, unpublished data from our laboratory observed an increase in CD31 fluorescence expression in rabbit VFs 14-days after 6-daily intramuscular injections of methylprednisolone. Although the current study did not observe any changes in CD31 during the 7-days following intramuscular methylprednisolone injections, it may be that the pro-vascular effects of this GC may only be apparent in the weeks following treatment. Increased vascularity - in combination with the unpublished findings of reduced ZO-1 in the VF of methylprednisolone-treated rabbits - may lead to a greater likelihood of damage to vessels and VF hemorrhage.

Some studies suggest that repeated GC treatment is associated with decreased expression of GCR.¹⁵¹ In the current study, there were no observed changes in GCR fluorescence expression

in VF tissue after repeated systemic treatment of dexamethasone or methylprednisolone, indicating that the anti-inflammatory and immunosuppressive properties of these GCs are likely still maintained in the week after 6-daily intramuscular injections.

4.3 Occurrence of Vocal Fold Atrophy After Intracordal Dexamethasone Injection

Glucocorticoid injections have been associated with skeletal muscle atrophy in multiple tissue types and models, including the VFs. With the frequency of GC use for laryngeal indications, particularly dexamethasone, it was imperative that the potential of GC-induced VF atrophy be investigated further using a well-established, controlled, *in-vivo* experimental paradigm. In the current study, there was no evidence of GC-induced atrophy. This finding was determined from no observed changes in atrophy-associated genes or TA morphological changes between the treatment group and controls.

A single intracordal injection of dexamethasone has been clinically utilized and shown to improve subjective voice measures²⁵¹ objective voice measures, and lesion size.²⁵² Although the current study used the highest commercially available dose of dexamethasone at a clinically relevant injection volume, repeated intracordal injections may be required to elicit TA skeletal muscle atrophy. The retrospective case series by Shi et al. 2016¹⁵⁹ observed the occurrence of VF atrophy after 5-6 weekly subepithelial injections of 0.1 mL of 10 mg/mL dexamethasone, but the analysis was limited to only endoscopic ratings of atrophy presence. Therefore, interpretations of whether atrophy was localized to the epithelium, lamina propria, or skeletal muscle were unachievable. A study by Hashimoto et al. (2021)²⁵³ investigating the temporal atrophic effects of four triamcinolone injections in rat VFs observed significant decreases in the area of hyaluronic

acid and thickness of the lamina propria, but no differences in TA muscle fiber CSA. Our study was limited to only exploring the potential atrophic effects of a single intracordal injection of dexamethasone on the TA muscle.

Although further studies are required to elucidate the possible local atrophic effects of serial intracordal GC injections, the current findings support the safety of a single intracordal injection of dexamethasone when treating various laryngeal pathologies.

4.4 Limitations

A limitation that was acknowledged is the uniqueness in the structure of the rabbit VF tissue and how this may influence how findings can be generalized to drug effects on human VFs. Although rabbits demonstrate similarities to humans in the context of VF tissue, microarchitectural properties, and ECM components, the rabbit only has 2-4 layers of VF SSE and a 2-layered LP,^{99,206,207} while humans have 5-10 SSE layers and a tertiary intermediate LP layer.^{24,254} Additionally, while humans have both type I and II muscle fibers in their TA muscle, rabbits have been reported to only have type II muscle fibers,²⁵⁵ which are believed to be less resistant to skeletal muscle atrophy.²⁵⁶ Although no atrophy was observed in these experiments, it is unclear whether different muscle fiber types have different resistance levels of skeletal muscle atrophy induced by GCs. Additionally, GCs are typically administered for laryngeal indications that frequently involve an inflammatory response in the VFs or surrounding tissue. It is reasonable to believe that this inflammatory response - characterized by an influx of immune cells, the release of inflammatory mediators, and chemoattraction of other cell types - can influence how GCs

interact with the VF tissue. However, the VFs used in the study were uninjured. Therefore, generalization of GC effects on injured VF tissue is limited.

A second limitation of this study was the absence of analysis of endocrine biomarkers, food intake, and waste output. It is unclear if body mass loss in rabbits receiving intramuscular methylprednisolone injections was influenced by potential GC effects on IGF-1, decreases in appetite, or increases in urine/fecal output. It is also unclear if there was atrophy in the injected iliocostalis/longissimus muscle or surrounding connective tissue. Future studies will account for food intake and fecal output, as well as the inclusion of skeletal muscles and endocrine biomarkers that may be affected by systemic GCs.

A third limitation was the location of the intracordal GC injection in the rabbit VF. In almost all instances of clinical GC intracordal injection, the surgeon will inject the bolus into the superficial LP, avoiding the vocal ligament and TA muscle.²⁵⁷ Due to the significantly smaller size of the rabbit VF, delineation of the superficial LP from the vocal ligament and TA muscle during endoscopic injection was challenging. Consequently, the rabbits receiving intracordal GC injections received the bolus into the TA muscle, which is atypical in clinical practice.

A fourth limitation was the lack of inclusion of female rabbits. Although attempts were made to incorporate female rabbits in all experimental cohorts, vendor supplies at the time of purchase were limited to male rabbits. While it is well established that human VF compositions differ between males and females, information regarding the differences and similarities between male and female rabbit VFs is virtually non-existent. To more precisely use *in-vivo* animal models to conclude VF biology to the general human population, future studies should include similar distributions of both male and female animals.

5.0 Conclusion and Clinical Implications

Immunolabeling of key integral membrane proteins in rabbits and humans revealed similar localization in the VFs between species, supporting the utility of rabbits as a model to investigate treatments for voice disorders. Rabbits treated with daily intramuscular dexamethasone revealed increases in VF epithelial and endothelial TJ expression, which may indicate improved VF barrier integrity and provide better protection of the underlying connective tissue. Although global body mass loss occurred with daily intramuscular methylprednisolone treatment, there were no observed drug effects associated with changes in TA muscle morphology. Similarly, rabbits receiving a bilateral intracordal injection of dexamethasone did not reveal any changes in TA muscle morphology or atrophy associated gene expression, supporting the use of a single intracordal injection of dexamethasone in treating laryngeal indications.

The differential effects of GCs discovered in the current study emphasize the important role physicians have to tailor GC selection based on patient-specific needs when treating voice disorders. For example, individuals who have a compromised VF epithelial barrier, as seen in patients with laryngopharyngeal reflux,^{236,237} may benefit from dexamethasone treatment. Similarly, physicians may want to avoid using serial methylprednisolone treatment in patients who have difficulty maintaining healthy body weight, as this GC was observed to be associated with rapid weight loss. These findings will provide physicians with additional objective evidence when selecting GCs for treating voice disorders as well as other conditions where GCs are utilized.

6.0 Future Directions

The etiology of voice disorders is wide-ranging with varying treatment efficacy. The current oversimplified clinical paradigm dichotomizes voice disorders into two distinct categories: mucosal injury and neuromuscular dysfunction. A concern with the current dichotomous classification of these two diagnoses is the disregard of potential interactions with the various tissue types of the VF. There is a large body of evidence describing the potential interactions between mucosa and muscle in lower airway diseases. For example, patients with asthma who have mucosal inflammation were also observed to have increased contractile properties²⁵⁸ and hypertrophy of the airway muscles.^{259,260} There is also evidence of altered expression of contractile proteins in airway muscles in instances of severe mucosal inflammation.²⁶¹ In the context of VF tissue, preliminary investigations have recently observed bidirectional interactions between mucosa and muscle. Most notably, studies observed the favorable down-regulation of genes associated with fibrosis in the presence of rat laryngeal myoblast controlled media and the unfavorable suppression of myogenesis in the presence of rat laryngeal fibroblast controlled media.²⁶² These data combined with our collective interest in developing novel and efficacious treatments for patients with voice-related disabilities provide the foundation for the current proposal.

I have recently taken a position as an Associate Research Scientist at the NYU Grossman School of Medicine. I seek to expand this area of investigation with the ultimate goal of improved insight into mechanisms of voice-related disabilities and improvement of therapeutic strategies for these challenging patients. I plan to combine *in vitro* studies of myoblasts, fibroblasts, and macrophages to investigate the interactions between different cell and tissue types within the VF,

and how these interactions may influence response to injury. Additionally, established models of preclinical iatrogenic VF injury will be employed. Specifically, I will investigate the effects of iatrogenic injury to the mucosa as a potential mediator of abnormal laryngeal muscle physiology.

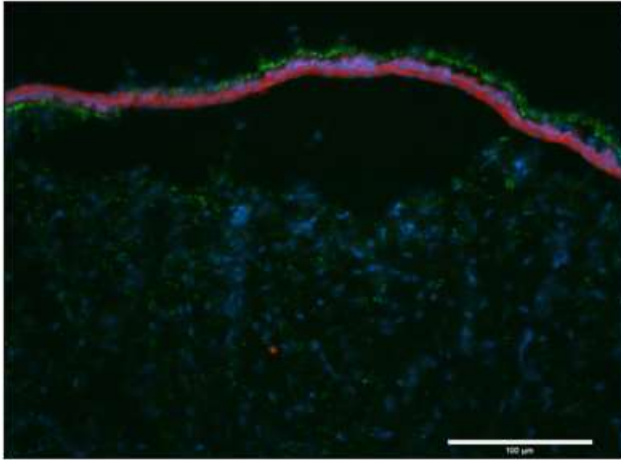
Ultimately, I seek to evolve as an independent investigator committed to elucidating the mechanisms underlying voice disorders to develop novel therapeutics for patients with voice-related disabilities. The training I received at the University of Pittsburgh in Dr. Rousseau's Laryngeal Biology Laboratory, in combination with expertise from Dr. Branski's laboratory, will allow me to integrate myself as an active member of the NYU Grossman School of Medicine scientific community to enhance my progression as an independent investigator.

Appendix A Subjective localization rating form

- *Directions*

The following slides contain images of rabbit and human vocal fold sections. The nuclei of the cells are labeled **blue**. Elastin fibers are represented by **green** auto fluorescence. The protein that you are going to localize is labeled **red**. Rabbit samples were captured at 20x magnification and contain the epithelium, superficial lamina propria, and deep lamina propria. There are also muscle fibers present in some rabbit samples. Human samples were captured at 10x and 20 x magnification. The human samples captured at x20 contain the epithelium, and superficial lamina propria. The human samples captured at 10x contain the epithelium, superficial lamina propria, intermediate lamina propria. To the right of each image, there will be boxes to "check off" which tissue structures you see containing **red** labeling. You can check multiple boxes.

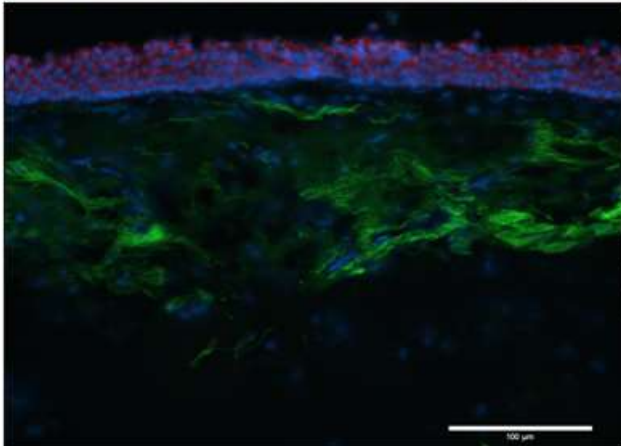
- *Rabbit (top) and human (bottom) VF samples (labeled for e-cadherin in red). Images were labeled with "X's" by a blinded rater which determined positive labeling in the apical epithelium and basal epithelium in both samples*



• Rabbit X20 magnification

Please check what structures are labeled red

Apical epithelium	X
Basal epithelium	X
Basement Membrane	
Superficial LP	
Deep LP	



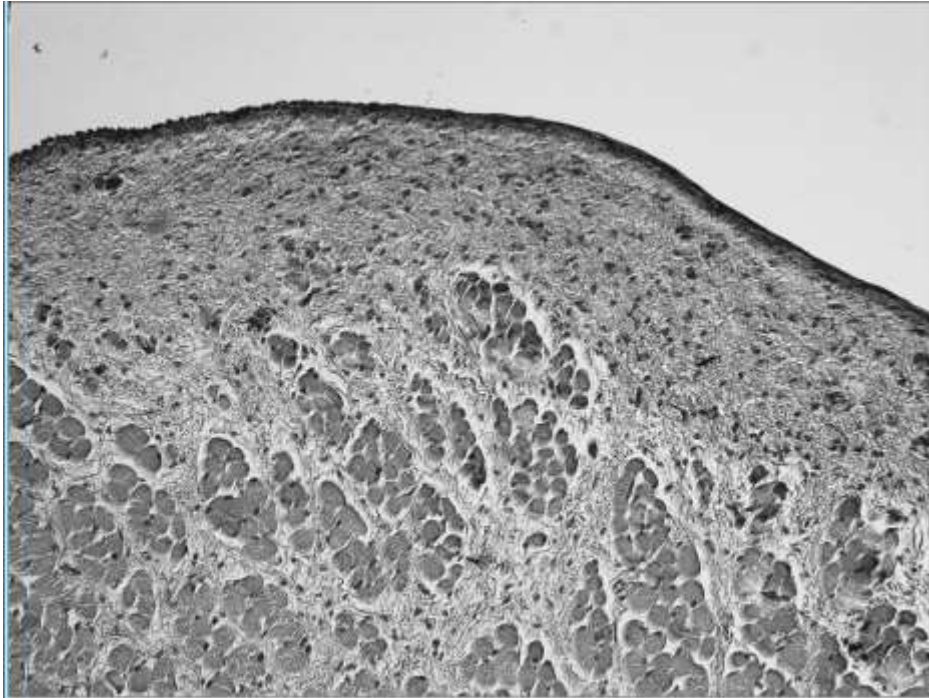
• Human X20 Magnification

Please check what structures are labeled red

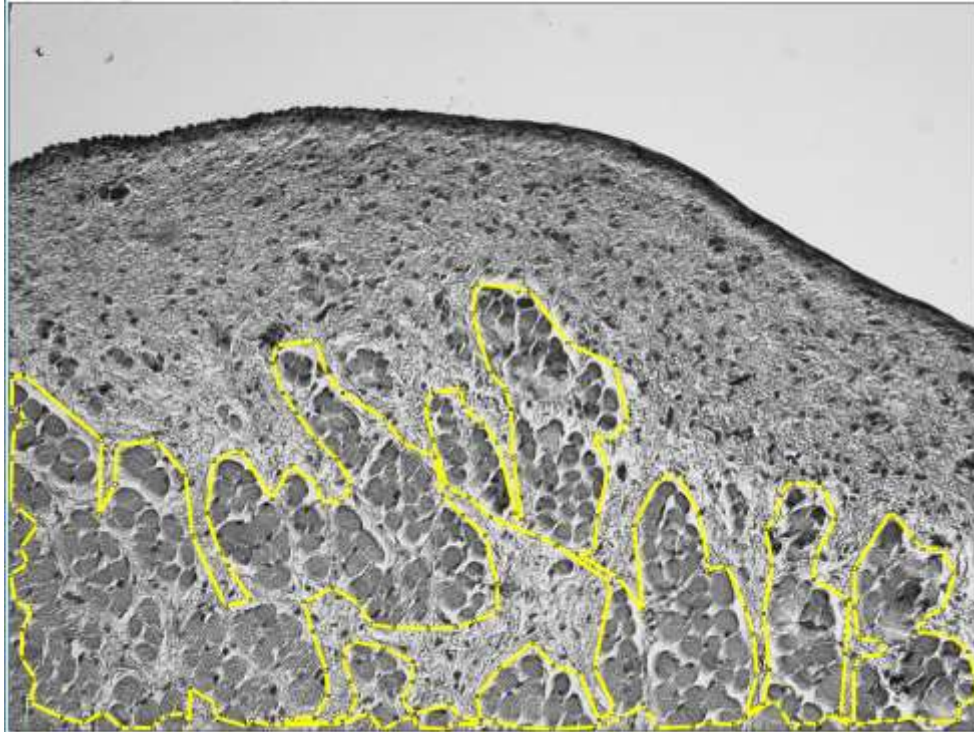
Apical epithelium	X
Basal epithelium	X
Basement Membrane	
Superficial LP	

Appendix B Depiction of muscle fiber CSA quantification

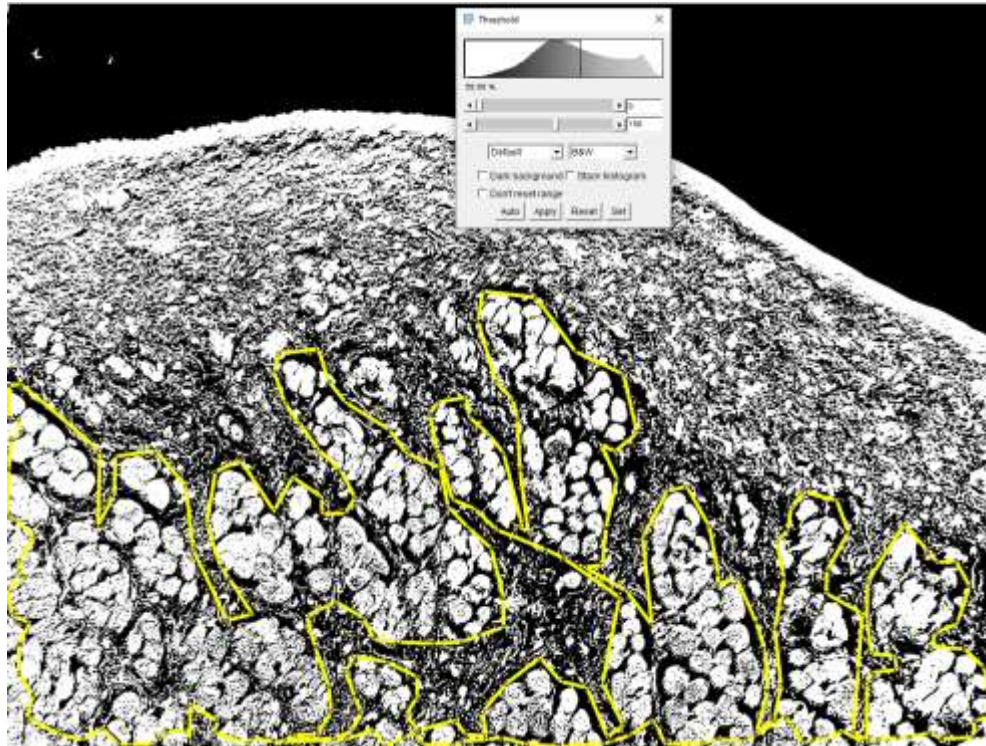
1. Import ND2 H&E image into ImageJ.



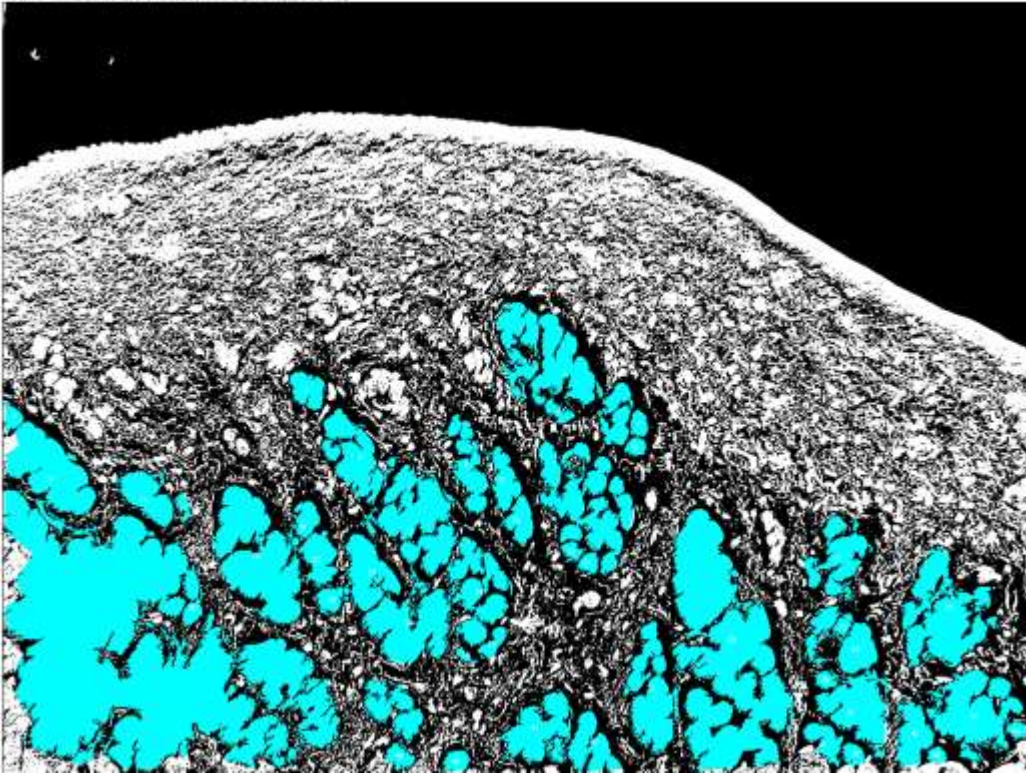
2. Manually select region of interest consisting of TA muscle using ImageJ's "polygon" tracing function.



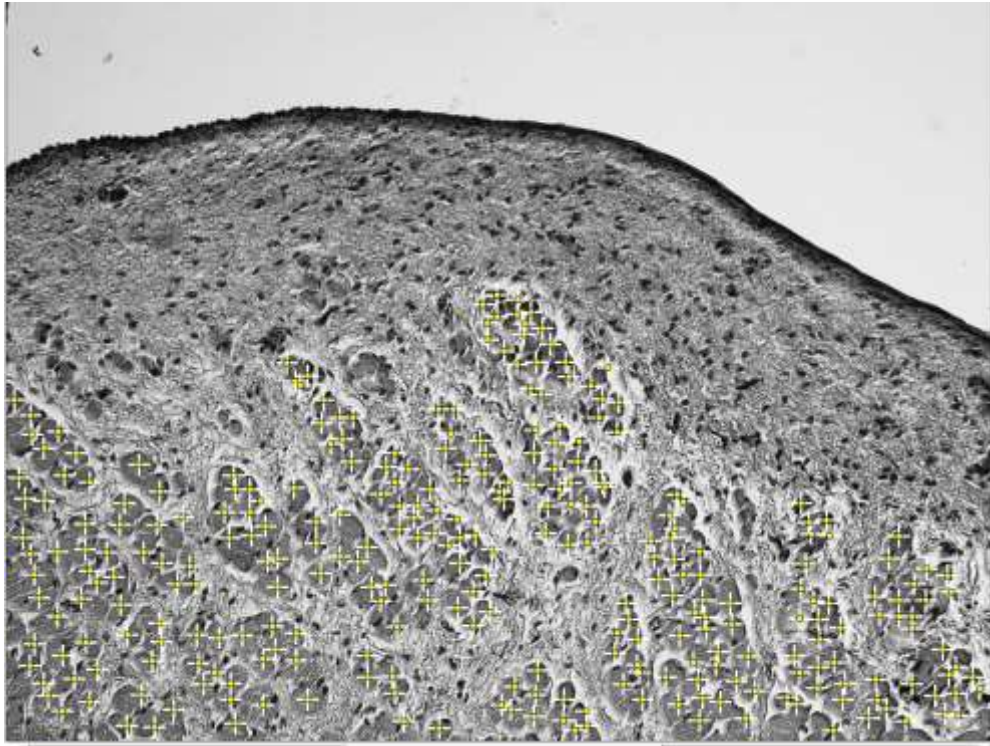
3. Use “Default” thresholding to obtain a high contrast image.



4. Use the “Analyze Particle” function to obtain pixel measures of muscle fibers.



- Using the multi-selection tool, obtain a manual count of each muscle fiber.



- Use the following formula to obtain the average individual muscle fiber CSA:

$$\frac{\text{Total muscle fiber area}}{\text{Muscle fiber count}} = \bar{x} \text{ Individual muscle fiber CSA.}$$

Bibliography

1. Roy N, Merrill RM, Gray SD, Smith EM. Voice disorders in the general population: Prevalence, risk factors, and occupational impact. *Laryngoscope*. 2005;115(11):1988-1995. doi:10.1097/01.mlg.0000179174.32345.41
2. Cohen SM, Kim J, Roy N, Asche C, Courey M. Direct health care costs of laryngeal diseases and disorders. *Laryngoscope*. 2012;122(7):1582-1588. doi:10.1002/lary.23189
3. Verdolini K, Ramig LO. Review: occupational risks for voice problems. *Logopedics Phoniatrics Vocology*. 2001;26(1):37-46. doi:10.1080/14015430119969
4. Cohen SM, Dupont WD, Courey MS. Quality-of-life impact of non-neoplastic voice disorders: a meta-analysis. *Ann Otol Rhinol Laryngol*. 2006;115(2):128-134. doi:10.1177/000348940611500209
5. Aronson A, Bless D. Clinical voice disorders. New York. NY: Thieme. Published online 2009.
6. Boone DR, Plante E. *Human Communication and Its Disorders*. Prentice Hall; 1993.
7. Roy N, Merrill R, Thibeault S, Parsa R, Gray S, Smith E. Voice disorders in teachers and the general population. *Journal of speech, language, and hearing research: JSLHR*. 2004;47:281-293. doi:10.1044/1092-4388(2004/023)
8. Coyle SM, Weinrich BD, Stemple JC. Shifts in relative prevalence of laryngeal pathology in a treatment-seeking population. *Journal of Voice*. 2001;15(3):424-440.
9. Martins RHG, do Amaral HA, Tavares ELM, Martins MG, Gonçalves TM, Dias NH. Voice disorders: etiology and diagnosis. *Journal of voice*. 2016;30(6):761-e1.
10. Cohen SM, Kim J, Roy N, Asche C, Courey M. Prevalence and causes of dysphonia in a large treatment-seeking population. *The Laryngoscope*. 2012;122(2):343-348. doi:10.1002/lary.22426
11. Martins RHG, Branco A, Tavares ELM, Gramuglia ACJ. Clinical Practice: Vocal nodules in dysphonic children. *Eur J Pediatr*. 2013;172(9):1161-1165. doi:10.1007/s00431-013-2048-x
12. Houtte EV, Lierde KV, D'Haeseleer E, Claeys S. The prevalence of laryngeal pathology in a treatment-seeking population with dysphonia. *The Laryngoscope*. 2010;120(2):306-312. doi:10.1002/lary.20696

13. Nunes RB, Behlau M, Nunes MB, Paulino JG. Clinical diagnosis and histological analysis of vocal nodules and polyps. *Brazilian Journal of Otorhinolaryngology*. 2013;79(4):434-440. doi:10.5935/1808-8694.20130078
14. Nardone HC, Recko T, Huang L, Nuss RC. A retrospective review of the progression of pediatric vocal fold nodules. *JAMA Otolaryngol Head Neck Surg*. 2014;140(3):233. doi:10.1001/jamaoto.2013.6378
15. Baken RJ, Orlikoff RF. *Clinical Measurement of Speech & Voice*. 2nd edition. Cengage Learning; 1999.
16. Thibeault SL, Rousseau B, Welham NV, Hirano S, Bless DM. Hyaluronan levels in acute vocal fold scar. *The Laryngoscope*. 2004;114(4):760-764. doi:10.1097/00005537-200404000-00031
17. Ward PD, Thibeault SL, Gray SD. Hyaluronic acid: its role in voice. *Journal of Voice*. 2002;16(3):303-309. doi:10.1016/S0892-1997(02)00101-7
18. Titze IR, Hunter EJ. Normal vibration frequencies of the vocal ligament. *The Journal of the Acoustical Society of America*. 2004;115(5):2264-2269. doi:10.1121/1.1698832
19. Dietrich M, Verdolini Abbott K, Gartner-Schmidt J, Rosen CA. The frequency of perceived stress, anxiety, and depression in patients with common pathologies affecting voice. *Journal of Voice*. 2008;22(4):472-488. doi:10.1016/j.jvoice.2006.08.007
20. Seifert E, Kollbrunner J. Stress and distress in non-organic voice disorder. *SWISS MED WKLY*.:11.
21. Hsiao TY, Liu CM, Hsu CJ, Lee SY, Lin KN. Vocal fold abnormalities in laryngeal tension-fatigue syndrome. *J Formos Med Assoc*. 2001;100(12):4.
22. Bertelsen C, Zhou S, Hapner ER, Johns MM. Sociodemographic characteristics and treatment response among aging adults with voice disorders in the United States. *JAMA Otolaryngology–Head & Neck Surgery*. 2018;144(8):719-726.
23. Gray SD. Cellular physiology of the vocal folds. *Otolaryngologic Clinics of North America*. 2000;33(4):679-697. doi:10.1016/S0030-6665(05)70237-1
24. Arens C, Glanz H, Wönckhaus J, Hersemeyer K, Kraft M. Histologic assessment of epithelial thickness in early laryngeal cancer or precursor lesions and its impact on endoscopic imaging. *Eur Arch Otorhinolaryngol*. 2007;264(6):645-649. doi:10.1007/s00405-007-0246-8
25. Leydon C, Sivasankar M, Falciglia DL, Atkins C, Fisher KV. Vocal fold surface hydration: A review. *J Voice*. 2009;23(6):658-665. doi:10.1016/j.jvoice.2008.03.010
26. Skou JC. The identification of the sodium pump. *Biological Reports*. 1998;18(4):155-159.

27. Nielsen S, Chou CL, Marples D, Christensen EI, Kishore BK, Knepper MA. Vasopressin increases water permeability of kidney collecting duct by inducing translocation of aquaporin-CD water channels to plasma membrane. *Proceedings of the National Academy of Sciences*. 1995;92(4):1013-1017.
28. Wolburg H, Lippoldt A. Tight junctions of the blood–brain barrier: Development, composition and regulation. *Vascular Pharmacology*. 2002;38(6):323-337.
29. Tsukita S, Yamazaki Y, Katsuno T, Tamura A, Tsukita S. Tight junction-based epithelial microenvironment and cell proliferation. *Oncogene*. 2008;27(55):6930-6938. doi:10.1038/onc.2008.344
30. Sivasankar M, Erickson E, Rosenblatt M, Branski RC. Hypertonic challenge to porcine vocal folds: Effects on epithelial barrier function. *Otolaryngol Head Neck Surg*. 2010;142(1):79-84. doi:10.1016/j.otohns.2009.09.011
31. Rousseau B, Suehiro A, Echemendia N, Sivasankar M. Raised intensity phonation compromises vocal fold epithelial barrier integrity. *Laryngoscope*. 2011;121(2):346-351. doi:10.1002/lary.21364
32. Zhang Q, Fisher K. Tight junction-related barrier contributes to the electrophysiological asymmetry across vocal fold epithelium. Deli MA, ed. *PLoS ONE*. 2012;7(3):e34017. doi:10.1371/journal.pone.0034017
33. Gill GA, Buda A, Moorghen M, Dettmar PW, Pignatelli M. Characterisation of adherens and tight junctional molecules in normal animal larynx; determining a suitable model for studying molecular abnormalities in human laryngopharyngeal reflux. *Journal of Clinical Pathology*. 2005;58(12):1265-1270. doi:10.1136/jcp.2004.016972
34. Takeichi M. Cadherins: a molecular family important in selective cell-cell adhesion. *Annual Review of Biochemistry*. 1990;59(1):237-252.
35. Gray SD, Pignatari SS, Harding P. Morphologic ultrastructure of anchoring fibers in normal vocal fold basement membrane zone. *Journal of Voice*. 1994;8(1):48-52.
36. Clark RA, Nielsen LD, Welch MP, McPherson JM. Collagen matrices attenuate the collagen-synthetic response of cultured fibroblasts to TGF-beta. *Journal of cell science*. 1995;108(3):1251-1261.
37. Moore J, Thibeault S. Insights into the role of elastin in vocal fold health and disease. *Journal of Voice*. 2011;26(3):269-275. doi:10.1016/j.jvoice.2011.05.003
38. Gray SD, Alipour F, Titze IR, Hammond TH. Biomechanical and histologic observations of vocal fold fibrous proteins. *Ann Otol Rhinol Laryngol*. 2000;109(1):77-85. doi:10.1177/000348940010900115

39. Gray SD, Titze IR, Chan R, Hammond TH. Vocal fold proteoglycans and their influence on biomechanics. *The Laryngoscope*. 1999;109(6):845-854. doi:10.1097/00005537-199906000-00001
40. Voinchet V, Vasseur P, Kern J. Efficacy and safety of hyaluronic acid in the management of acute wounds. *American Journal of Clinical Dermatology*. 2006;7(6):353-357. doi:10.2165/00128071-200607060-00003
41. Weigel PH, Fuller GM, LeBoeuf RD. A model for the role of hyaluronic acid and fibrin in the early events during the inflammatory response and wound healing. *Journal of Theoretical Biology*. 1986;119(2):219-234. doi:10.1016/S0022-5193(86)80076-5
42. Hammond TH, Zhou R, Hammond E, Pawlak A, Gray S. The intermediate layer: a morphologic study of the elastin and hyaluronic acid constituents of normal human vocal folds. *National Center for Voice and Speech Status and Progress Report*. 1995;8(July):49-54.
43. Hirano M. Phonosurgery: basic and clinical investigations. *Otol (Fukuoka)*. 1975;21:239-242.
44. Pawlak AS, Hammond E, Hammond T, Gray SD. Immunocytochemical study of proteoglycans in vocal folds. *Annals of Otology, Rhinology & Laryngology*. 1996;105(1):6-11.
45. Butler JE, Hammond TH, Gray SD. Gender-related differences of hyaluronic acid distribution in the human vocal fold. *The Laryngoscope*. 2001;111(5):907-911.
46. Gray SD. Molecular and cellular structure of vocal fold tissue. *Vocal fold physiology*. Published online 1993:1-17.
47. Hirano M. Morphological structure of the vocal cord as a vibrator and its variations. *Folia phoniatrica et logopaedica*. 1974;26(2):89-94.
48. Sanders I, Wu B, Biller H. Phonatory specializations of human laryngeal muscles. *Trans Am Laryngol Assoc*. 1994;115:153.
49. Sanders I, Han Y, Wang J, Biller H. Muscle spindles are concentrated in the superior vocalis subcompartment of the human thyroarytenoid muscle. *Journal of Voice*. 1998;12(1):7-16.
50. Cielo CA, Elias VS, Brum DM, Ferreira FV. Thyroarytenoid muscle and vocal fry: a literature review. *Revista da Sociedade Brasileira de Fonoaudiologia*. 2011;16(3):362-369. doi:10.1590/S1516-80342011000300020
51. Hirano M. Morfological structure of the vocal fold as a vibrator and its variations. *Folia Phoniatr (Basel)*. 1974;26:89-4.
52. Alipour F, Titze I. Combined simulation of two dimensional airflow and vocal fold vibration. *Status and Progress Report, National Center for Voice and Speech*. 1995;8:9-14.

53. Oren L, Khosla S, Gutmark E. Intraglottal geometry and velocity measurements in canine larynges. *The Journal of the Acoustical Society of America*. 2014;135(1):380-388.
54. Jaworek AJ, Earasi K, Lyons KM, Daggumati S, Hu A, Sataloff RT. Acute infectious laryngitis: A case series. *Ear, Nose & Throat Journal*. 2018;97(9):306-313. doi:10.1177/014556131809700920
55. Ng ML, Gilbert HR, Lerman JW. Some aerodynamic and acoustic characteristics of acute laryngitis. *Journal of Voice*. 1997;11(3):356-363. doi:10.1016/S0892-1997(97)80015-X
56. Woo P, Casper J, Colton R, Brewer D. Diagnosis and treatment of persistent dysphonia after laryngeal surgery: A retrospective analysis of 62 patients. *Laryngoscope*. 1994;104:1084-1091. doi:10.1288/00005537-199409000-00007
57. Rosen CA, Lombard LE, Murry T. Acoustic, Aerodynamic, and Videostroboscopic Features of Bilateral Vocal Fold Lesions. *Ann Otol Rhinol Laryngol*. 2000;109(9):823-828. doi:10.1177/000348940010900907
58. Wilgus TA. Inflammation as an orchestrator of cutaneous scar formation: a review of the literature. *Plastic and aesthetic research*. 2020;7.
59. Dworkin JP. Laryngitis: types, causes, and treatments. *Otolaryngologic Clinics of North America*. 2008;41(2):419-436. doi:10.1016/j.otc.2007.11.011
60. Richter J. Do we know the cause of reflux disease? *European journal of gastroenterology & hepatology*. 1999;11 Suppl 1:S3-9.
61. Childs LF, Rickert S, Wengerman OC, Lebovics R, Blitzer A. Laryngeal manifestations of relapsing polychondritis and a novel treatment option. *Journal of Voice*. 2012;26(5):587-589. doi:10.1016/j.jvoice.2011.07.012
62. Swain SK, Sahu MC, Parida JR. Wegener's granulomatosis causing subglottic stenosis: Experiences at a tertiary care hospital of the Eastern India. *Journal of Taibah University Medical Sciences*. Published online 2016. doi:10.1016/j.jtumed.2016.01.005
63. Hamdan AL, Sarieddine D. Laryngeal manifestations of rheumatoid arthritis. *Autoimmune Diseases*. 2013;2013. doi:10.1155/2013/103081
64. Habib MA. Intra-articular steroid injection in acute rheumatoid arthritis of the larynx. *Journal of Laryngology and Otolaryngology*. 1977;91(10):909-910. doi:10.1017/S0022215100084541
65. Johns MM. Update on the etiology, diagnosis, and treatment of vocal fold nodules, polyps, and cysts. *Current Opinion in Otolaryngology & Head and Neck Surgery*. 2003;11(6):456-461.

66. Branski R, Verdolini K, Sandulache V, Rosen C, Hebda P. Vocal fold wound healing: A review for clinicians. *Journal of Voice*. 2006;20(3):432-442. doi:10.1016/j.jvoice.2005.08.005
67. Naunheim MR, Carroll TL. Benign vocal fold lesions: update on nomenclature, cause, diagnosis, and treatment. *Current Opinion in Otolaryngology & Head and Neck Surgery*. 2017;25(6):453-458. doi:10.1097/MOO.0000000000000408
68. Benninger MS, Alessi D, Archer S, et al. Vocal fold scarring: Current concepts and management. *Otolaryngology—head and neck surgery*. 1996;115(5):474-482. doi:10.1016/S0194-5998(96)70087-6
69. Singer AJ, Clark R. Mechanisms of disease: cutaneous wound healing. *The New England Journal of Medicine*. 1999;341(1):738-746.
70. Baumgartner HR, Tschopp TB, Weiss HJ. Platelet interaction with collagen fibrils in flowing blood. II. Impaired adhesion aggregation in bleeding disorders. A comparison with subendothelium. *Thrombosis and Haemostasis*. Published online 1977. doi:10.1055/s-0038-1649197
71. Larrabee WF, Lanier BJ, Mickle D. Effect of epinephrine on local cutaneous blood flow. *Head & Neck Surgery*. 1987;9(5):287-289. doi:10.1002/hed.2890090507
72. Rickles FR, Patierno S, Fernandez PM. Tissue factor, thrombin, and cancer. *Chest*. Published online 2003. doi:10.1378/chest.124.3_suppl.58S
73. Hawkey C. COX-2 inhibitors. *The Lancet*. 1999;353(9149):307-314. doi:10.1016/S0140-6736(98)12154-2
74. Li J, Chen J, Kirsner R. Pathophysiology of acute wound healing. *Clinics in Dermatology*. Published online 2007. doi:10.1016/j.clindermatol.2006.09.007
75. Ng MFY. The role of mast cells in wound healing. 2010;7(1):55-61.
76. Velnar T, Bailey T, Smrkolj V. The wound healing process: An overview of the cellular and molecular mechanisms. *Journal of International Medical Research*. Published online 2009. doi:10.1177/147323000903700531
77. Beldon P. Basic science of wound healing. *Surgery*. 2010;28(9):409-412. doi:10.1016/j.mpsur.2010.05.007
78. Kirsner RS, Eaglstein WH. The wound healing process. *Dermatologic Clinics*. Published online 1993. doi:10.1016/0738-081X(84)90022-1
79. Clark RA, Nielsen LD, Welch MP, McPherson JM. Collagen matrices attenuate the collagen-synthetic response of cultured fibroblasts to TGF-beta. *Journal of cell science*. Published online 1995.

80. Schreml S, Szeimies RM, Prantl L, Landthaler M, Babilas P. Wound healing in the 21st century. *Journal of American Dermatology*. 2010;63:866-881. doi:10.1016/j.jaad.2009.10.048
81. Seifert AW, Maden M. New insights into vertebrate skin regeneration. *International review of cell and molecular biology*. 2014;310:129-169.
82. Hopf HW, Kelly M, Shapshak D. Oxygen and the basic mechanisms of wound healing. In: *Physiology and Medicine of Hyperbaric Oxygen Therapy*. Saunders; 2008:203-228.
83. Caley MP, Martins VLC, O'Toole EA. Metalloproteinases and Wound Healing. *Advances in Wound Care*. Published online 2015. doi:10.1089/wound.2014.0581
84. Montes GS. Structural biology of the fibres of the collagenous and elastic systems. *Cell Biology International*. Published online 1996. doi:10.1006/cbir.1996.0004
85. Lapiere CM, Nusgens B, Pierard GE. Interaction between collagen type I and type III in conditioning bundles organization. *Connective Tissue Research*. Published online 1977. doi:10.3109/03008207709152608
86. Verdolini K, Rosen CA, Branski RC, Hebda PA. Shifts in biochemical markers associated with wound healing in laryngeal secretions following phonotrauma: A preliminary study. *Annals of Otolaryngology, Rhinology and Laryngology*. Published online 2003. doi:10.1177/000348940311201205
87. Lim X, Tateya I, Tateya T, Muñoz-Del-Río A, Bless DM. Immediate inflammatory response and scar formation in wounded vocal folds. *Annals of Otolaryngology, Rhinology and Laryngology*. Published online 2006. doi:10.1177/000348940611501212
88. Welham NV, Lim X, Tateya I, Bless DM. Inflammatory factor profiles one hour following vocal fold injury. *Annals of Otolaryngology, Rhinology and Laryngology*. 2008;117(2):145-152. doi:10.1177/000348940811700213
89. Tateya T, Tateya I, Sohn JH, Bless DM. Histological study of acute vocal fold injury in a rat model. *Annals of Otolaryngology, Rhinology and Laryngology*. Published online 2006. doi:10.1177/000348940611500406
90. Rousseau B, Ge PJ, Ohno T, French LC, Thibeault SL. Extracellular matrix gene expression after vocal fold injury in a rabbit model. *Annals of Otolaryngology, Rhinology and Laryngology*. 2008;117(8):598-603. doi:10.1177/000348940811700809
91. Rousseau B, Ge P, French LC, Zealear DL, Thibeault SL, Ossoff RH. Experimentally induced phonation increases matrix metalloproteinase-1 gene expression in normal rabbit vocal fold. *Otolaryngology—Head and Neck Surgery*. 2008;138(1):62-68. doi:10.1016/j.otohns.2007.10.024

92. Rousseau B, Suehiro A, Echemendia N, Sivasankar M. Raised intensity phonation compromises vocal fold epithelial barrier integrity. *Laryngoscope*. Published online 2011. doi:10.1002/lary.21364
93. Rousseau B, Kojima T, Novaleski CK, et al. Recovery of vocal fold epithelium after acute phonotrauma. *Cells, tissues, organs*. 2017;204(2):93-104. doi:10.1159/000472251
94. Kojima T, Valenzuela C V., Novaleski CK, et al. Effects of phonation time and magnitude dose on vocal fold epithelial genes, barrier integrity, and function. *The Laryngoscope*. 2014;124(12):2770-2778. doi:10.1002/lary.24827
95. Branski RC, Verdolini K, Rosen CA, Hebda PA. Acute vocal fold wound healing in a rabbit model. *Annals of Otolaryngology, Rhinology and Laryngology*. 2005;114(1):19-24. doi:10.1177/000348940511400105
96. Tateya T, Sohn JH, Tateya I, Bless DM. Histologic characterization of rat vocal fold scarring. *Annals of Otolaryngology, Rhinology & Laryngology*. 2005;114(3):183-191.
97. Rousseau B, Sohn J, Tateya I, Montequin DW, Bless DM. Functional outcomes of reduced hyaluronan in acute vocal fold scar. *Annals of Otolaryngology, Rhinology and Laryngology*. 2004;113(10):767-776. doi:10.1177/000348940411301001
98. Thibeault SL, Rousseau B, Welham NV, Hirano S, Bless DM. *Hyaluronan Levels in Acute Vocal Fold Scar.*; 2004. <https://onlinelibrary.wiley.com/doi/pdf/10.1097/00005537-200404000-00031>
99. Thibeault SL, Gray SD, Bless DM, Chan RW, Ford CN. Histologic and rheologic characterization of vocal fold scarring. *Journal of Voice*. 2002;16(1):96-104. doi:10.1016/S0892-1997(02)00078-4
100. Rousseau B, Hirano S, Scheidt TD, et al. Characterization of vocal fold scarring in a canine model. *Laryngoscope*. 2003;113(4):620-627. doi:10.1097/00005537-200304000-00007
101. Rousseau B, Hirano S, Chan RW, et al. Characterization of chronic vocal fold scarring in a rabbit model. *Journal of Voice*. 2004;18(1):116-124. doi:10.1016/j.jvoice.2003.06.001
102. Kotby M, Nassar A, Seif E, Helal E, Saleh M. Ultrastructural features of vocal fold nodules and polyps. *Acta Oto-Laryngologica*. 1988;105(5-6):477-482.
103. Courey MS, Scott MA, Shohet JA, Ossoff RH. Immunohistochemical characterization of benign laryngeal lesions. *Annals of Otolaryngology, Rhinology & Laryngology*. 1996;105(7):525-531.
104. Çetinkaya F, Tüfekçi BS, Kutluk G. A comparison of nebulized budesonide, and intramuscular, and oral dexamethasone for treatment of croup. *International Journal of Pediatric Otorhinolaryngology*. 2004;68(4):453-456. doi:10.1016/J.IJPORL.2003.11.017

105. Cruz MN, Stewart G, Rosenberg N. Use of dexamethasone in the outpatient management of acute laryngotracheitis. *Pediatrics*. 1995;96(2 Pt 1):220-223.
106. Rafii B, Sridharan S, Taliercio S, et al. Glucocorticoids in laryngology: A review. *Laryngoscope*. 2014;124(7):1668-1673. doi:10.1002/lary.24556
107. Govil N, Rafii BY, Paul BC, Ruiz R, Amin MR, Branski RC. Glucocorticoids for vocal fold disease: A survey of otolaryngologists. *Journal of Voice*. Published online 2014. doi:10.1016/j.jvoice.2013.04.015
108. Mortensen M. Laryngeal steroid injection for vocal fold scar. *Current Opinion in Otolaryngology and Head and Neck Surgery*. 2010;18(6):487-491. doi:10.1097/MOO.0b013e32833fe112
109. Woo JH, Kim DY, Kim JW, Oh EA, Lee SW. Efficacy of percutaneous vocal fold injections for benign laryngeal lesions: Prospective multicenter study. *Acta Oto-Laryngologica*. 2011;131(12):1326-1332. doi:10.3109/00016489.2011.620620
110. Tateya I, Omori K, Kojima H, Hirano S, Kaneko K, Ito J. Steroid injection for Reinke's edema using fiberoptic laryngeal surgery. *Acta Oto-Laryngologica*. Published online 2003. doi:10.1080/00016480310001321
111. Tateya I, Omori K, Kojima H, Hirano S, Kaneko K ichi, Ito J. Steroid injection to vocal nodules using fiberoptic laryngeal surgery under topical anesthesia. *European Archives of Oto-Rhino-Laryngology*. 2004;261(9):489-492. doi:10.1007/s00405-003-0720-x
112. Mortensen M, Woo P. Office steroid injections of the larynx. *Laryngoscope*. Published online 2006. doi:10.1097/01.mlg.0000231455.19183.8c
113. Lee SH, Yeo JO, Choi JI, et al. Local steroid injection via the cricothyroid membrane in patients with a vocal nodule. *Archives of Otolaryngology - Head and Neck Surgery*. Published online 2011. doi:10.1001/archoto.2011.168
114. Velden VHJ Van Der. Glucocorticoids: mechanisms of action and anti-inflammatory. 1998;237:229-237.
115. Barnes PJ, Adcock IM. How Do Corticosteroids Work in Asthma? *Annals of Internal Medicine*. Published online 2003. doi:10.7326/0003-4819-139-5_part_1-200309020-00012
116. Grzanka A, Misiołek M, Golusiński W, Jarzab J. Molecular mechanisms of glucocorticoids action: Implications for treatment of rhinosinusitis and nasal polyposis. *European Archives of Oto-Rhino-Laryngology*. Published online 2011. doi:10.1007/s00405-010-1330-z
117. Wicke C, SW B, JM S, et al. Effects of steroids and retinoids on wound healing. *Archives of Surgery*. 2000;135(11):1265-1270. doi:10.1001/archsurg.135.11.1265

118. Ingle JW, Helou LB, Li NYK, Hebda PA, Rosen CA, Abbott K V. Role of steroids in acute phonotrauma: A basic science investigation. *Laryngoscope*. Published online 2014. doi:10.1002/lary.23691
119. Gayo A, Mozo L, Suárez A, Tuñon A, Lahoz C, Gutiérrez C. Glucocorticoids increase IL-10 expression in multiple sclerosis patients with acute relapse. *Journal of Neuroimmunology*. 1998;85(2):122-130. doi:10.1016/S0165-5728(97)00262-2
120. Rhen T, Cidlowski JA. Antiinflammatory action of glucocorticoids - New mechanisms for old drugs. *New England Journal of Medicine*. Published online 2005. doi:10.1056/NEJMra050541
121. Auphan N, DiDonato JA, Rosette C, Helmberg A, Karin M. Immunosuppression by glucocorticoids: Inhibition of NF- κ B activity through induction of I κ B synthesis. *Science*. Published online 1995. doi:10.1126/science.270.5234.286
122. Webster JI, Tonelli L, Sternberg EM. Neuroendocrine regulation of immunity. *Annu Rev Immunol*. 2002;20:125-163. doi:10.1146/annurev.immunol.20.082401.104914
123. Barnes PJ. How corticosteroids control inflammation: Quintiles Prize Lecture 2005. *British Journal of Pharmacology*. 2006;148(3):245-254. doi:10.1038/sj.bjp.0706736
124. McKay LI, Cidlowski JA. Molecular control of immune/inflammatory responses: Interactions between nuclear factor- κ B and steroid receptor-signaling pathways. *Endocrine Reviews*. Published online 1999. doi:10.1210/er.20.4.435
125. Cato ACB, Wade E. Molecular mechanisms of anti-inflammatory action of glucocorticoids. *BioEssays*. 1996;18(5):371-378. doi:10.1002/bies.950180507
126. Scheinman RI, Gualberto A, Jewell CM, Cidlowski JA, Baldwin AS. Characterization of mechanisms involved in transrepression of NF- κ B by activated glucocorticoid receptors. *Pneumologie*. Published online 1997.
127. Buttgerit F, Burmester GR, Brand MD. Bioenergetics of immune functions: Fundamental and therapeutic aspects. *Immunology Today*. Published online 2000.
128. Du J, Wang Y, Hunter R, et al. Dynamic regulation of mitochondrial function by glucocorticoids. *Proceedings of the National Academy of Sciences of the United States of America*. Published online 2009. doi:10.1073/pnas.0812671106
129. Stahn C, Buttgerit F. Genomic and nongenomic effects of glucocorticoids. *Nature Clinical Practice Rheumatology*. 2008;4(10):525-533. doi:10.1038/ncprheum0898
130. Higgins AJ, Lees P. The acute inflammatory process, arachidonic acid metabolism and the mode of action of anti-inflammatory drugs. *Equine Veterinary Journal*. Published online 1984. doi:10.1111/j.2042-3306.1984.tb01893.x

131. Löwenberg M, Verhaar AP, Bilderbeek J, et al. Glucocorticoids cause rapid dissociation of a T-cell-receptor-associated protein complex containing LCK and FYN. *EMBO reports*. 2006;7(10):1023-1029. doi:10.1038/sj.embor.7400775
132. Smink JJ, Buchholz IM, Hamers N, et al. Short-term glucocorticoid treatment of piglets causes changes in growth plate morphology and angiogenesis. *Osteoarthritis and Cartilage*. 2003;11(12):864-871. doi:10.1016/S1063-4584(03)00187-0
133. Lu Y, Yu Q, Guo W, Hao Y, Sun W, Cheng L. Effect of glucocorticoids on the function of microvascular endothelial cells in the human femoral head bone. *Adv Clin Exp Med*. 2020;29(3):345-353. doi:10.17219/acem/112602
134. Vinukonda G, Dummula K, Malik S, et al. Effect of Prenatal Glucocorticoids on Cerebral Vasculature of the Developing Brain. *Stroke*. 2010;41(8):1766-1773. doi:10.1161/STROKEAHA.110.588400
135. Chetta A, Zanini A, Foresi A, et al. Vascular Component of Airway Remodeling in Asthma Is Reduced by High Dose of Fluticasone. *Am J Respir Crit Care Med*. 2003;167(5):751-757. doi:10.1164/rccm.200207-7100C
136. Kao JS, Fluhr JW, Man MQ, et al. Short-Term Glucocorticoid Treatment Compromises Both Permeability Barrier Homeostasis and Stratum Corneum Integrity: Inhibition of Epidermal Lipid Synthesis Accounts for Functional Abnormalities. *J Invest Dermatol*. 2003;120(3):456-464. doi:10.1046/j.1523-1747.2003.12053.x
137. Sheu HM, Lee JYY, Chai CY, Kuo KW. Depletion of stratum corneum intercellular lipid lamellae and barrier function abnormalities after long-term topical corticosteroids. *British Journal of Dermatology*. 1997;136(6):884-890. doi:10.1046/j.1365-2133.1997.01827.x
138. Wild GE, Waschke KA, Bitton A, Thomson ABR. The mechanisms of prednisone inhibition of inflammation in Crohn's disease involve changes in intestinal permeability, mucosal TNF α production and nuclear factor kappa B expression. *Alimentary Pharmacology & Therapeutics*. 2003;18(3):309-317. doi:10.1046/j.1365-2036.2003.01611.x
139. Boivin MA, Ye D, Kennedy JC, Al-Sadi R, Shepela C, Ma TY. Mechanism of glucocorticoid regulation of the intestinal tight junction barrier. *American Journal of Physiology-Gastrointestinal and Liver Physiology*. 2007;292(2):G590-G598. doi:10.1152/ajpgi.00252.2006
140. Hue CD, Cho FS, Cao S, Bass CR "Dale," Meaney DF, Morrison B. Dexamethasone Potentiates in Vitro Blood-Brain Barrier Recovery after Primary Blast Injury by Glucocorticoid Receptor-Mediated Upregulation of ZO-1 Tight Junction Protein. *J Cereb Blood Flow Metab*. 2015;35(7):1191-1198. doi:10.1038/jcbfm.2015.38
141. Romero IA, Radewicz K, Jubin E, et al. Changes in cytoskeletal and tight junctional proteins correlate with decreased permeability induced by dexamethasone in cultured rat brain endothelial cells. *Neuroscience Letters*. 2003;344(2):112-116. doi:10.1016/S0304-3940(03)00348-3

142. Singer KL, Stevenson B, Woos PL, Firestone S, GL. Relationship of Serine/Threonine Phosphorylation/Dephosphorylation Signaling to Glucocorticoid Regulation of Tight Junction Permeability and ZO-1 Distribution in Nontransformed Mammary Epithelial Cells. :8.
143. Cucullo L, Hallene K, Dini G, Dal Toso R, Janigro D. Glycerophosphoinositol and dexamethasone improve transendothelial electrical resistance in an in vitro study of the blood–brain barrier. *Brain research*. 2004;997(2):147-151.
144. Campolo M, Ahmad A, Crupi R, et al. Combination therapy with melatonin and dexamethasone in a mouse model of traumatic brain injury. *The Journal of endocrinology*. 2013;217. doi:10.1530/JOE-13-0022
145. Thal SC, Schaible EV, Neuhaus W, et al. Inhibition of Proteasomal Glucocorticoid Receptor Degradation Restores Dexamethasone-Mediated Stabilization of the Blood–Brain Barrier After Traumatic Brain Injury*. *Critical Care Medicine*. 2013;41(5):1305-1315. doi:10.1097/CCM.0b013e31827ca494
146. Förster C, Silwedel C, Golenhofen N, et al. Occludin as direct target for glucocorticoid-induced improvement of blood–brain barrier properties in a murine in vitro system. *The Journal of Physiology*. 2005;565(2):475-486. doi:10.1113/jphysiol.2005.084038
147. Hall JE, Suehiro A, Rousseau B, Branski RC, Garrett CG. Investigation of Triamcinolone in Acute Phonotrauma. *Otolaryngol Head Neck Surg*. 2011;145(2_suppl):P193-P193. doi:10.1177/0194599811415823a192
148. Kielgast F, Schmidt H, Braubach P, et al. Glucocorticoids Regulate Tight Junction Permeability of Lung Epithelia by Modulating Claudin 8. *Am J Respir Cell Mol Biol*. 2016;54(5):707-717. doi:10.1165/rcmb.2015-0071OC
149. Ramamoorthy S, Cidlowski JA. Exploring the Molecular Mechanisms of Glucocorticoid Receptor Action from Sensitivity to Resistance. *Endocr Dev*. 2013;24:41-56. doi:10.1159/000342502
150. G R, A M, A L, et al. Glucocorticoid receptors are down-regulated in inflamed colonic mucosa but not in peripheral blood mononuclear cells from patients with inflammatory bowel disease. *Eur J Clin Invest*. 1999;29(4):330-336. doi:10.1046/j.1365-2362.1999.00460.x
151. Wasilewska A, Zoch-Zwierz W. Expression of glucocorticoid receptors in nephrotic children depending on total prednisone dose. *J Pediatr Endocrinol Metab*. 2005;18(8):799-806. doi:10.1515/jpem.2005.18.8.799
152. Lippman M. Clinical implications of glucocorticoid receptors in human leukemia. *American Journal of Physiology-Endocrinology and Metabolism*. 1982;243(2):E103-E108. doi:10.1152/ajpendo.1982.243.2.E103

153. Bhavsar P, Hew M, Khorasani N, et al. Relative corticosteroid insensitivity of alveolar macrophages in severe asthma compared with non-severe asthma. *Thorax*. 2008;63(9):784-790. doi:10.1136/thx.2007.090027
154. Chang PJ, Bhavsar PK, Michaeloudes C, Khorasani N, Chung KF. Corticosteroid insensitivity of chemokine expression in airway smooth muscle of patients with severe asthma. *Journal of Allergy and Clinical Immunology*. 2012;130(4):877-885.
155. Chang PJ, Michaeloudes C, Zhu J, et al. Impaired Nuclear Translocation of the Glucocorticoid Receptor in Corticosteroid-Insensitive Airway Smooth Muscle in Severe Asthma. *Am J Respir Crit Care Med*. 2015;191(1):54-62. doi:10.1164/rccm.201402-0314OC
156. Schakman O, Gilson H, Kalista S, Thissen JP. Mechanisms of Muscle Atrophy Induced by Glucocorticoids. *Horm Res*. 2009;72(1):36-41. doi:10.1159/000229762
157. Salehian, MD B, Kejriwal, MD K. GLUCOCORTICOID-INDUCED MUSCLE ATROPHY: MECHANISMS AND THERAPEUTIC STRATEGIES. *Endocrine Practice*. 1999;5(5):277-281. doi:10.4158/EP.5.5.277
158. Lecker SH, Solomon V, Mitch WE, Goldberg AL. Muscle Protein Breakdown and the Critical Role of the Ubiquitin-Proteasome Pathway in Normal and Disease States. *J Nutr*. 1999;129(1):227S-237S. doi:10.1093/jn/129.1.227S
159. Shi LL, Giraldez-Rodriguez LA, Johns MM. The risk of vocal fold atrophy after serial corticosteroid injections of the vocal fold. *Journal of Voice*. 2016;30(6):762-e11. doi:10.1016/j.jvoice.2015.10.004
160. Jin HJ, Lee SH, Lee SU, et al. Morphological and Histological Changes of Rabbit Vocal Fold after Steroid Injection. *Otolaryngol Head Neck Surg*. 2013;149(2):277-283. doi:10.1177/0194599813489657
161. Wing SS, Haas AL, Goldberg AL. Increase in ubiquitin-protein conjugates concomitant with the increase in proteolysis in rat skeletal muscle during starvation and atrophy denervation. *Biochem J*. 1995;307(Pt 3):639-645.
162. Clavel S, Coldefy AS, Kurkdjian E, Salles J, Margaritis I, Derijard B. Atrophy-related ubiquitin ligases, atrogin-1 and MuRF1 are up-regulated in aged rat Tibialis Anterior muscle. *Mechanisms of Ageing and Development*. 2006;127(10):794-801. doi:10.1016/j.mad.2006.07.005
163. Schiaffino S, Mammucari C. Regulation of skeletal muscle growth by the IGF1-Akt/PKB pathway: insights from genetic models. *Skelet Muscle*. 2011;1:4. doi:10.1186/2044-5040-1-4
164. Gumucio JP, Mendias CL. Atrogin-1, MuRF-1, and sarcopenia. *Endocrine*. 2013;43(1):12-21. doi:10.1007/s12020-012-9751-7

165. Callis J. The Ubiquitination Machinery of the Ubiquitin System. *Arabidopsis Book*. 2014;12. doi:10.1199/tab.0174
166. Hershko A, Ciechanover A. The Ubiquitin System for Protein Degradation. *Annual Review of Biochemistry*. 1992;61(1):761-807. doi:10.1146/annurev.bi.61.070192.003553
167. Mitch WE, Goldberg AL. Mechanisms of Muscle Wasting — The Role of the Ubiquitin–Proteasome Pathway. Epstein FH, ed. *N Engl J Med*. 1996;335(25):1897-1905. doi:10.1056/NEJM199612193352507
168. Nakayama KI, Nakayama K. Ubiquitin ligases: cell-cycle control and cancer. *Nature Reviews Cancer*. 2006;6(5):369-381. doi:10.1038/nrc1881
169. Foletta VC, White LJ, Larsen AE, Léger B, Russell AP. The role and regulation of MAFbx/atrogenin-1 and MuRF1 in skeletal muscle atrophy. *Pflugers Arch - Eur J Physiol*. 2011;461(3):325-335. doi:10.1007/s00424-010-0919-9
170. de Boer MD, Selby A, Atherton P, et al. The temporal responses of protein synthesis, gene expression and cell signalling in human quadriceps muscle and patellar tendon to disuse. *J Physiol (Lond)*. 2007;585(Pt 1):241-251. doi:10.1113/jphysiol.2007.142828
171. Jones SW, Hill RJ, Krasney PA, O’conner B, Peirce N, Greenhaff PL. Disuse atrophy and exercise rehabilitation in humans profoundly affects the expression of genes associated with the regulation of skeletal muscle mass. *The FASEB Journal*. 2004;18(9):1025-1027. doi:10.1096/fj.03-1228fje
172. Chen YW, Gregory CM, Scarborough MT, Shi R, Walter GA, Vandeborne K. Transcriptional pathways associated with skeletal muscle disuse atrophy in humans. *Physiological Genomics*. 2007;31(3):510-520. doi:10.1152/physiolgenomics.00115.2006
173. Gustafsson T, Osterlund T, Flanagan JN, et al. Effects of 3 days unloading on molecular regulators of muscle size in humans. *Journal of Applied Physiology*. 2010;109(3):721-727. doi:10.1152/jappphysiol.00110.2009
174. Bodine SC, Latres E, Baumhueter S, et al. Identification of ubiquitin ligases required for skeletal Muscle Atrophy. *Science*. 2001;31(3):510-520. doi:10.1126/science.1065874
175. Moresi V, Williams AH, Meadows E, et al. Myogenin and Class II HDACs Control Neurogenic Muscle Atrophy by Inducing E3 Ubiquitin Ligases. *Cell*. 2010;143(1):35-45. doi:10.1016/j.cell.2010.09.004
176. Lecker SH, Jagoe RT, Gilbert A, et al. Multiple types of skeletal muscle atrophy involve a common program of changes in gene expression. *FASEB j*. 2004;18(1):39-51. doi:10.1096/fj.03-0610com
177. Satchek JM, Hyatt JPK, Raffaello A, et al. Rapid disuse and denervation atrophy involve transcriptional changes similar to those of muscle wasting during systemic diseases. *The FASEB Journal*. 2007;21(1):140-155. doi:10.1096/fj.06-6604com

178. McFarlane C, Plummer E, Thomas M, et al. Myostatin induces cachexia by activating the ubiquitin proteolytic system through an NF- κ B-independent, FoxO1-dependent mechanism. *Journal of Cellular Physiology*. 2006;209(2):501-514. doi:10.1002/jcp.20757
179. Patel K, Amthor H. The function of Myostatin and strategies of Myostatin blockade—new hope for therapies aimed at promoting growth of skeletal muscle. *Neuromuscular Disorders*. 2005;15(2):117-126. doi:10.1016/j.nmd.2004.10.018
180. Goodman CA, McNally RM, Hoffmann FM, Hornberger TA. Smad3 Induces Atrogin-1, Inhibits mTOR and Protein Synthesis, and Promotes Muscle Atrophy In Vivo. *Mol Endocrinol*. 2013;27(11):1946-1957. doi:10.1210/me.2013-1194
181. Zhao J, Brault JJ, Schild A, et al. FoxO3 coordinately activates protein degradation by the autophagic/lysosomal and proteasomal pathways in atrophying muscle cells. *Cell Metab*. 2007;6(6):472-483. doi:10.1016/j.cmet.2007.11.004
182. Bollinger LM, Witczak CA, Houmard JA, Brault JJ. SMAD3 augments FoxO3-induced MuRF-1 promoter activity in a DNA-binding-dependent manner. *American Journal of Physiology-Cell Physiology*. 2014;307(3):C278-C287. doi:10.1152/ajpcell.00391.2013
183. Sandri M, Sandri C, Gilbert A, et al. Foxo Transcription Factors Induce the Atrophy-Related Ubiquitin Ligase Atrogin-1 and Cause Skeletal Muscle Atrophy. *Cell*. 2004;117(3):399-412. doi:10.1016/S0092-8674(04)00400-3
184. Mendias CL, Lynch EB, Davis ME, et al. Changes in Circulating Biomarkers of Muscle Atrophy, Inflammation, and Cartilage Turnover in Patients Undergoing Anterior Cruciate Ligament Reconstruction and Rehabilitation. *Am J Sports Med*. 2013;41(8):1819-1826. doi:10.1177/0363546513490651
185. Lalani R, Bhasin S, Byhower F, et al. Myostatin and insulin-like growth factor-I and -II expression in the muscle of rats exposed to the microgravity environment of the NeuroLab space shuttle flight. *Journal of Endocrinology*. 2000;167(3):417-428. doi:10.1677/joe.0.1670417
186. Wehling M, Cai B, James, Tidball G. Modulation of myostatin expression during modified muscle use. *FASEB Journal*. 2000;14:103-110.
187. Kostyo JL, Redmond AF. Role of protein synthesis in the inhibitory action of adrenal steroid hormones on amino acid transport by muscle. *Endocrinology*. 1966;73(3):531-540. doi:10.1210/endo-79-3-531
188. Gayan-Ramirez G, Vanderhoydonc F, Verhoeven G, Decramer M. Acute Treatment with Corticosteroids Decreases IGF-1 and IGF-2 Expression in the Rat Diaphragm and Gastrocnemius. *Am J Respir Crit Care Med*. 1999;159(1):283-289. doi:10.1164/ajrccm.159.1.9803021
189. Inder WJ, Jang C, Obeyesekere VR, Alford FP. Dexamethasone administration inhibits skeletal muscle expression of the androgen receptor and IGF-1 – implications for steroid-

- induced myopathy. *Clinical Endocrinology*. 2010;73(1):126-132. doi:10.1111/j.1365-2265.2009.03683.x
190. Nakao R, Hirasaka K, Goto J, et al. Ubiquitin ligase Cbl-b is a negative regulator for insulin-like growth factor 1 signaling during muscle atrophy caused by unloading. *Mol Cell Biol*. 2009;29(17):4798-4811. doi:10.1128/MCB.01347-08
191. Schakman O, Kalista S, Barbé C, Loumaye A, Thissen JP. Glucocorticoid-induced skeletal muscle atrophy. *The International Journal of Biochemistry & Cell Biology*. 2013;45(10):2163-2172. doi:10.1016/j.biocel.2013.05.036
192. Ma K, Mallidis C, Artaza J, Taylor W, Gonzalez-Cadavid N, Bhasin S. Characterization of 5'-regulatory region of human myostatin gene: regulation by dexamethasone in vitro. *American Journal of Physiology-Endocrinology and Metabolism*. 2001;281(6):E1128-E1136. doi:10.1152/ajpendo.2001.281.6.E1128
193. Ma K, Mallidis C, Bhasin S, et al. Glucocorticoid-induced skeletal muscle atrophy is associated with upregulation of myostatin gene expression. *American journal of physiology Endocrinology and metabolism*. 2003;285(2):NaN-NaN. doi:10.1152/ajpendo.00487.2002
194. Qin J, Du R, Yang YQ, et al. Dexamethasone-induced skeletal muscle atrophy was associated with upregulation of myostatin promoter activity. *Research in Veterinary Science*. 2013;94(1):84-89. doi:10.1016/j.rvsc.2012.07.018
195. Gilson H, Schakman O, Combaret L, et al. Myostatin Gene Deletion Prevents Glucocorticoid-Induced Muscle Atrophy. *Endocrinology*. 2007;148(1):452-460. doi:10.1210/en.2006-0539
196. Yin HN, Chai JK, Yu YM, et al. Regulation of Signaling Pathways Downstream of IGF-I/Insulin by Androgen in Skeletal Muscle of Glucocorticoid-Treated Rats: *The Journal of Trauma: Injury, Infection, and Critical Care*. 2009;66(4):1083-1090. doi:10.1097/TA.0b013e31817e7420
197. Yamamoto D, Maki T, Herningtyas EH, et al. Branched-chain amino acids protect against dexamethasone-induced soleus muscle atrophy in rats. *Muscle Nerve*. 2010;41(6):819-827. doi:10.1002/mus.21621
198. Garrett CG, Coleman JR, Reinisch L. Comparative histology and vibration of the vocal folds: Implications for experimental studies in microlaryngeal surgery. *The Laryngoscope*. 2000;110(5):814-824. doi:10.1097/00005537-200005000-00011
199. Maytag AL, Robitaille MJ, Rieves AL, Madsen J, Smith BL, Jiang JJ. Use of the rabbit larynx in an excised larynx setup. *Journal of Voice*. 2013;27(1):24-28. doi:10.1016/j.jvoice.2012.08.004
200. Alipour F, Jaiswal S, Vigmostad S. Vocal fold elasticity in the pig, sheep, and cow larynges. *Journal of Voice*. 2011;25(2):130-136. doi:10.1016/j.jvoice.2009.09.002

201. Jiang JJ, Raviv JR, Hanson DG. Comparison of the phonation-related structures among pig, dog, white-tailed deer, and human larynges. *Ann Otol Rhinol Laryngol*. 2001;110(12):1120-1125. doi:10.1177/000348940111001207
202. Ge PJ, French LC, Ohno T, Zeale DL, Rousseau B. Model of evoked rabbit phonation. *Annals of Otolology, Rhinology and Laryngology*. 2009;118(1):51-55. doi:10.1177/000348940911800109
203. Swanson ER, Abdollahian D, Ohno T, Ge P, Zeale DL, Rousseau B. Characterization of raised phonation in an evoked rabbit phonation model. *The Laryngoscope*. 2009;119(7):1439-1443. doi:10.1002/lary.20532
204. Swanson ER, Ohno T, Abdollahian D, Rousseau B. Effects of raised-intensity phonation on inflammatory mediator gene expression in normal rabbit vocal fold. *Otolaryngology-Head and Neck Surgery*. 2010;143(4):567-572. doi:10.1016/j.otohns.2010.04.264
205. Novaleski CK, Kimball EE, Mizuta M, Rousseau B. Acute exposure to vibration is an apoptosis-inducing stimulus in the vocal fold epithelium. *Tissue and Cell*. 2016;48(5):407-416. doi:10.1016/j.tice.2016.08.007
206. Kurita S. A comparative study of the layer structure of the vocal fold. *Jibi To Rinsho Kai*. 1981;28(4):3-21.
207. Gray SD, Hammond TH. *BIOMECHANICAL AND HISTOLOGIC OBSERVATIONS OF VOCAL FOLD FIBROUS PROTEINS.*; 2000. <https://journals.sagepub.com/doi/pdf/10.1177/000348940010900115>
208. Bless DM, Welham NV. Characterization of vocal fold scar formation, prophylaxis, and treatment using animal models. *Current Opinion in Otolaryngology & Head and Neck Surgery*. 2010;18(6):481-486. doi:10.1097/MOO.0b013e3283407d87
209. Govil N, Rafii BY, Paul BC, Ruiz R, Amin MR, Branski RC. Glucocorticoids for vocal fold disease: A survey of otolaryngologists. *Journal of Voice*. 2014;28(1):82-87. doi:10.1016/j.jvoice.2013.04.015
210. Cope D, Bova R. Steroids in Otolaryngology: *The Laryngoscope*. 2008;118(9):1556-1560. doi:10.1097/MLG.0b013e31817c0b4d
211. Mortensen M. Laryngeal steroid injection for vocal fold scar. *Current Opinion in Otolaryngology and Head and Neck Surgery*. 2010;18(6):487-491. doi:10.1097/MOO.0b013e328333fe112
212. Baehr LM, Furlow JD, Bodine SC. Muscle sparing in muscle RING finger 1 null mice: response to synthetic glucocorticoids. *J Physiol (Lond)*. 2011;589(Pt 19):4759-4776. doi:10.1113/jphysiol.2011.212845

213. Suehiro A, Bock JM, Hall JE, Gaelyn Garrett C, Rousseau B. Feasibility and acute healing of vocal fold microflap incisions in a rabbit model. *Laryngoscope*. 2012;122(3):600-605. doi:10.1002/lary.22470
214. Kojima T, Deusen MV, Jerome WG, et al. Quantification of Acute Vocal Fold Epithelial Surface Damage with Increasing Time and Magnitude Doses of Vibration Exposure. *PLOS ONE*. 2014;9(3):e91615. doi:10.1371/journal.pone.0091615
215. Lim X, Tateya I, Tateya T, Muñoz-Del-Río A, Bless DM. Immediate inflammatory response and scar formation in wounded vocal folds. *Annals of Otolology, Rhinology and Laryngology*. 2006;115(12):921-929. doi:10.1177/000348940611501212
216. Rousseau B, Sohn J, Tateya I, Montequin DW, Bless DM. Functional outcomes of reduced hyaluronan in acute vocal fold scar. *Annals of Otolology, Rhinology and Laryngology*. 2004;113(10):767-776. doi:10.1177/000348940411301001
217. Smith S, Ossoff JP, Coleman JR, et al. Histomorphometric and laryngeal videostroboscopic analysis of the effects of corticosteroids on microflap healing in the dog larynx. *Annals of Otolology, Rhinology and Laryngology*. 1999;108(2):119-217 Aquaporin deletion in mice reduces intraocular pressure and aqueous fluid production. doi:10.1177/000348949910800203
218. Institute of Laboratory Animal Resources (US). Committee on Care, Use of Laboratory Animals. *Guide for the Care and Use of Laboratory Animals*. US Department of Health and Human Services, Public Health Service, National ...; 1986.
219. Dexamethasone 4 mg tablets - Summary of Product Characteristics (SmPC) - (emc). Accessed December 7, 2020. <https://www.medicines.org.uk/emc/product/7395/smpc#gref>
220. Methylprednisolone Dosage Guide with Precautions - Drugs.com. Accessed December 7, 2020. <https://www.drugs.com/dosage/methylprednisolone.html>
221. Howe KL, Achuthan P, Allen J, et al. Ensembl 2021. *Nucleic Acids Research*. 2021;49(D1):D884-D891. doi:10.1093/nar/gkaa942
222. Cohen J. Weighted kappa: Nominal scale agreement provision for scaled disagreement or partial credit. *Psychological Bulletin*. 1968;70(4):213-220. doi:10.1037/h0026256
223. Viera AJ, Garrett JM. Understanding interobserver agreement: The kappa statistic. *Family Medicine*. 2005;37(5):360-363.
224. Ahmed MER, Bando H, Hirota R, et al. Localization and regulation of aquaporins in the murine larynx. *Acta Oto-Laryngologica*. 2012;132(4):439-446. doi:10.3109/00016489.2011.644253
225. Zhang D, Vetrivel L, Verkman AS. Aquaporin deletion in mice reduces intraocular pressure and aqueous fluid production. *J Gen Physiol*. 2002;119(6):561-569. doi:10.1085/jgp.20028597

226. Bai C, Matthay MA, Verkman AS. Lung fluid transport in aquaporin-1 and aquaporin-4 knockout mice. *J Clin Invest.* 1999;103(4):555. doi:10.1172/JCI4138
227. King LS, Nielsen S, Agre P, Brown RH. Decreased pulmonary vascular permeability in aquaporin-1-null humans. *Proceedings of the National Academy of Sciences.* 2002;99(2):1059-1063.
228. Nielsen S, King LS, Christensen BM, Agre P. Aquaporins in complex tissues. II. Subcellular distribution in respiratory and glandular tissues of rat. *American Journal of Physiology-Cell Physiology.* 1997;273(5):C1549-C1561. doi:10.1152/ajpcell.1997.273.5.C1549
229. Song Y, Ma T, Matthay MA, Verkman AS. Role of Aquaporin-4 in Airspace-to-Capillary Water Permeability in Intact Mouse Lung Measured by a Novel Gravimetric Method. *Journal of General Physiology.* 2000;115(1):17-27. doi:10.1085/jgp.115.1.17
230. Binder DK, Oshio K, Ma T, Verkman AS, Manley GT. Increased seizure threshold in mice lacking aquaporin-4 water channels. *NeuroReport.* 2004;15(2):259-262.
231. Saadoun S, Papadopoulos MC, Watanabe H, Yan D, Manley GT, Verkman AS. Involvement of aquaporin-4 in astroglial cell migration and glial scar formation. *Journal of Cell Science.* 2005;118(24):5691-5698. doi:10.1242/jcs.02680
232. Hara-Chikuma M, Sohara E, Rai T, et al. Progressive Adipocyte Hypertrophy in Aquaporin-7-deficient Mice: ADIPOCYTE GLYCEROL PERMEABILITY AS A NOVEL REGULATOR OF FAT ACCUMULATION. *J Biol Chem.* 2005;280(16):15493-15496. doi:10.1074/jbc.C500028200
233. Andersson KE, McCloskey KD. Lamina propria: The functional center of the bladder? *Neurourology and Urodynamics.* 2014;33(1):9-16. doi:10.1002/nau.22465
234. Fisher KV, Telser a, Phillips JE, Yeates DB. Regulation of vocal fold transepithelial water fluxes. *Journal of applied physiology (Bethesda, Md : 1985).* 2001;91(3):1401-1411.
235. Hallén L, Johansson C, Laurent C, Dahlqvist Å. Hyaluronan localization in the rabbit larynx. *The Anatomical Record.* 1996;246(4):441-445. doi:10.1002/(SICI)1097-0185(199612)246:4<441::AID-AR3>3.0.CO;2-Y
236. Gill GA, Buda A, Moorghen M, Dettmar PW, Pignatelli M. Characterisation of adherens and tight junctional molecules in normal animal larynx; determining a suitable model for studying molecular abnormalities in human laryngopharyngeal reflux. *Journal of Clinical Pathology.* 2005;58(12):1265-1270. doi:10.1136/jcp.2004.016972
237. Bulmer D, Ross PE, Axford SE, et al. Cell biology of laryngeal epithelial defenses in health and disease: Further studies. *Annals of Otology, Rhinology and Laryngology.* 2003;112(6):481-491. doi:10.1177/000348940111001203

238. Kojima T, Valenzuela CV, Novaleski CK, et al. Effects of phonation time and magnitude dose on vocal fold epithelial genes, barrier integrity, and function. *The Laryngoscope*. 2014;124(12):2770-2778. doi:10.1002/lary.24827
239. Suzuki R, Katsuno T, Kishimoto Y, et al. Process of tight junction recovery in the injured vocal fold epithelium: Morphological and paracellular permeability analysis. *The Laryngoscope*. 2018;128(4):E150-E156. doi:10.1002/lary.26959
240. Ma J, Wang P, Liu Y, Zhao L, Li Z, Xue Y. Krüppel-Like Factor 4 Regulates Blood-Tumor Barrier Permeability via ZO-1, Occludin and Claudin-5. *Journal of Cellular Physiology*. 2014;229(7):916-926. doi:10.1002/jcp.24523
241. Sassoon CSH, Zhu E, Pham HT, et al. Acute effects of high-dose methylprednisolone on diaphragm muscle function. *Muscle Nerve*. 2008;38(3):1161-1172. doi:10.1002/mus.21048
242. Skjærbæk C, Frystyk J, Grøfte T, et al. Serum free insulin-like growth factor-I is dose-dependently decreased by methylprednisolone and related to body weight changes in rats. *Growth Hormone & IGF Research*. 1999;9(1):74-80. doi:10.1054/ghir.1999.0090
243. Won Jahng J, Kim NY, Ryu V, et al. Dexamethasone reduces food intake, weight gain and the hypothalamic 5-HT concentration and increases plasma leptin in rats. *European Journal of Pharmacology*. 2008;581(1-2):64-70. doi:10.1016/j.ejphar.2007.11.029
244. Liu XY, Shi JH, Du WH, et al. Glucocorticoids decrease body weight and food intake and inhibit appetite regulatory peptide expression in the hypothalamus of rats. *Experimental and Therapeutic Medicine*. 2011;2(5):977-984. doi:10.3892/etm.2011.292
245. Zakrzewska KE, Cusin I, Stricker-Krongrad A, et al. Induction of obesity and hyperleptinemia by central glucocorticoid infusion in the rat. *Diabetes*. 1999;48(2):365-370. doi:10.2337/diabetes.48.2.365
246. Buchbinder R. Short course prednisolone for adhesive capsulitis (frozen shoulder or stiff painful shoulder): a randomised, double blind, placebo controlled trial. *Annals of the Rheumatic Diseases*. 2004;63(11):1460-1469. doi:10.1136/ard.2003.018218
247. Halvorsen P, Ræder J, White PF, et al. The effect of dexamethasone on side effects after coronary revascularization procedures. *Anesthesia & Analgesia*. 2003;96(6):1578-1583.
248. Scudamore CL, Jepson MA, Hirst BH, Hugh R, Miller P. The rat mucosal mast cell chymase, RMCP-11, alters epithelial cell monolayer permeability in association with altered distribution of the tight junction proteins ZO-1 and occludin. *European Journal of Cell Biology*. 1998;75(4):321-330. doi:10.1016/S0171-9335(98)80065-4
249. Shen ZY, Zhang J, Song HL, Zheng WP. Bone-marrow mesenchymal stem cells reduce rat intestinal ischemia-reperfusion injury, ZO-1 downregulation and tight junction disruption via a TNF- α -regulated mechanism. *World J Gastroenterol*. 2013;19(23):3583-3595. doi:10.3748/wjg.v19.i23.3583

250. Erickson EL, Leydon C, Thibeault SL. Vocal fold epithelial barrier in health and injury: A research review. *Journal of Speech, Language, and Hearing Research*. 2014;57(June):1679-1691. doi:10.1044/2014
251. Al-Ali M, Anderson J. The role of steroid injection for vocal folds lesions in professional voice users. *Journal of Otolaryngology-Head & Neck Surgery*. 2020;49(1):1-7.
252. Wang CT, Lai MS, Hsiao TY. Comprehensive Outcome Researches of Intralesional Steroid Injection on Benign Vocal Fold Lesions. *Journal of Voice*. 2015;29(5):578-587. doi:10.1016/j.jvoice.2014.11.002
253. Hashimoto K, Kaneko M, Kinoshita S, et al. Effects of repeated intracordal glucocorticoid injection on the histology and gene expression of rat vocal folds. *Journal of Voice*. Published online July 2021. doi:10.1016/j.jvoice.2021.06.013
254. Hallén L, Johansson C, Laurent C, Dahlqvist AA. Hyaluronan localization in the rabbit larynx. *Anatomical Record*. 1996;246(4):441-445. doi:10.1002/(SICI)1097-0185(199612)246:4<441::AID-AR3>3.0.CO;2-Y
255. Hoh JFY. Laryngeal muscle fibre types. *Acta Physiologica Scandinavica*. 2005;183(2):133-149. doi:10.1111/j.1365-201X.2004.01402.x
256. Wang Y, Pessin JE. Mechanisms for fiber-type specificity of skeletal muscle atrophy. *Curr Opin Clin Nutr Metab Care*. 2013;16(3):243-250. doi:10.1097/MCO.0b013e328360272d
257. Wang CT. Vocal Fold Steroid Injection. In: *Vocal Fold Injection*. Springer; 2021:141-150.
258. Seow CY, Schellenberg RR, Paré PD. Structural and Functional Changes in the Airway Smooth Muscle of Asthmatic Subjects. 1998;158:8.
259. Ebina M, Takahashi T, Chiba T, Motomiya M. Cellular hypertrophy and hyperplasia of airway smooth muscles underlying bronchial asthma: A 3-D morphometric study. *American Review of Respiratory Disease*. 720;148. doi:10.1164/ajrccm/148.3.720
260. Dunnill M. The pathology of asthma, with special reference to changes in the bronchial mucosa. *Journal of clinical pathology*. 13(1):27-33.
261. Léguillette R, Laviolette M, Bergeron C, et al. Myosin, Transgelin, and Myosin Light Chain Kinase. 2009;179:11.
262. Nakamura R, Doyle C, Bing R, Johnson AM, Branski RC. Preliminary investigation of In vitro, bidirectional vocal fold muscle-mucosa interactions. *Ann Otol Rhinol Laryngol*. Published online July 1, 2021:00034894211028497. doi:10.1177/00034894211028497

